Title
Topics in Scattering Amplitudes

Author
Dennen, Tristan Lucas

Publication Date
2012

Peer reviewed|Thesis/dissertation

University of California
Los Angeles

Topics in Scattering Amplitudes

A dissertation submitted in partial satisfaction
of the requirements for the degree
Doctor of Philosophy in Physics

by

Tristan Lucas Dennen

2012

Abstract of the Dissertation

Topics in Scattering Amplitudes

by

Tristan Lucas Dennen

Doctor of Philosophy in Physics

University of California, Los Angeles, 2012

Professor Zvi Bern, Chair

In Part 1, we combine on-shell methods with the six-dimensional helicity formalism of Cheung and O'Connell to construct tree-level and multiloop scattering amplitudes. As a nontrivial multiloop example, we confirm that the recently constructed four-loop four-point amplitude of N=4 super-Yang-Mills theory, including nonplanar contributions, is valid for dimensions less than or equal to six. We demonstrate that the tree-level amplitudes of maximal super-Yang-Mills theory in six dimensions, when stripped of their overall momentum and supermomentum delta functions, are covariant with respect to the six-dimensional dual conformal group. We demonstrate that this property is also present for loop amplitudes.

In Part 2, we explore consequences of the recently discovered duality between color and kinematics, which states that kinematic numerators in a diagrammatic expansion of gauge-theory amplitudes can be arranged to satisfy Jacobi-like identities in one-to-one correspondence to the associated color factors. The related squaring relations express gravity amplitudes in terms of gauge-theory ingredients. We then present a Yang-Mills Lagrangian whose diagrams through five points manifestly satisfy the duality between color and kinematics. Finally, we compute the coefficient of the potential three-loop divergence in pure N=4 supergravity and show that it vanishes, contrary to expectations from symmetry arguments.

The dissertation of Tristan Lucas Dennen is approved.

Christian Haesemeyer

Per Kraus

Eric D'Hoker

Zvi Bern, Committee Chair

University of California, Los Angeles

2012

Table of Contents

Acknowledgments

This work was performed in collaboration with Zvi Bern, John Joseph Carrasco, Scott Davies, Yu-tin Huang, Harald Ita, Michael Kiermaier, and Warren Siegel. Chapters 1 and 2 are adapted from refs. [1, 2]. Chapter 3 is adapted from ref. [3]. Chapter 4 is adapted from ref. [4]. Chapter 5 is adapted from ref. [5]. Chapter 6 is adapted from ref. [6]. In each case, I have removed sections to which I made little contribution. What remains is largely my work.

I am grateful for the financial support of a Department of Energy Fellowship in High Energy Theory, and a Dissertation Year Fellowship from the University of California, Los Angeles.

Vita

2007	B.S. (Physics and Mathematics), Emory University, Atlanta, Georgia
2008–2011	Teaching Assistant, Department of Physics and Astronomy, UCLA.
2009–present	Graduate Student Researcher, Department of Physics and Astronomy, UCLA.

Publications

T. Dennen, Y. -t. Huang and W. Siegel, JHEP **1004**, 127 (2010) [arXiv:0910.2688 [hep-th]].

Z. Bern, J. J. Carrasco, T. Dennen, Y. -t. Huang and H. Ita, Phys. Rev. D **83**, 085022 (2011) [arXiv:1010.0494 [hep-th]].

T. Dennen and Y. -t. Huang, JHEP **1101**, 140 (2011) [arXiv:1010.5874 [hep-th]].

Z. Bern, T. Dennen, Y. -t. Huang and M. Kiermaier, Phys. Rev. D **82**, 065003 (2010) [arXiv:1004.0693 [hep-th]].

Z. Bern and T. Dennen, Phys. Rev. Lett. **107**, 081601 (2011) [arXiv:1103.0312 [hep-th]].

Z. Bern, S. Davies, T. Dennen and Y. -t. Huang, arXiv:1202.3423 [hep-th].

Part I

On-Shell Techniques in Six-Dimensional Maximally-Supersymmetric Yang-Mills Theory

CHAPTER 1

Superspace for 6D Maximal Super Yang-Mills

1.1 Introduction

In recent years many surprising results were discovered in the S-matrix of maximal supersymmetric theories in four dimensions. These include new symmetries and structures [7, 8, 9, 10] , representations [11, 12, 13, 14, 15, 16, 17] of tree-level amplitudes, and unexpected UV behaviour in loop perturbation theory [18, 19, 20, 21, 22, 23, 24, 25]. Many of these advancements rely heavily on newly developed on-shell methods such as recursion relations to construct tree amplitudes, and generalized unitarity to obtain loop corrections by simply sewing tree amplitudes. More precisely, one can now use either the CSW method [12, 13], which constructs general amplitudes from MHV vertices, or the BCFW [14] construction, which expresses an n-point amplitude as direct products of lower point amplitudes, to efficiently construct tree amplitudes for either gauge or gravity theory. Modern unitarity methods [26, 27, 28] then allow one to construct loop amplitudes by expressing them in terms of a set of integrals that reproduces the cuts of the amplitude. Tree amplitudes are then used to construct the coefficients of these integrals.

While these current approaches rely on a four-dimensional spinor-helicity formalism [29, 30], many interesting questions are inherently D-dimensional. For example in the study of divergences in maximal supersymmetric theories, one usually encounters various bounds (at given loop level) on the dimension at which the first potential divergence should appear [18, 19, 20, 31]. To study this bound, one is required to compute the divergences of the D-dimensional theory. On the other hand even in QCD one loop amplitudes, D-dimensional tree amplitudes are useful for obtaining rational terms when using unitarity methods [32].

Therefore a spinor helicity formalism similar to four dimensions will be helpful for these purposes.

Here we restrict ourselves to six dimensions, where the spinor-helicity formalism is very similar to four dimensions, as recently demonstrated by Cheung and O'Connell [33]. The Lorentz group SO(5,1) has the covering group SU*(4). The vector forms an antisymmetric representation of SU*(4), and the on-shell condition is naturally solved by introducing SU*(4) spinors, $p^{AB} = \lambda^{Aa}\lambda^B_a$, $p_{AB} = \tilde{\lambda}_{A\dot{a}}\tilde{\lambda}^{\dot{a}}_B$. The indices $a, \dot{a}$ transform under the little group SO(4)$\simeq$SU(2)$\times$ SU(2).

In this chapter, we will introduce Grassmann variables along with the spinors to form an on-shell superspace for $\mathcal{N} = (1,1)$ super Yang-Mills theory. The Yang-Mills field strength is in the $(\frac{1}{2}, \frac{1}{2})$ representation of the little group. Since for maximal $\mathcal{N} = (1,1)$ theory the full multiplet should be contained in a single superfield, the non-chiral nature of the field strength then implies a non-chiral on-shell superspace. Being non-chiral has the advantage of representing the amplitudes in a more symmetric fashion, instead of viewing the amplitudes from the MHV (or $\overline{\text{MHV}}$) point of view. We will also treat BCFW on-shell recursion, giving all the details necessary to generate tree-level superamplitudes with arbitrarily many legs.

1.2 Six-Dimensional Spinor Helicity

We begin by reviewing the six-dimensional spinor-helicity formalism recently developed by Cheung and O'Connell [33]. In six-dimensional Minkowski space, the Lorentz group is SO(5,1), whose covering group is SU*(4). The vector is in the anti-symmetric representation of SU*(4), and can be expressed as

$$p_{AB} = p_\mu \sigma^\mu_{AB}\,, \qquad\qquad p^{AB} = p_\mu \tilde{\sigma}^{\mu AB}\,, \tag{1.1}$$

where $\{A, B \cdots\}$ are the fundamental representation indices of SU*(4). Here the σ^μ_{AB} and $\tilde{\sigma}^{\mu AB}$ are antisymmetric 4×4 matrices which play a role analogous to the Pauli matrices in four dimensions. Our Clifford algebra conventions may be found in Appendix A. The scalar

product of two vectors is defined as a contraction with the SU*(4) invariant tensor ϵ_{ABCD}.

The Dirac equation for Weyl spinors in six dimensions can be written as,

$$p_\mu \sigma^\mu_{AB} \lambda_p^{Ba} = 0\,, \qquad\qquad p_\mu \tilde{\sigma}^{\mu AB}\, \tilde{\lambda}_{pB\dot{a}} = 0\,, \tag{1.2}$$

and gives rise to two independent solutions for each of the Weyl spinors, λ^{Ba} and $\tilde{\lambda}_{B\dot{a}}$. Each solution is labeled by an index a or $\dot{a}$, which are spinor indices of the little group SU(2)×SU(2). We may lower and raise the little group indices with the matrices ϵ_{ab} and $\epsilon^{\dot{a}\dot{b}}$,

$$\lambda_a = \epsilon_{ab}\lambda^b\,, \qquad\qquad \tilde{\lambda}^{\dot{a}} = \epsilon^{\dot{a}\dot{b}}\tilde{\lambda}_{\dot{b}}\,, \tag{1.3}$$

and $\epsilon_{12} = -1$, $\epsilon^{12} = 1$, for this case as well. Spinor inner products are defined by contractions of the SU*(4) indices,

$$\langle i^a | j_{\dot{b}}] = \lambda_i^{Aa}\tilde{\lambda}_{jA\dot{b}} = [j_{\dot{b}}|i^a\rangle\,. \tag{1.4}$$

Other common quantities are spinors contracted with the SU*(4)-invariant Levi-Civita tensor,

$$\begin{aligned} \langle i^a j^b k^c l^d\rangle &\equiv \epsilon_{ABCD}\lambda_i^{Aa}\lambda_j^{Bb}\lambda_k^{Cc}\lambda_l^{Dd}\,, \\ [i_{\dot{a}} j_{\dot{b}} k_{\dot{c}} l_{\dot{d}}] &\equiv \epsilon^{ABCD}\tilde{\lambda}_{iA\dot{a}}\tilde{\lambda}_{jB\dot{b}}\tilde{\lambda}_{kC\dot{c}}\tilde{\lambda}_{lD\dot{d}}\,. \end{aligned} \tag{1.5}$$

The on-shell massless condition can be solved using bosonic six-dimensional chiral spinors in a way similar to the well-known four-dimensional case. The antisymmetry of p_{AB} together with the on-shell condition $p^2 \sim \epsilon^{ABCD}p_{AB}p_{CD} = \det(\not{p}) = 0$ gives the bispinor representation,

$$p^{AB} = \lambda^{Aa}\,\epsilon_{ab}\lambda^{Bb}\,, \qquad p_{AB} = \tilde{\lambda}_{A\dot{a}}\,\epsilon^{\dot{a}\dot{b}}\tilde{\lambda}_{B\dot{b}}\,, \qquad \lambda^{Aa}\tilde{\lambda}_{A\dot{a}} = 0\,. \tag{1.6}$$

One can also express the vector momenta directly in terms of the spinors via,

$$p^\mu = -\frac{1}{4}\langle p^a|\sigma^\mu|p^b\rangle\epsilon_{ab} = -\frac{1}{4}[p_{\dot{a}}|\tilde{\sigma}^\mu|p_{\dot{b}}]\epsilon^{\dot{a}\dot{b}}\,. \tag{1.7}$$

Spinor strings also appear in amplitudes. These are given by

$$\begin{aligned}
\langle i_a|j_{\dot{a}}] &= (\lambda_i)_a^A(\tilde{\lambda}_j)_{A\dot{a}} \\
\langle i^a|\not{p}_1\not{p}_2\cdots\not{p}_{2n+1}|j^b\rangle &= (\lambda_i)^{A_1 a}\,(p_1)_{A_1A_2}\,(p_2)^{A_2A_3}\cdots(p_{2n+1})_{A_{2n+1}A_{2n+2}}\,(\lambda_j)^{A_{2n+2}b}\,, \\
\langle i^a|\not{p}_1\not{p}_2\cdots\not{p}_{2n}|j_{\dot{b}}] &= (\lambda_i)^{A_1 a}\,(p_1)_{A_1A_2}\,(p_2)^{A_2A_3}\,\cdots(p_{2n})^{A_{2n}A_{2n+1}}\,(\tilde{\lambda}_j)_{A_{2n+1}\dot{b}}\,.
\end{aligned} \tag{1.8}$$

There are four polarization states for vector particles. Following Cheung and O'Connell, the polarization vectors can be written as [33],

$$\epsilon^\mu_{a\dot{a}}(p,k) = \frac{1}{\sqrt{2}}\langle p_a|\sigma^\mu|k_b\rangle(\langle k_b|p^{\dot{a}}])^{-1} = (\langle p^a|k_{\dot{b}}])^{-1}\frac{1}{\sqrt{2}}[k_{\dot{b}}|\tilde{\sigma}^\mu|p_{\dot{a}}]\,, \tag{1.9}$$

where the a and $\dot{a}$ indices are labels for the four polarization states. As for the four-dimensional case, a null reference momentum k is needed to define the states. For each of the Weyl spinors $[i^{\dot{a}}|$ and $\langle j_a|$ the indices a and $\dot{a}$ label two helicity states respectively. The object $(\langle p^a|k_{\dot{b}}])^{-1} = -(\langle p_a|k^{\dot{b}}])/2p\cdot k$ is the inverse matrix of the spinor product $\langle p^a|k_{\dot{b}}]$ with respect to the helicity indices. As for the four-dimensional case, the polarization vectors are transverse, and a redefinition of the reference spinor can be shown to correspond to a gauge transformation.

In light of the proliferation of indices, we make a brief list:

$$\begin{aligned}
\text{SU}^*(4)\text{ fundamental labels:} &\qquad A, B, C, \ldots = 1, 2, 3, 4 \\
\text{SO(5,1) vector labels:} &\qquad \mu, \nu, \rho, \ldots = 0, 1, 2, \ldots 5 \\
\text{SU(2)}\times\text{SU(2) helicity labels:} &\qquad a, b, c, \ldots = 1, 2 \quad \text{and} \quad \dot{a}, \dot{b}, \dot{c}, \ldots = 1, 2\,.
\end{aligned} \tag{1.10}$$

1.3 Six-Dimensional $\mathcal{N} = (1,1)$ Superspace

Recent constructions of the S-matrix for maximal gauge and gravity theories make use of four-dimensional superspace. Here we construct the six-dimensional $\mathcal{N} = (1,1)$ on-shell superspace in similar fashion, i.e. by introducing Grassmann variables η_a^I, where I is the R index and a is the little group index, one can arrive at the usual superspace by contracting the little group indices with the spinors. In four dimensions, $I = 1,2,3,4$ and the little group is U(1), under which the Grassmann variables transform as $\eta^I \to e^{-i\theta}\eta^I, \bar{\eta}_I \to e^{i\theta}\bar{\eta}_I$. The relation to the usual superspace can be seen with the help of the spinors

$$4\,D: \quad \theta^{I\alpha} = \lambda^\alpha \eta^I, \quad \bar{\theta}_{J\dot{\alpha}} = \tilde{\lambda}_{\dot{\alpha}} \bar{\eta}_J.$$

One can do similar for six dimensions. Maximal super Yang-Mills in six dimensions has $\mathcal{N} = (1,1)$ supersymmetry, with R-symmetry group USp(2)×USp(2)=SU(2)×SU(2). We introduce η^{aI} and $\tilde{\eta}_{\dot{a}I'}$ where the I, I' are the $\mathrm{SU}(2)_R$ symmetry indices. Note that η and $\tilde{\eta}$ are complex and independent. The full six-dimensional superspace variables are then

$$6\,D: \quad q^{AI} = \lambda_a^A \eta^{aI}, \quad \tilde{q}_{AI'} = \tilde{\lambda}_{A\dot{a}} \tilde{\eta}^{\dot{a}}_{I'}.$$

In four-dimensional maximal super Yang-Mills theory, one can express the full amplitude using either chiral or anti-chiral superspace, i.e. only half of the full superspace, since this is enough to contain all physical degrees of freedom. This is due to the self-CPT conjugate nature of the physical spectrum. A similar result holds in six dimensions. However since the supertwistors are self-conjugate, only half of the degrees of freedom for η^{aI} and $\tilde{\eta}_{\dot{a}I'}$ are independent. Therefore to construct our on-shell superspace we need to truncate the $\eta, \tilde{\eta}$s. Since we wish to use the little group index to label our states, we will truncate using the R-indices.

Note that this situation is equivalent to the issue of trying to construct off-shell $\mathcal{N} > 1$ superspace, where chiral constraints usually lead to field equations. One of the well known

examples is the $\mathcal{N} = 2$ harmonic superspace [34] in four dimensions. Here one introduces harmonic variables $u_I^{\pm}$ to parameterize the SU(2)/U(1) coset. These variables are then used to separate the θ variables into two separate sets ($\theta_\alpha^+ = u_I^+ \theta_\alpha^I$, $\bar{\theta}_{\dot{\alpha}}^+ = u^{+I}\bar{\theta}_{I\dot{\alpha}}$) and $+ \to -$. Then the prepotential, which contains the physical gauge field, depends only on a subspace (the "analytic superspace") which only includes $\theta^+, \bar{\theta}^+$. The harmonic variables can be viewed as providing a linear combination of the R-symmetry index, and therefore separating the supercharges into subsets.[1]

Therefore, in our on-shell superspace formalism, the on-shell superfield appears as a polynomial in a pair of anticommuting coordinates $\eta_a, \tilde{\eta}^{\dot{a}}$ which carry SU(2)×SU(2) little group indices,

$$\begin{aligned}\Phi(\eta,\tilde{\eta}) &= \phi + \chi^a \eta_a + \phi'(\eta)^2 + \tilde{\chi}_{\dot{a}}\tilde{\eta}^{\dot{a}} + g^a{}_{\dot{a}}\eta_a\tilde{\eta}^{\dot{a}} + \tilde{\psi}_{\dot{a}}(\eta)^2\tilde{\eta}^{\dot{a}} \\ &\quad + \phi''(\tilde{\eta})^2 + \psi^a\eta_a(\tilde{\eta})^2 + \phi'''(\eta)^2(\tilde{\eta})^2\,, \end{aligned} \tag{1.11}$$

where $(\eta)^2 \equiv \frac{1}{2}\epsilon^{ab}\eta_b\eta_a$ and $(\tilde{\eta})^2 \equiv \frac{1}{2}\epsilon_{\dot{a}\dot{b}}\tilde{\eta}^{\dot{b}}\tilde{\eta}^{\dot{a}}$. Using these fields, we can obtain superamplitudes in the usual way. The different component amplitudes can be read off from their η expansions. For example, the four-gluon amplitude $\langle g^a{}_{\dot{a}}(1)\, g^b{}_{\dot{b}}(2)\, g^c{}_{\dot{c}}(3)\, g^d{}_{\dot{d}}(4)\rangle$ appears as the coefficient of $\eta_{1a}\tilde{\eta}_1^{\dot{a}}\eta_{2b}\tilde{\eta}_2^{\dot{b}}\eta_{3c}\tilde{\eta}_3^{\dot{c}}\eta_{4d}\tilde{\eta}_4^{\dot{d}}$ in the four-point superamplitude $\mathcal{A}_4$. These amplitudes are functions of momenta p_i and supermomenta $q_i, \tilde{q}_i$ defined by,

$$q_i^A = \lambda_i^{Aa}\eta_{ia}, \qquad \tilde{q}_{iB} = \tilde{\lambda}_{iB\dot{b}}\tilde{\eta}_i^{\dot{b}}\,. \tag{1.12}$$

For a general discussion of higher-dimensional on-shell superspaces, see ref. [36].

[1] Of course these new bosonic R-coordinates also provide the infinite auxiliary fields that are necessary to close the susy algebra off-shell. Different choices (or a subset) of these coordinates represent different off-shell formulations, for example there is also the N=2 projective superspace [35].

1.4 3-Point Kinematics

While amplitudes are generically written in terms of Lorentz invariants, the 3-point amplitude has the problem of vanishing Lorentz invariants due to kinematic constraints: $p_i \cdot p_j = 0$. In four dimensions this is solved by using complex momenta or going to split signature with real momenta, then λ and $\tilde{\lambda}$ are no longer related and one can set either $\langle ij \rangle$ or $[ij]$ to zero without constraining the other. Since we intend to use on-shell recursion as a systematic way of generating higher point amplitudes from three-point amplitudes, we must do something similar in six dimensions. In this case, the Lorentz-invariant inner product of a fundamental and an anti-fundamental spinor has vanishing determinant, i.e. the 2×2 matrix $\langle i_a | j_{\dot{a}}]$ has rank one, which means we can factorize it into a bispinor as $\langle i_a | j_{\dot{a}}] = u_{ia} \tilde{u}_{j\dot{a}}$. Consistently defining the SU(2) spinors u_i and $\tilde{u}_j$ for all of the spinor products $\langle i_a | j_{\dot{a}}]$, we have (for $\{i, j\}$ cyclically ordered),

$$\langle i_a | j_{\dot{a}}] = u_{ia} \tilde{u}_{j\dot{a}} \,, \qquad\qquad \langle j_a | i_{\dot{a}}] = -u_{ja} \tilde{u}_{i\dot{a}} \,. \tag{1.13}$$

Momentum conservation implies the following important and useful property:

$$u_1^c \langle 1_c | = u_2^c \langle 2_c | = u_3^c \langle 3_c | \,, \qquad\qquad \tilde{u}_{1\dot{c}} [1^{\dot{c}}| = \tilde{u}_{2\dot{c}} [2^{\dot{c}}| = \tilde{u}_{3\dot{c}} [3^{\dot{c}}| \,. \tag{1.14}$$

In Ref. [33], Cheung and O'Connell also introduce pseudoinverses w and $\tilde{w}$ of these spinors, which are ultimately the key to writing down the three-point amplitude. These pseudoinverses are defined by

$$u_a w_b - u_b w_a = \epsilon_{ab} \,, \qquad\qquad \tilde{u}_{\dot{a}} \tilde{w}_{\dot{b}} - \tilde{u}_{\dot{b}} \tilde{w}_{\dot{a}} = \epsilon_{\dot{a}\dot{b}} \,. \tag{1.15}$$

Being pseudoinverses, w and $\tilde{w}$ are not uniquely specified by this definition. Specifically, w_{ja} is only defined up to a shift $w_{ja} \to w_{ja} + b_j u_{ja}$ (and likewise for $\tilde{w}$). This ambiguity can be

partially removed by requiring

$$w_1^a \lambda_{1a}^A + w_2^a \lambda_{2a}^A + w_3^a \lambda_{3a}^A = 0\,, \qquad\qquad \tilde{w}_{1\dot{a}} \tilde{\lambda}_{1A}^{\dot{a}} + \tilde{w}_{2\dot{a}} \tilde{\lambda}_{2A}^{\dot{a}} + \tilde{w}_{3\dot{a}} \tilde{\lambda}_{3A}^{\dot{a}} = 0\,. \quad (1.16)$$

Then w_i^a are defined up to shifts with $b_1 + b_2 + b_3 = 0$. Even though there is still ambiguity, this will help us determine the full amplitude by requiring invariance under this shift.

The 3-pt Yang-Mills amplitude is given by

$$A_3 = i\Gamma_{abc}\tilde{\Gamma}_{\dot{a}\dot{b}\dot{c}} = i(u_1 u_2 w_3 + u_1 w_2 u_3 + w_1 u_2 u_3)_{abc}(\tilde{u}_1 \tilde{u}_2 \tilde{w}_3 + \tilde{u}_1 \tilde{w}_2 \tilde{u}_3 + \tilde{w}_1 \tilde{u}_2 \tilde{u}_3)_{\dot{a}\dot{b}\dot{c}}. \quad (1.17)$$

This was presented in Ref. [33], and can be derived for example from Feynman diagrams and the spinor definitions presented in this chapter.

The supersymmetrization of this amplitude is given by

$$\mathcal{A}_3^{\text{tree}}(1,2,3) \;=\; -i\big(\mathbf{u_1 u_2} + \mathbf{u_2 u_3} + \mathbf{u_3 u_1}\big)\left(\sum_{\mathbf{i=1}}^{\mathbf{3}} \mathbf{w_i}\right)\big(\tilde{\mathbf{u}}_\mathbf{1}\tilde{\mathbf{u}}_\mathbf{2} + \tilde{\mathbf{u}}_\mathbf{2}\tilde{\mathbf{u}}_\mathbf{3} + \tilde{\mathbf{u}}_\mathbf{3}\tilde{\mathbf{u}}_\mathbf{1}\big)\left(\sum_{\mathbf{i=1}}^{\mathbf{3}} \tilde{\mathbf{w}}_\mathbf{i}\right), \quad (1.18)$$

where $\mathbf{u_i}$ and $\mathbf{w_i}$ are defined in terms of u_i^a and w_i^a as,

$$\mathbf{u_i} = \mathbf{u_i^a}\eta_{\mathbf{ia}}, \quad \tilde{\mathbf{u}}_\mathbf{i} = \tilde{\mathbf{u}}_{\mathbf{i\dot{a}}}\tilde{\eta}_\mathbf{i}^{\dot{\mathbf{a}}}, \quad \mathbf{w_i} = \mathbf{w_i^a}\eta_{\mathbf{ia}}, \quad \tilde{\mathbf{w}}_\mathbf{i} = \tilde{\mathbf{w}}_{\mathbf{i\dot{a}}}\tilde{\eta}_\mathbf{i}^{\dot{\mathbf{a}}}\,. \quad (1.19)$$

One can confirm that this expression is correct by picking out particular component amplitudes. For example, the coefficient of $\eta_1^a \eta_2^b \eta_3^c \tilde{\eta}_1^{\dot{a}}\ \tilde{\eta}_2^{\dot{b}} \tilde{\eta}_3^{\dot{c}}$ reproduces eq. (1.17). Similarly, the coefficient of $\eta_2^a \eta_{2a} \eta_1^c \tilde{\eta}_1^{\dot{a}} \tilde{\eta}_2^{\dot{b}} \tilde{\eta}_3^{\dot{c}}$ gives

$$iu_{1c}(\tilde{u}_{1\dot{a}} \tilde{u}_{2\dot{b}} \tilde{w}_{3\dot{c}} + \tilde{u}_{1\dot{a}} \tilde{w}_{2\dot{b}} \tilde{u}_{3\dot{c}} + \tilde{w}_{1\dot{a}} \tilde{u}_{2\dot{b}} \tilde{u}_{3\dot{c}}),$$

which is the amplitude for two gauginos and one gauge boson $(g_1, \tilde{\lambda}_2, \tilde{\lambda}_3)$.

1.5 Recursive Construction of Tree-level Amplitudes

We now turn to BCFW on-shell recursion relations [37], which offer a means for constructing tree amplitudes in a form where we can exploit the six-dimensional helicity techniques. It also provides a convenient means for generating tree amplitudes needed in higher-loop calculations.

1.5.1 BCFW recursion

The BCFW shift using six-dimensional spinor helicity was given in ref. [33], and the supersymmetric version in [1]. Here we give a brief summary and the relevant bosonic shifts. We begin by picking two external lines, say $1, 2$ as special, and deform them by a null vector proportional to a complex parameter z,

$$p_1(z) = p_1 + zr, \qquad p_2(z) = p_2 - zr\,, \tag{1.20}$$

where r is a null vector satisfying $p_1 \cdot r = p_2 \cdot r = 0$. These conditions ensure that the deformed momenta remain on-shell, $p_1^2(z) = p_2^2(z) = 0$, and the overall momentum conservation of the amplitude is unaltered.

Since a tree amplitude is a rational function of momenta with no more than a single pole in any given kinematic invariant, this deformation will result in a complex function with only simple poles in z. Each pole in z will correspond to a propagator that is a sum of a subset of external momenta that includes only one of the shifted momenta,

$$P_{2j}(z)^2 \equiv (p_2(z) + \ldots + p_j)^2 = P_{2j}^2 + 2zr \cdot P_{2j}\,. \tag{1.21}$$

The location of the pole is given by solving the on-shell condition $P_{2j}(z)^2 = 0$,

$$z_{2j} = -\frac{P_{2j}^2}{2r \cdot P_{2j}}\,. \tag{1.22}$$

As in common usage, we denote the shifted momenta evaluated at the value of z locating a

pole with a hatted symbol " ˆ ", e.g. $\hat{p}_2 \equiv p_2(z = z_{2j})$.

If a shifted amplitude vanishes as $z \to \infty$, then standard complex variable theory implies that it is uniquely determined by its residues in z. For $D \geq 4$ dimensions, it is straightforward to find choices of shifts where this property holds for Yang-Mills theories [38, 33]. The poles correspond to configurations where propagators go on shell and where the amplitude factorizes into a product of lower-point amplitudes. Each residue is then simply a sum of products of two lower-point tree amplitudes on either side of the propagator, with the shifted momenta evaluated at the location of the pole. If legs 1 and 2 are shifted, the BCFW recursion relation gives us the unshifted amplitude as,

$$A_n^{\text{tree}}(0) = \sum_{j=3}^{n-1} \sum_h A_L\left(\hat{p}_2, \ldots, p_j, -\hat{P}_{2j}^{(-h)}\right) \frac{i}{P_{2j}^2} A_R\left(\hat{P}_{2j}^{(h)}, p_{j+1}, \ldots, \hat{p}_1\right)\Big|_{z=z_{2j}}, \tag{1.23}$$

where A_L and A_R are lower-point tree amplitudes on the left and right sides of the propagator and are evaluated at shifted momenta with $z = z_{2j}$. The first sum in the above equation is over all diagrams that produce poles, while the second is over all helicity states that cross the internal leg $\hat{P}$.

In six dimensions, the conditions $p_1 \cdot r = p_2 \cdot r = 0$ can be solved by choosing r to be proportional to the polarization of line 1, $r \sim \epsilon_{1a\dot{a}}$, and choosing the reference spinor for the polarization vector to be λ_2. This satisfies the needed constraints and leads to sufficiently good behavior at large z. Since $\epsilon_{1a\dot{a}}$ has extra SU(2)×SU(2) little-group indices, one introduces an auxiliary matrix $X^{a\dot{a}}$ to contract the indices so that,

$$r^{AB} = \frac{1}{\sqrt{2}} X^{a\dot{a}} (\epsilon_1^{AB})_{a\dot{a}} = -X^{a\dot{a}} \frac{\lambda_{1a}^{[A} \lambda_{2b}^{B]}}{[1^{\dot{a}}|2_b\rangle} = X^{a\dot{a}} \frac{{}^{[A}\not{p}_2 |1_{\dot{a}}] \langle 1_a|^{B]}}{s_{12}}, \tag{1.24}$$

and the condition $r^2 = 0$ now becomes $\det X = 0$. This can automatically be satisfied by choosing $X_{a\dot{a}} = x_a \tilde{x}_{\dot{a}}$, where the x_a and $\tilde{x}_{\dot{a}}$ are arbitrary. These arbitrary variables will cancel out once one sums over all contributions. When implementing the recursion relations numerically, these variables are helpful since they can identify errors when one checks whether the result is independent of the choice of x_a, $\tilde{x}_{\dot{a}}$. The above shift can be translated into a

redefinition of the spinors,

$$\begin{aligned}
\lambda_1^{Aa}(z) &= \lambda_1^{Aa} - \frac{z}{s_{12}} X^a{}_{\dot{a}} [1^{\dot{a}}|2^b\rangle \lambda_{2b}^A \,, \qquad & \lambda_2^{Ab}(z) = \lambda_2^{Ab} - \frac{z}{s_{12}} X^a{}_{\dot{a}} \lambda_{1a}^A [1^{\dot{a}}|2^b\rangle \,, \\
\tilde{\lambda}_{1A\dot{a}}(z) &= \tilde{\lambda}_{1A\dot{a}} + \frac{z}{s_{12}} X^a{}_{\dot{a}} \langle 1_a|2_{\dot{b}}] \tilde{\lambda}_{2A}^{\dot{b}} \,, \qquad & \tilde{\lambda}_{2A\dot{b}}(z) = \tilde{\lambda}_{2A\dot{b}} + \frac{z}{s_{12}} X^a{}_{\dot{a}} \tilde{\lambda}_{1A}^{\dot{a}} \langle 1_a|2_{\dot{b}}] \,. \qquad (1.25)
\end{aligned}$$

In section 1.5.2, we will describe the supersymmetrized BCFW recursion relations to generate the tree amplitudes needed in calculations of multiloop amplitudes of $\mathcal{N} = 4$ sYM theory.

1.5.2 Supersymmetric BCFW recursion

In order to investigate high loop orders we need high-point tree amplitudes. To obtain these, we use supersymmetric forms of the BCFW recursion relations. This also serves as a warmup for the unitarity cuts, because the state sums generated by integration over Grassmann parameters at loop level are similar to the state sums in supersymmetric forms of the BCFW recursion relations. As discussed in ref. [1], the super-BCFW recursion relations can be obtained by shifting the Grassmann variables,

$$\begin{aligned}
\eta_{1a}(z) &= \eta_{1a} - z X_{a\dot{a}} [1^{\dot{a}}|2^b\rangle \eta_{2b}/s_{12} \,, \qquad & \eta_{2b}(z) = \eta_{2b} - z X^a{}_{\dot{a}} [1^{\dot{a}}|2_b\rangle \eta_{1a}/s_{12} \,, \\
\tilde{\eta}_1^{\dot{a}}(z) &= \tilde{\eta}_1^{\dot{a}} + z X^{a\dot{a}} [2_{\dot{b}}|1_a\rangle \tilde{\eta}_2^{\dot{b}}/s_{12} \,, \qquad & \tilde{\eta}_2^{\dot{b}}(z) = \tilde{\eta}_2^{\dot{b}} + z X^a{}_{\dot{a}} [2^{\dot{b}}|1_a\rangle \tilde{\eta}_1^{\dot{a}}/s_{12} \,, \qquad (1.26)
\end{aligned}$$

in addition to the shifts of the spinors in eq. (1.25). This is designed to maintain supermomentum conservation, i.e. $q_1^A + q_2^A = q_{\hat{1}}^A + q_{\hat{2}}^A$ and $\tilde{q}_{1A} + \tilde{q}_{2A} = \tilde{q}_{\hat{1}A} + \tilde{q}_{\hat{2}A}$. These shifts on η can be rephrased as shifts directly on the supermomenta by combining with the spinorial shifts in eq. (1.25) and using the trick,

$$\delta^a{}_b = -\frac{1}{s_{12}} \langle 1^a|\not{p}_2|1_b\rangle \,. \qquad (1.27)$$

After the necessary rearrangements, we have,

$$\begin{aligned}
q_1^A(z) &= q_1^A + \frac{z}{s_{12}^2} X^a{}_{\dot{a}} [1^{\dot{a}}|2^b\rangle \lambda_{2b}^A \langle 1_a|2_{\dot{b}}] \tilde{\lambda}_{2B}^{\dot{b}} q_1^B - \frac{z}{s_{12}} \lambda_1^{Aa} X_{a\dot{a}} \tilde{\lambda}_{1B}^{\dot{a}} q_2^B \,, \\
q_2^A(z) &= q_2^A - \frac{z}{s_{12}} \lambda_{1a}^A X^a{}_{\dot{a}} \tilde{\lambda}_{1B}^{\dot{a}} q_2^B - \frac{z}{s_{12}^2} X^a{}_{\dot{a}} [1^{\dot{a}}|2_b\rangle \lambda_2^{Ab} \langle 1_a|2_{\dot{b}}] \tilde{\lambda}_{2B}^{\dot{b}} q_1^B \,, \\
\tilde{q}_{1A}(z) &= \tilde{q}_{1A} + \frac{z}{s_{12}^2} X^a{}_{\dot{a}} \langle 1_a|2_{\dot{b}}] \tilde{\lambda}_{2A}^{\dot{b}} [1^{\dot{a}}|2^b\rangle \lambda_{2b}^B \tilde{q}_{1B} + \frac{z}{s_{12}} \tilde{\lambda}_{1A\dot{a}} X^{a\dot{a}} \lambda_{1a}^B \tilde{q}_{2B} \,, \\
\tilde{q}_{2A}(z) &= \tilde{q}_{2A} + \frac{z}{s_{12}} X^a{}_{\dot{a}} \tilde{\lambda}_{1A}^{\dot{a}} \lambda_{1a}^B \tilde{q}_{2B} + \frac{z}{s_{12}^2} X^a{}_{\dot{a}} \tilde{\lambda}_{2A\dot{b}} [2^{\dot{b}}|1_a\rangle [1^{\dot{a}}|2^b\rangle \lambda_{2b}^B \tilde{q}_{1B} \,. \qquad (1.28)
\end{aligned}$$

As we will see, these supermomentum shifts help us avoid dealing directly with the supercoordinates η in the recursion.

The intermediate state sum in the recursion is realized as an integration over the Grassmann coordinates $\eta_P, \tilde{\eta}_P$ of the intermediate leg (labeled as P), and the remainder of this section is devoted to systematically carrying out these integrations.

To set up high-point recursion, it is useful to first organize the types of contributions. If we track the factors containing Grassmann parameters, and drop other factors, the n-point tree amplitudes have the schematic form,

$$\mathcal{A}_n \;\sim\; \delta^4\Big(\sum\nolimits_i q_i^A\Big)\delta^4\Big(\sum\nolimits_i \tilde{q}_{iB}\Big) q^{n-4}\tilde{q}^{n-4} \quad \text{for } n \geq 4 \,, \qquad (1.29)$$

where the fermionic delta function is defined as,

$$\delta^4\Big(\sum\nolimits_i q_i^A\Big) \equiv \frac{1}{4!}\,\epsilon_{BCDE}\Big(\sum\nolimits_i q_i^B\Big)\Big(\sum\nolimits_i q_i^C\Big)\Big(\sum\nolimits_i q_i^D\Big)\Big(\sum\nolimits_i q_i^E\Big) \,, \qquad (1.30)$$

and likewise for the antichiral supermomentum $\tilde{q}_A$. We have left an unbalanced index A as a reminder that the delta function is over the four SU*(4) components. The supermomentum delta functions for $n \geq 4$ impose algebraic constraints on $\eta_P, \tilde{\eta}_P$ under the fermionic integration. We can follow the same strategy as used in four dimensions to consider the delta-function constraints as a set of algebraic equations to be systematically solved [39]. A

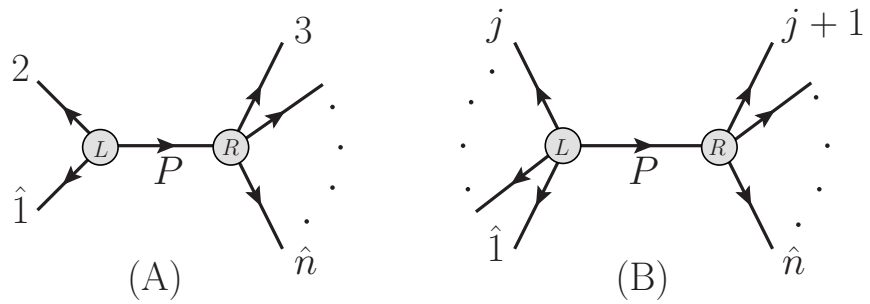

Figure 1.1: Two categories of BCFW diagrams. (A) contains a three-point subamplitude, which does not have the full supermomentum delta function $\delta^4(q)\delta^4(\tilde{q})$. (B) contains no three-point subamplitude, thus all delta functions are of degree four.

key identity for carrying this out is

$$\delta^4(q_1^A + q_2^A + Q^A) \;=\; s_{12}\,\delta^2\Big(\eta_{1a} + s_{12}^{-1}\langle 1_a|\not{p}_2 Q\Big)\delta^2\Big(\eta_{2b} + s_{12}^{-1}\langle 2_b|\not{p}_1 Q\Big)\,. \tag{1.31}$$

A similar antichiral identity also holds. These identities are analogous to ones used in four dimensions [9].

Before proceeding, though, we are obliged to address a glitch in the spinor-helicity formalism: the spinors do not properly distinguish between particles and antiparticles, causing phase inconsistencies in diagrams containing fermions. This glitch and prescriptions for resolving it have already been discussed in the four-dimensional case, for example, in ref. [40, 39]. Here we use the prescription that if p is incoming, so that this momentum is $-p$ in our all-outgoing convention, then we take,

$$\lambda_{(-p)}^{Aa} \equiv i\lambda_p^{Aa}, \qquad \tilde{\lambda}_{(-p)A\dot{a}} \equiv i\tilde{\lambda}_{pA\dot{a}}\,. \tag{1.32}$$

In this way, we maintain the relationship between momenta and spinors, i.e.,

$$(-p)^{AB} = \lambda_{(-p)}^{Aa}\lambda_{(-p)a}^{B} = -\lambda_p^{Aa}\lambda_{pa}^{B}\,. \tag{1.33}$$

Along the same lines, we demand that $q_{(-p)}^A = -q_p^A$, which we achieve with the same pre-

scription for the supercoordinates η: whenever $-p$ is outgoing, we choose,

$$\eta_{(-p)a} \equiv i\eta_{pa}, \qquad \tilde{\eta}^{\dot{a}}_{(-p)} \equiv i\tilde{\eta}^{\dot{a}}_{p}. \tag{1.34}$$

Beyond four points, we can split all BCFW diagrams into two categories, as shown in Fig. 1.1. We consider these two cases in turn.

Case (A):

In cases where one has to sew a three-point superamplitude to a higher-point tree superamplitude, illustrated in Fig. 1.1(A), the Grassmann integration has the form,

$$\int d^2\eta_P d^2\tilde{\eta}_P \; \mathcal{A}_{3L} \times \delta^4\Big(\sum_{i\in R} q_i^B\Big)\delta^4\Big(\sum_{i\in R}\tilde{q}_{iC}\Big) q^{n-5}\tilde{q}^{n-5}\,, \tag{1.35}$$

where the summations are over all external lines of the right tree amplitude including shifted legs, and the integration measure is $d^2\eta_P d^2\tilde{\eta}_P = \frac{1}{4} d\eta_P^a d\eta_{Pa} d\tilde{\eta}_{P\dot{a}} d\tilde{\eta}_P^{\dot{a}}$.

To perform this integral, we view the factors in the three-point amplitude (1.18) as algebraic constraints on the supercoordinates $\eta_P, \tilde{\eta}_P$ imposing,

$$\begin{aligned}
&\mathbf{u_{\hat{1}}} = \mathbf{u_2}\,, \qquad \mathbf{u_P} = \tfrac{\mathbf{1}}{\mathbf{2}}(\mathbf{u_{\hat{1}}} + \mathbf{u_2}), \qquad \mathbf{w_P} = -\mathbf{w_{\hat{1}}} - \mathbf{w_2},\\
&\tilde{\mathbf{u}}_{\hat{\mathbf{1}}} = \tilde{\mathbf{u}}_{\mathbf{2}}\,, \qquad \tilde{\mathbf{u}}_{\mathbf{P}} = \tfrac{\mathbf{1}}{\mathbf{2}}(\tilde{\mathbf{u}}_{\hat{\mathbf{1}}} + \tilde{\mathbf{u}}_{\mathbf{2}}), \qquad \tilde{\mathbf{w}}_{\mathbf{P}} = -\tilde{\mathbf{w}}_{\hat{\mathbf{1}}} - \tilde{\mathbf{w}}_{\mathbf{2}}\,.
\end{aligned} \tag{1.36}$$

Since there are two components each in η_{Pa} and $\tilde{\eta}_P^{\dot{a}}$, the three-point amplitude is sufficient to localize the η_P integrals. The solutions to the constraint equations are

$$\begin{aligned}
\eta_{Pa} &= \tfrac{1}{2} w_{Pa}(\mathbf{u_{\hat{1}}} + \mathbf{u_2}) + \mathbf{u_{Pa}}(\mathbf{w_{\hat{1}}} + \mathbf{w_2})\,,\\
\tilde{\eta}_P^{\dot{a}} &= -\tfrac{1}{2}\tilde{w}_P^{\dot{a}}(\tilde{\mathbf{u}}_{\hat{\mathbf{1}}} + \tilde{\mathbf{u}}_{\mathbf{2}}) - \tilde{\mathbf{u}}_{\mathbf{P}}^{\dot{\mathbf{a}}}(\tilde{\mathbf{w}}_{\hat{\mathbf{1}}} + \tilde{\mathbf{w}}_{\mathbf{2}})\,,
\end{aligned} \tag{1.37}$$

with the understanding that we are free to replace $\mathbf{u_{\hat{1}}} \leftrightarrow \mathbf{u_2}$ and $\tilde{\mathbf{u}}_{\hat{\mathbf{1}}} \leftrightarrow \tilde{\mathbf{u}}_{\mathbf{2}}$ at any step, due to the leftover factors of $(\mathbf{u_{\hat{1}}} - \mathbf{u_2})$ and $(\tilde{\mathbf{u}}_{\hat{\mathbf{1}}} - \tilde{\mathbf{u}}_{\mathbf{2}})$.

In practice, it is much easier to deal with supermomenta q_i than the u and w variables. It is straightforward to demonstrate that eq. (1.37) implies the substitutions,

$$q_P^A = -q_{\hat{1}}^A - q_2^A\,, \qquad\qquad \tilde{q}_{PA} = -\tilde{q}_{\hat{1}A} - \tilde{q}_{2A}\,. \tag{1.38}$$

Thus one can substitute the result for q_P in the tree amplitude on the right, avoiding the more complicated eq. (1.37), and extract out the full supermomentum-conservation delta function. At this stage, we are left with the task of integrating,

$$\delta^4\Big(\sum_{i\in\mathcal{E}} q_i^A\Big)\delta^4\Big(\sum_{i\in\mathcal{E}} \tilde{q}_{iB}\Big) q^{n-5}\tilde{q}^{n-5}\int d^2\eta_P d^2\tilde{\eta}_P \mathcal{A}_{3L}\,, \tag{1.39}$$

where the two delta functions correspond to the overall supermomentum conservation, and $\mathcal{E}$ is the set of all external legs of the full amplitude. The remaining integral has the solution,

$$\int d^2\eta_P d^2\tilde{\eta}_P \mathcal{A}_{3L} = i(\mathbf{u_{\hat{1}}} - \mathbf{u_2})(\tilde{\mathbf{u}}_{\hat{\mathbf{1}}} - \tilde{\mathbf{u}}_{\mathbf{2}})\,, \tag{1.40}$$

which can be re-written in terms of the $q, \tilde{q}$ as,

$$i\bigg(-\frac{q_{\hat{1}}\not{p}_K\not{p}_2\tilde{q}_{\hat{1}}}{s_{\hat{1}K}} - q_{\hat{1}}\tilde{q}_2 + q_2\tilde{q}_{\hat{1}} + \frac{q_2\not{p}_K\not{p}_{\hat{1}}\tilde{q}_2}{s_{2K}}\bigg)\,, \tag{1.41}$$

where p_K is an arbitrary null reference vector. The sewing of a three-point amplitude with a general tree amplitude will thus result in the form,

$$\delta^4\Big(\sum_{i\in\mathcal{E}} q_i^A\Big)\delta^4\Big(\sum_{i\in\mathcal{E}} \tilde{q}_{iB}\Big) q^{n-5}\tilde{q}^{n-5}\bigg(-\frac{q_{\hat{1}}\not{p}_K\not{p}_2\tilde{q}_{\hat{1}}}{s_{\hat{1}K}} - q_{\hat{1}}\tilde{q}_2 + q_2\tilde{q}_{\hat{1}} + \frac{q_2\not{p}_K\not{p}_{\hat{1}}\tilde{q}_2}{s_{2K}}\bigg)\,, \tag{1.42}$$

where all $q, \tilde{q}$s are in terms of external lines and $q_{\hat{1}}$ is the shifted q_1 with z taking on the value at the pole.

Case (B):

For the case with no three-point subamplitudes, illustrated in Fig. 1.1(B), we can always

eliminate q_P and $\tilde{q}_P$ from the "R" amplitude, using the "L" delta functions. The Grassmann integral will then be of the form,

$$\delta^4\Big(\sum_{i\in\mathcal{E}} q_i^A\Big)\delta^4\Big(\sum_{i\in\mathcal{E}} \tilde{q}_{iB}\Big) f(q,\tilde{q}) \int d^2\eta_P d^2\tilde{\eta}_P\, \delta^4\Big(\sum_{i\in L} q_i^C\Big)\delta^4\Big(\sum_{i\in L} \tilde{q}_{iD}\Big)\,. \tag{1.43}$$

Focusing on the chiral integral, we proceed by splitting the delta function using eq. (1.31) on legs j and P, which gives,

$$\begin{aligned}
\int d^2\eta_P \delta^4\Big(\sum_{i\in L} q_i^C\Big) &= s_{jP}\,\delta^2\Big(\eta_{ja} + s_{jP}^{-1}\langle j_a|\not{P}(q_{\hat{1}}+\ldots+q_{j-1})\Big) \\
&= s_{jP}\,\delta^2\Big(s_{jP}^{-1}\langle j_a|\not{P}(q_{\hat{1}}+\ldots+q_j)\Big) \\
&= -s_{jP}^{-1}(q_{\hat{1}}+\ldots+q_j)\not{P}\not{p}_j\not{P}(q_{\hat{1}}+\ldots+q_j) \\
&= (q_{\hat{1}}+\ldots+q_j)^A(p_{\hat{1}}+\ldots+p_j)_{AB}(q_{\hat{1}}+\ldots+q_j)^B\,,
\end{aligned} \tag{1.44}$$

where $P = p_{\hat{1}} + p_2 + \cdots + p_j$, and we used the identity (1.27) between the first and second lines. Likewise, the antichiral integration contributes,

$$\int d^2\tilde{\eta}_P \delta^4\Big(\sum_{i\in L} \tilde{q}_{iD}\Big) = (\tilde{q}_{\hat{1}}+\ldots+\tilde{q}_j)_A(p_{\hat{1}}+\ldots+p_j)^{AB}(\tilde{q}_{\hat{1}}+\ldots+\tilde{q}_j)_B\,. \tag{1.45}$$

1.6 Analytic Low-point Amplitudes

In ref. [1], the three-, four- and five-particle tree-level superamplitudes were worked out analytically using the BCFW recursion. The four-point superamplitude is the simplest case. This is given by

$$\mathcal{A}_4^{\text{tree}}(1,2,3,4) = -\frac{i}{s_{12}s_{23}}\,\delta^4\Big(\sum_{i=1}^4 q_i^A\Big)\delta^4\Big(\sum_{i=1}^4 \tilde{q}_{iB}\Big)\,. \tag{1.46}$$

The five-point tree-level superamplitude is

$$\begin{aligned}\mathcal{A}_5^{\text{tree}} &= i\,\frac{\delta^4\Big(\sum_i q_i^A\Big)\delta^4\Big(\sum_i \tilde{q}_{iB}\Big)}{s_{12}s_{23}s_{34}s_{45}s_{51}}\Big\{q_1^A(p_2p_3p_4p_5)_A{}^B\tilde{q}_{1B} + \text{cyclic} \\ &\quad + \frac{1}{2}\left[q_1^A\tilde{\Delta}_{2A} + q_3^A\tilde{\Delta}_{4A} + (q_3+q_4)^A\tilde{\Delta}_{5A} + (\text{chiral conjugate})\right]\Big\}\,, \qquad (1.47)\end{aligned}$$

where $\tilde{\Delta}_{2A} = (p_2p_3p_4p_5 - p_2p_5p_4p_3)_A{}^B\tilde{q}_{2B}$, $\tilde{\Delta}_{4A} = (p_4p_5p_1p_2 - p_4p_2p_1p_5)_A{}^B\tilde{q}_{4B}$, etc. The five-particle amplitude is given here in a particularly compact form which lacks explicit cyclic symmetry, although the symmetry does hold on the support of the fermionic delta functions.

In the next chapter, we will use these expressions as input into the BCFW recursion to generate higher-point amplitudes, which we use to calculate unitarity cuts of multi-loop amplitudes.

CHAPTER 2

Generalized Unitarity and Six-Dimensional Helicity

2.1 Introduction

The unitarity method [41, 42, 43, 44, 45, 46, 47, 48, 49, 50, 51, 52, 53, 54] gives a means for constructing complete loop amplitudes directly from on-shell tree amplitudes. These methods are efficient and display a relatively tame growth in complexity with increasing number of external particles or loops, especially when compared to traditional Feynman-diagrammatic approaches. With this approach, it is usually advantageous to simplify the input tree amplitudes as much as possible prior to applying them in loop calculations. A key tool for simplifying massless tree amplitudes strictly in four dimensions has been spinor helicity [55, 56]. However, if we use dimensional regularization or any form of massive regularization, massless four-dimensional spinor helicity techniques are no longer directly applicable within the loops.

In this chapter we will describe a unitarity-based approach using the six-dimensional spinor-helicity formalism of Cheung and O'Connell [33] to avoid these limitations. Here we are concerned primarily with multiloop scattering amplitudes in $\mathcal{N} = 4$ super-Yang-Mills (sYM) theory. The supersymmetric theory needs an efficient formalism to organize its spectrum of states, especially at high-loop orders, in much the same way as done in four dimensions using an on-shell superspace [57, 9, 58, 39]. As we discuss, both aspects can be addressed using the six-dimensional spinor helicity formalism described in Chapter 1.

In the past, the main bottleneck for carrying out next-to-leading-order QCD calculations has been the difficulty of evaluating one-loop amplitudes [59]. The unitarity method offers a universal solution to this difficulty that scales well with the number of external legs. Any

contributions which can be captured by four-dimensional techniques — the so called "cut-constructible pieces" — may be computed efficiently using four-dimensional helicity states in the cuts [41, 45, 49, 60]. The remaining rational contributions tend to be the most complex (and time consuming) parts of calculations, though there are a number of techniques for dealing with such pieces. In the bootstrap approach, the rational pieces are constructed by on-shell recursion in four dimensions [61, 60]. Another approach uses D-dimensional generalized unitarity [43, 44, 62, 47, 50, 53]. A six-dimensional unitarity procedure for any one-loop QCD amplitude has been given in ref. [53] using the on-shell procedure of reducing integrals in ref. [48]. A related approach makes use of the relation between massive states in four dimensions and those in extra dimensions to reduce the integrals obtained from unitarity cuts [43, 54]. The six-dimensional helicity approach described here is well suited for either of the latter two approaches for carrying out integral reductions.

We will consider multiloop $\mathcal{N} = 4$ sYM amplitudes. To set this up, we make use of the six-dimensional on-shell superspace presented in the previous chapter. General constructions of on-shell superspaces have been discussed in ref. [36]. In strictly four dimensions, there is a well-developed on-shell superspace [57, 9, 58, 39] for tracking contributions from different states in the multiplet. However, as already noted above this leaves open the question of whether contributions are missed by using four-dimensional momenta in the unitarity cuts or in the recent BCFW constructions of planar loop integrands [63, 64]. This is especially important when constructing amplitudes for use in $D > 4$ studies, but even in dimensionally regularized four-dimensional expressions, when divergences are present, there can be nonvanishing contributions from terms that vanish naively in four dimensions. This becomes more important as the loop order or the number of external legs grows, allowing for a greater number of potentially problematic terms. Besides terms with explicit dependence on extra-dimensional momenta, such terms can be formed from antisymmetric combinations of momenta which vanish in four dimensions. For example, we know that dimensionally regularized two-loop six-point amplitudes in $\mathcal{N} = 4$ sYM theory have such terms [65]. In theories with fewer supersymmetries, such terms occur with more frequency, and, for example, appear in one-loop QCD amplitudes [43].

To illustrate the supersymmetric formalism, we first describe a two-particle cut of the one-loop four-point $\mathcal{N} = 4$ amplitude, then move on to a three-particle cut of the planar two-loop four-point amplitude [66]. Finally, we turn to the rather nontrivial case of four-loop four-point amplitudes in this theory, including the nonplanar terms. The latter amplitude has recently been computed [67], using mainly four-dimensional techniques. Direct calculations of four-point gluon amplitudes in $\mathcal{N} = 1$ sYM in $D = 10$ dimensions, which upon dimensional reduction gives $\mathcal{N} = 4$ sYM theory, confirm that all terms are captured by calculating directly in four dimensions, through three loops.[1] At four loops, similar $D = 10$ checks have been performed in the planar case, up to a mild assumption that no term has a worse power count than the amplitude [68]. However, in the case of nonplanar contributions, there is no complete check that the expressions built using four-dimensional momenta in the cuts are complete, although a number of strong consistency checks have been performed [67]. In this chapter we confirm that the expressions for the amplitudes of ref. [67] are valid for $D \leq 6$, as expected.

At four points, the integrands of $\mathcal{N} = 4$ sYM do not depend explicitly on the space-time dimension, but only implicitly through Lorentz dot products, as already noted in refs. [66, 69, 70, 68, 71, 67] and explicitly confirmed here at four loops. This suggests that the dual conformal properties, which impose strong constraints on the form of the integrands in four dimensions, will impose similar constraints in higher dimensions. In addition, dual conformal invariance can be extended to the massive Higgs-regulated case [72]. These facts suggest that the dual conformal properties of planar $\mathcal{N} = 4$ sYM amplitudes should have extensions away from four dimensions. Motivated by this, in Chapter 3 we will write down generators for dual conformal transformations in six dimensions and prove transformation properties to all loop orders.

[1] This property is special to maximal supersymmetry, and we have no expectation that it should hold for other theories.

2.2 The Unitarity Method

The modern unitarity method constructs loop amplitudes directly from on-shell tree amplitudes [41], by combining unitarity cuts into complete expressions for amplitudes. The most convenient cuts generally are those that reduce the loop amplitude integrands into a sum of products of tree amplitudes,

$$A_n^{\text{loop}}\big|_{\text{cut}} = \sum_{\text{states}} A^{\text{tree}} A^{\text{tree}} \cdots A^{\text{tree}} A^{\text{tree}} \,. \tag{2.1}$$

To construct the full amplitude, we can apply a merging procedure for combining cuts [62]. For more complicated cases, it is best to build an ansatz first in terms of some arbitrary parameters. The arbitrary parameters are then determined by comparing the cuts of the ansatz against the generalized unitarity cuts (2.1). If an inconsistency is found, the ansatz is not general enough and must be enlarged. In four dimensions, a particularly simple set of cuts to evaluate is those with the maximal numbers of cut propagators [45]. Often it is convenient to build the ansatz for the amplitude by starting with generalizations of these types of maximal cuts and then systematically relaxing the cut conditions one at a time [51, 70, 67]. This approach, known as the method of maximal cuts, offers a systematic procedure for obtaining complete amplitudes, including nonplanar contributions, at any loop order in massless theories. One can carry out cut calculations either analytically or numerically comparing to a target ansatz at high precision.[2]

An important concept is "spanning cuts", or a complete set of cuts for determining an amplitude. For the color-ordered one-loop four-point amplitude a spanning set is the usual s and t channel two-particle cuts. More generally, spanning cuts are determined by requiring that all potential terms that can contribute, including contact terms, can be detected by the cuts. In section 2.3 we use such a spanning set of cuts to confirm the six-dimensional validity of the complete four-loop four-point amplitude of $\mathcal{N} = 4$ sYM theory, calculated in refs. [67, 71] using mostly four-dimensional methods.

[2]Since this procedure does not involve any integration, high precision is straightforward. One can also choose rational numbers for the kinematic points.

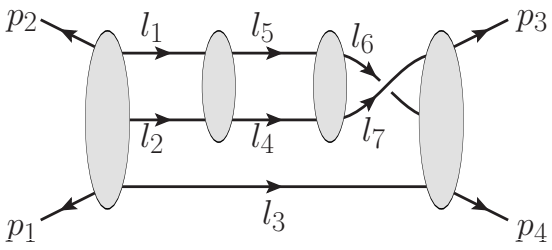

Figure 2.1: A sample cut of the four-loop four-point amplitude.

2.3 Multiloop applications with maximal supersymmetry

In this section we consider the construction of multiloop amplitudes in maximally supersymmetric Yang-Mills in six dimensions. After some general comments, we turn to one-loop and two-loop warmups before discussing four-point amplitudes at four and six loops.

2.3.1 General considerations

In unitarity cuts, one must sum over states for multiple particles. The supersum then corresponds to integrating over the $\eta, \tilde{\eta}$ coordinates of these lines. For example, when sewing the four-loop cut displayed in Fig. 2.1, the sum over states is implemented by the Grassmann integration,

$$\int \prod_{i=1}^{7} \left(d^2\eta_{l_i} d^2\tilde{\eta}_{l_i} \right) \mathcal{A}_5^{(1)} \mathcal{A}_4^{(2)} \mathcal{A}_4^{(3)} \mathcal{A}_5^{(4)} \,, \tag{2.2}$$

where the superscript $\mathcal{A}_4^{(j)}$ labels the four distinct tree amplitudes composing the cut.

The strategy for dealing with such supersums is similar to the strategy used at tree level; we use eq. (1.31) to localize as many η integrals as possible. In cuts with no three-point subamplitudes, such as the cut in Fig. 2.1, there is a supermomentum delta function on each tree amplitude. Each delta function can be used to localize two pairs of $\eta_l, \tilde{\eta}_l$ via eq. (1.31); in a cut with m tree amplitudes, a total of $2(m-1)$ pair of $\eta_l, \tilde{\eta}_l$ can be localized in this manner, with one overall $\delta^4(\sum_{\mathcal{E}} q)\delta^4(\sum_{\mathcal{E}} \tilde{q})$ extracted outside of the integral. We note that when solving the delta-function constraints, care must be taken to avoid circular solutions.

In general, the fermionic delta functions will be insufficient to localize all of the η integrals; the remaining integrals must be handled in a different manner. One approach is to expand the left-over integrand as a polynomial in $\eta_{l_i}, \tilde{\eta}_{l_i}$ and interpret the fermionic integral as instructions to pick out the coefficient of $\prod_i (\eta_{l_i})^2 (\tilde{\eta}_{l_i})^2$. We will apply this approach to a two-loop example in the next Section 2.3.3.

Cuts that have three-point subamplitudes are generally more difficult, and may need to be handled on an *ad hoc* basis. One can usually make progress by combining three-point subamplitudes into higher-point amplitudes and perform the remaining η integrals as before.

We note that for four-point loop amplitudes, after extracting out the overall supermomentum delta functions, the number of remaining $\eta, \tilde{\eta}$s will always match the number of Grassmann integrations. Therefore, the four-point loop amplitudes will depend on $\eta, \tilde{\eta}$ only through the supermomentum delta functions, i.e. they will be proportional to a four-point tree superamplitude.

To illustrate these techniques we now work out a few examples. (The cut of Fig. 2.1 is evaluated in some detail in appendix B.)

2.3.2 One-loop four-point example

Here we compute a two-particle cut of the one-loop 4-point amplitude for six-dimensional maximal super Yang-Mills. It was shown in D-dimensional maximal super Yang-Mills that the two-particle cut for the one-loop 4-point amplitude takes the following form [73]

$$\sum_{s_1,s_2} A_{\text{tree}}(k_2^{s_2}, 1, 2, -k_1^{s_1}) A_{\text{tree}}(-k_2^{s_2}, 3, 4, k_1^{s_1}) = -ist A_{\text{tree}}(1,2,3,4) \frac{1}{(p_1 - k_1)^2 (p_3 - k_2)^2}$$

where s_1, s_2 label the internal states and are summed over. We now reproduce this relation

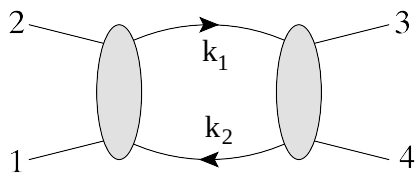

Figure 2.2: Two-particle cut for one-loop 4-point amplitude.

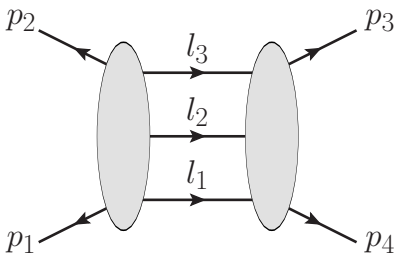

Figure 2.3: The three-particle cut of a two-loop four-point amplitude.

in six dimensions. Using superspace to sum the internal states:

$$
\begin{aligned}
& \sum_{s_1,s_2} A_{\text{tree}}(k_2^{s_2}, 1, 2, -k_1^{s_1}) A_{\text{tree}}(-k_2^{s_2}, 3, 4, k_1^{s_1}) \\
= \quad & -\int d^2\eta_{k_1} \int d^2\eta_{k_2} \int d^2\tilde{\eta}_{k_2} \int d^2\tilde{\eta}_{k_2} \frac{\delta^4(\sum_R q^A)\delta^4(\sum_R \tilde{q}_A)}{(p_1-k_1)^2 s} \frac{\delta^4(\sum_L q^B)\delta^4(\sum_L \tilde{q}_B)}{s(p_3-k_2)^2} \\
= \quad & -\int d^2\eta_{k_1} \int d^2\eta_{k_2} \int d^2\tilde{\eta}_{k_2} \int d^2\tilde{\eta}_{k_2} \frac{\delta^4(\sum_{full} q^A)\delta^4(\sum_{full} \tilde{q}_A)}{(p_1-k_1)^2 s} \frac{\delta^4(\sum_L q^B)\delta^4(\sum_L \tilde{q}_B)}{s(p_3-k_2)^2} \\
= \quad & -\frac{\delta^4(\sum_{full} q^A)\delta^4(\sum_{full} \tilde{q}_A)}{(p_1-k_1)^2 s} \frac{(k_1\cdot k_2)^2}{s(p_3-k_2)^2} = -ist A_{\text{tree}}(1,2,3,4) \frac{1}{(p_1-k_1)^2(p_3-k_2)^2}
\end{aligned}
$$

where we used $k_1 - k_2 = p_1 + p_2$.

2.3.3 Two-loop four-point example

Now we evaluate the three-particle cut illustrated in Fig. 2.3, which is more complicated than the one-loop example because it contains two five-point subamplitudes:

$$C^{\text{2-loop}} = \int \prod_{i=1}^{3} d^2\eta_{l_i} d^2\tilde{\eta}_{l_i}\, \mathcal{A}_{5L}^{\text{tree}}(p_1, p_2, l_3, l_2, l_1)\mathcal{A}_{5R}^{\text{tree}}(p_3, p_4, -l_1, -l_2, -l_3)\,. \tag{2.3}$$

We choose the following convenient representations for the five-point tree superamplitudes:

$$\begin{aligned}
\mathcal{A}_{5L}^{\text{tree}} &= i\,\frac{\delta^4(\sum_L q)\delta^4(\sum_L \tilde{q})}{s_{l_3l_2}s_{l_2l_1}s_{l_11}s_{12}s_{2l_3}}\Big\{q_{l_3}^A(l_2l_1p_1p_2)_A{}^B\tilde{q}_{l_3B} + \text{cyclic} \\
&\quad + \frac{1}{2}\left[q_{l_3}^A\tilde{\Delta}_{l_2A}^L + q_{l_1}^A\tilde{\Delta}_{1A}^L + (q_{l_1}+q_1)^A\tilde{\Delta}_{2A}^L + (\text{chiral conjugate})\right]\Big\}\,, \\
\mathcal{A}_{5R}^{\text{tree}} &= i\,\frac{\delta^4(\sum_R q)\delta^4(\sum_R \tilde{q})}{s_{l_1l_2}s_{l_2l_3}s_{l_33}s_{34}s_{4l_1}}\Big\{q_{l_1}^A(l_2l_3p_3p_4)_A{}^B\tilde{q}_{l_1B} + \text{cyclic} \\
&\quad + \frac{1}{2}\left[-q_{l_1}^A\tilde{\Delta}_{(-l_2)A}^R - q_{l_3}^A\tilde{\Delta}_{3A}^R + (q_3-q_{l_3})^A\tilde{\Delta}_{4A}^R + (\text{chiral conjugate})\right]\Big\}\,,
\end{aligned} \tag{2.4}$$

where the L, R superscript of the Δ's denote which side of the cut they are defined with respect to. For example, we have,

$$\begin{aligned}
\tilde{\Delta}_{l_2A}^L &= (l_2l_1p_1p_2 - l_2p_2p_1l_1)_A{}^B\tilde{q}_{l_2B}\,, \\
\tilde{\Delta}_{(-l_2)A}^R &= -(l_2l_3p_3p_4 - l_2p_4p_3l_3)_A{}^B\tilde{q}_{l_2B}\,.
\end{aligned} \tag{2.5}$$

As discussed previously, one can extract an overall supermomentum delta function $\delta^4(\sum_{\mathcal{E}} q)\delta^4(\sum_{\mathcal{E}} \tilde{q})$ outside of the integral, leaving behind a degree eight delta function, which can be used to localize two pairs of ηs and $\tilde{\eta}$s. Here we choose to localize η_{l_1}, η_{l_2} and their antichiral partners.

Thus the fermionic delta functions from the two tree amplitudes combine to give,

$$\begin{aligned}
&\delta^4\Big(\sum_L q\Big)\delta^4\Big(\sum_L \tilde{q}\Big)\delta^4\Big(\sum_R q\Big)\delta^4\Big(\sum_R \tilde{q}\Big) \\
&\quad = \quad \delta^4\Big(\sum_{\mathcal{E}} q\Big)\delta^4\Big(\sum_{\mathcal{E}} \tilde{q}\Big)s_{l_1l_2}^2 \\
&\qquad \times\delta^2\Big(\eta_{l_1a}+s_{l_1l_2}^{-1}\langle l_{1a}|\not{l}_2(q_{l_3}+q_1+q_2)\Big)\delta^2\Big(\eta_{l_2b}+s_{l_1l_2}^{-1}\langle l_{2b}|\not{l}_1(q_{l_3}+q_1+q_2)\Big) \\
&\qquad \times\delta^2\Big(\tilde{\eta}_{l_1}^{\dot{a}}+s_{l_1l_2}^{-1}[l_1^{\dot{a}}|\not{l}_2(\tilde{q}_{l_3}+\tilde{q}_1+\tilde{q}_2)\Big)\delta^2\Big(\tilde{\eta}_{l_2}^{\dot{b}}+s_{l_1l_2}^{-1}[l_2^{\dot{b}}|\not{l}_1(\tilde{q}_{l_3}+\tilde{q}_1+\tilde{q}_2)\Big)\,, \qquad (2.6)
\end{aligned}$$

which is a direct application of eq. (1.31). From the above, one can immediately see that the delta function localizes the $d^2\eta_{l_i}d^2\tilde{\eta}_{l_i}$ integral in eq. (2.3) for $i=1,2$.

After factoring out the fermionic delta functions in $\mathcal{A}_{5L}\mathcal{A}_{5R}$, the remaining function is of Grassmann degree four, and only terms proportional to $(\eta_{l_3})^2(\tilde{\eta}_{l_3})^2$ can saturate the remaining Grassmann integrals. Keeping in mind that $\eta_{l_1},\eta_{l_2},\tilde{\eta}_{l_1},\tilde{\eta}_{l_2}$ are localized through eq. (2.6), the contributing terms in the curly bracket in eq. (2.4) are,

$$\begin{aligned}
&\Big\{q_{l_3}^A(l_2l_1p_1p_2)_A{}^B\tilde{q}_{l_3B}+q_{l_2}^A(l_1p_1p_2l_3)_A{}^B\tilde{q}_{l_2B}+q_{l_1}^A(p_1p_2l_3l_2)_A{}^B\tilde{q}_{l_1B}+\frac{1}{2}\Big[q_{l_3}^A\tilde{\Delta}_{l_2A}^L+\tilde{q}_{l_3A}\Delta_{l_2}^{LA}\Big]\Big\} \\
&\times\Big\{q_{l_1}^A(l_2l_3p_3p_4)_A{}^B\tilde{q}_{l_1B}+q_{l_2}^A(l_3p_3p_4l_1)_A{}^B\tilde{q}_{l_2B}+q_{l_3}^A(p_3p_4l_1l_2)_A{}^B\tilde{q}_{l_3B}-\frac{1}{2}\Big[q_{l_1}^A\tilde{\Delta}_{(-l_2)A}^R+\tilde{q}_{l_A}\Delta_{(-l_2)}^{RA}\Big]\Big\}\,. \\
&\qquad (2.7)
\end{aligned}$$

Thus performing the final $d^2\eta_{l_3}d^2\tilde{\eta}_{l_3}$ integration gives for eq. (2.3),

$$\begin{aligned}
C^{\text{2-loop}} &= \frac{is_{23}\mathcal{A}_4^{\text{tree}}(p_1,p_2,p_3,p_4)}{s_{12}(l_3+l_2)^4(l_1+p_1)^2(p_2+l_3)^2(l_3-p_3)^2(p_4-l_1)^2} \\
&\quad\times\Big\{\langle l_3|\not{l}_2\not{l}_1\not{p}_1\not{p}_2+\frac{\not{l}_1\not{p}_1\not{p}_2\not{l}_3\not{l}_2\not{l}_1}{(l_1+l_2)^2}+\frac{\not{l}_2\not{l}_1\not{p}_1\not{p}_2\not{l}_3\not{l}_2}{(l_1+l_2)^2}|l_3] \\
&\qquad-\frac{1}{2}\Big[\langle l_3|\frac{(\not{l}_2\not{l}_1\not{p}_1\not{p}_2-\not{l}_2\not{p}_2\not{p}_1\not{l}_1)\not{l}_2\not{l}_1}{(l_1+l_2)^2}|l_3]-[l_3|\frac{(\not{l}_2\not{l}_1\not{p}_1\not{p}_2-\not{l}_2\not{p}_2\not{p}_1\not{l}_1)\not{l}_2\not{l}_1}{(l_1+l_2)^2}|l_3\rangle\Big]\Big\}^a_{\dot{a}} \\
&\quad\times\Big\{\langle l_3|\frac{\not{l}_2\not{l}_3\not{p}_3\not{p}_4\not{l}_1\not{l}_2}{(l_1+l_2)^2}+\frac{\not{l}_1\not{l}_2\not{l}_3\not{p}_3\not{p}_4\not{l}_1}{(l_1+l_2)^2}+\not{p}_3\not{p}_4\not{l}_1\not{l}_2|l_3] \\
&\qquad+\frac{1}{2}\Big[\langle l_3|\frac{(\not{l}_2\not{l}_3\not{p}_3\not{p}_4-\not{l}_2\not{p}_4\not{p}_3\not{l}_3)\not{l}_2\not{l}_1}{(l_1+l_2)^2}|l_3]-[l_3|\frac{(\not{l}_2\not{l}_3\not{p}_3\not{p}_4-\not{l}_2\not{p}_4\not{p}_3\not{l}_3)\not{l}_2\not{l}_1}{(l_1+l_2)^2}|l_3\rangle\Big]\Big\}^{\dot{a}}_a\,. \qquad (2.8)
\end{aligned}$$

This expression can be cleaned up further, but for our purposes it is simplest to evaluate it numerically. We have numerically checked that after dividing by the tree amplitude, this expression matches the analogous expression obtained using four-dimensional cuts [66, 69], but extended into six dimensions. Since the four-dimensional expression depends only on Lorentz dot products of momenta, this extension is carried out simply by treating the dot products as six-dimensional ones.

2.3.4 Multiloop $\mathcal{N} = 4$ super-Yang-Mills and $\mathcal{N} = 8$ supergravity

Following the procedure described above, one can directly check the six-dimensional unitarity cuts of more complicated multiloop $\mathcal{N} = 4$ sYM amplitudes. Up to three loops, the four-gluon amplitude is known to be valid in D dimensions (subject to mild power counting assumptions) [70]. As a nontrivial application of the methods described above, here we confirm that the complete four-loop four-particle amplitudes of $\mathcal{N} = 4$ sYM theory computed in ref. [67] are indeed valid for $D \leq 6$. In that paper, the amplitude was given as a linear combination of 50 integrals of the form,

$$stA_4^{\text{tree}} \int \left(\prod_{i=1}^{4} \frac{d^D l_i}{(2\pi)^D} \right) \frac{N_k(l_i, p_i)}{\prod_{j=1}^{16} l_j^2}, \tag{2.9}$$

where the numerator N_k is a polynomial of degree six in the loop and external momenta. Of these integrals, six are planar and the rest nonplanar. In ref. [67], many of the terms in the numerators were explicitly determined using cuts with $D = 4$ momenta and helicity states. Although a number of nontrivial checks were performed partially confirming their validity in $D > 4$ dimensions, it is still useful to have a complete confirmation valid especially for $D = 11/2$, which is the lowest dimension where an ultraviolet divergence can occur.

As explained in ref. [71], the validity of $\mathcal{N} = 4$ sYM amplitudes in D dimensions implies that the corresponding $\mathcal{N} = 8$ supergravity amplitudes are valid as well. This follows from the construction of $\mathcal{N} = 8$ supergravity amplitudes from corresponding $\mathcal{N} = 4$ sYM amplitudes using the unitarity method in conjunction with the KLT relations [74], which are

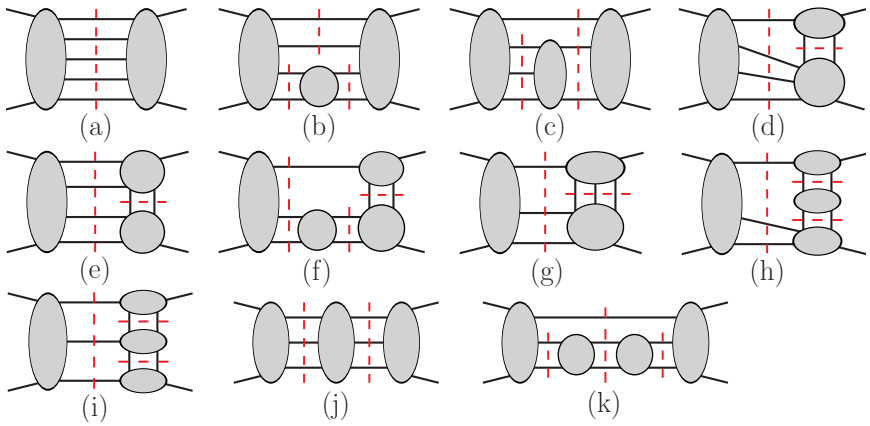

Figure 2.4: The eleven basic cuts decomposing a four-point four-loop amplitude into a product of tree amplitudes. Together with ones involving two-particle cuts, these are the basic ones for determining a massless four-point four-loop amplitude, including nonplanar contributions [71, 67]. The complete spanning set is given by taking all possible distinct permutations of cut and external legs.

known to be valid in D dimensions. We therefore need only confirm the $D = 6$ validity of the $\mathcal{N} = 4$ sYM amplitudes to confirm the result for $\mathcal{N} = 8$ supergravity for $4 < D \leq 6$. A key conclusion of ref. [71] is that the four-loop four-point amplitude of $\mathcal{N} = 8$ supergravity then cannot diverge in dimensions lower than $D = 11/2$, matching the behavior of $\mathcal{N} = 4$ sYM theory.

As discussed in refs. [71, 67], any four-point four-loop amplitude of a massless theory can be completely determined (up to scale-free integrals that integrate to zero in dimensional regularization) via a set of eleven basic cuts shown in Fig. 2.4 along with simpler ones containing two-particle cuts, not displayed. The complete spanning set is obtained by considering all permutations of the legs of each constituent tree amplitude. This set is constructed by demanding that all potential terms are detectable in at least one cut. To carry out our six-dimensional evaluation, we compare the cuts formed from the products of tree amplitudes against the corresponding cuts of the amplitudes as given in ref. [67]. In the latter form, after dividing by the tree amplitude, only Lorentz inner products remain in the amplitude, making numerical comparisons in six dimensions straightforward. In appendix B, we give an explicit analytic evaluation of the sample nonplanar cut shown in Fig. 2.1.

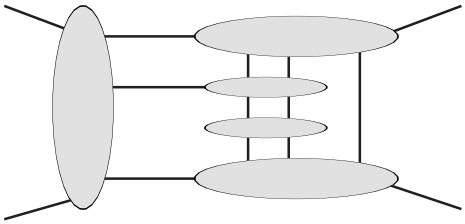

Figure 2.5: A nontrivial cut of the planar four-point six-loop $\mathcal{N} = 4$ sYM theory.

More generally, after extracting an overall supermomentum-conservation delta function from the cuts, the remaining delta functions localize most of the $\eta\tilde{\eta}$ integration, leaving behind six, four, and two pairs of $\eta\tilde{\eta}$ respectively for diagrams (a), (b,c,d,e,g,j), and (f,h,i,k). These extra pairs of $\eta\tilde{\eta}$s then saturate the remaining integration, as was the case in the two-loop example above. This then gives us a result for the state sum of these cuts, which we evaluate with six-dimensional kinematics constrained to satisfy the on-shell conditions.

We find appropriate numerical solutions to the cut conditions by sequentially building momenta that satisfy the on-shell conditions of each of the constituent tree amplitudes in a cut. For a constituent n-point tree amplitude, we need to impose momentum conservation and take the momenta on shell, $p_i^2 = 0$. For $n - 2$ of the legs, we can choose arbitrary null vectors, imposing the momentum conservation constraints on the final two legs. We label the sum of the arbitrary $n - 2$ momenta as $P = \sum_i^{n-2} p_i$. We then define $p_{n-1} \equiv (-P^2/2k \cdot P)\, k$, where k is an arbitrary null vector. With this choice then $p_n \equiv p_{n-1} + K$ automatically satisfies the on-shell condition $p_n^2 = 0$. (It can happen that momentum conservation constraints can lead to inconsistencies in this simple procedure, if a tree does not have at least two unspecified legs. Although this can always be avoided in our case, we note that such inconsistencies can be resolved by solving the cut conditions for groups of tree amplitudes instead of one by one.)

By systematically stepping through the spanning set of cuts described above, we confirm that for $D \leq 6$ the full amplitude is correctly constructed by the mostly four-dimensional evaluation of ref. [67], as expected.

Another interesting case is the four-point six-loop amplitude of $\mathcal{N} = 4$ sYM theory. At six loops, the planar amplitudes can be expressed as a linear combination of integrals similar to the four-loop form (2.9), except that the numerator N_k is a polynomial in the loop and external momenta of degree ten instead of degree six. In four dimensions, any Gram determinant $\det(p_i \cdot p_j)$ vanishes for p_i and p_j corresponding to any five independent momenta, since there can be no more than four linearly independent momenta. For the six-loop four-point amplitude we have a total of nine independent external and loop momenta. Thus with four-dimensional momenta and spinors in the cuts, the constructed amplitude is trivially invariant under the shifts,

$$N_m \to N_m + a_m \det(p_i \cdot p_j)\,, \tag{2.10}$$

although its form changes. The a_m are constants. If we impose dual conformal symmetry [75, 68, 51, 76], the planar numerators are fixed with $a_m = 0$. What about higher dimensions? Iterated two-particle cuts are simple to evaluate in D dimensions [66, 69], with the result that all a_m detectable in such cuts vanish. As a more nontrivial check, we evaluated the cut shown in Fig. 2.5 in six dimensions using the methods described above and numerically compared it against the same cut obtained via four-dimensional methods [51, 39, 67] and extended into six dimensions. Because this cut is composed of four- and five-point tree amplitudes, its evaluation in six dimensions is similar to the four-loop cut described in appendix B. We find that $a_m = 0$ in six dimensions to match the cut Fig. 2.5. Although we did not check a spanning set of cuts, this result strongly suggests that all a_m vanish.

CHAPTER 3

Dual Conformal Properties of Six-Dimensional Maximal Super Yang-Mills Amplitudes

3.1 Introduction

Dual superconformal symmetry [75, 9] has played an important role in understanding the structure of planar four-dimensional $\mathcal{N} = 4$ super-Yang-Mills (sYM) theory at both strong [8, 77, 78, 10] and weak coupling [79, 80]. In particular, the closure of the original and dual superconformal symmetries forms an infinite-dimensional Yangian symmetry [81], which has been extremely useful in determining the planar amplitudes of four-dimensional $\mathcal{N} = 4$ sYM [82, 83, 84, 85].

Because the realization of this symmetry relies heavily on four-dimensional twistor variables [86, 87, 88], it is not immediately apparent how the symmetry behaves away from four dimensions. This is an important question because the loop amplitudes are infrared divergent and require regularization in four dimensions, and the dimensional regulator breaks the symmetry [9, 80, 89]. Generically, any regularization scheme will result in either altering the dimensionality or the massless condition of the external momenta, both of which are essential to the definition of twistors. While one can modify the dual symmetry generators to account for massive regulators [90], thus making the symmetry exact, it is a priori not apparent that such a symmetry should exist without explicit calculation of the loop amplitudes, although it is expected to exist.

To clarify these issues, six-dimensional four-point sYM multiloop amplitudes were recently set up [2] using the six-dimensional spinor helicity formalism and on-shell superspace

of refs. [33, 1]. If one restricts the external momenta to a four-dimensional subspace, these should correspond to four-dimensional $\mathcal{N} = 4$ sYM amplitudes with loop momenta continued to six dimensions. Interestingly, four-dimensional dual conformal symmetry can be used to restrict the form of the multiloop planar integrand, and at four points, this integrand can be straightforwardly extended to six dimensions. Furthermore, the four-dimensional dual conformal boost generator can be extended to incorporate a massive regulator [82], which can be interpreted as extra-dimensional momenta.

In ref. [2] it was conjectured that the six-dimensional maximal sYM n-point tree amplitude, when stripped of the momentum and supermomentum delta functions, transforms covariantly under dual conformal inversion. More precisely, the delta-function-independent part of the amplitude inverts with the same inversion weight on all external lines. The delta functions then introduce extra inversion weight due to the mismatch of mass dimensions of the momentum and supermomentum delta functions. This conjecture was checked explicitly against the simple four-point tree amplitude.

In this chaper, we will show that the conjecture holds for all $n \geq 4$–point tree amplitudes. We will establish the proof by induction; assuming that the $(n-1)$–point amplitude inverts covariantly, via BCFW recursion relations [37], the n–point amplitude will invert in the same way. This proof follows a similar line given for the four-dimensional $\mathcal{N} = 4$ sYM theory in ref. [91].

At loop level, while it is expected that the six-dimensional loop integration measure spoils any dual conformal properties present at tree level, we can recover good behavior by restricting our attention to the integrand. Using the tree-level result, we will demonstrate that the multiloop planar integrands invert in the same fashion as in four dimensions; they are covariant with equal weight on all external lines, and with extra weight for the dual loop variables. We proceed by combining the tree-level result with the generalized unitarity method [41] to show that all planar cuts, after restoring the cut propagators, invert uniformly, and thus the planar multiloop integrand inverts in the same way.

By restricting the loop integration to a four-dimensional subspace, the six-dimensional

maximal sYM amplitudes can be interpreted as four-dimensional massively regulated $\mathcal{N} = 4$ sYM amplitudes. Furthermore, the four-dimensional loop integration measure inverts with the precise weight to cancel the extra weight of dual loop variables in the integrand. Because ultraviolet divergences are absent in four dimensions, and the massive regulator does not break the six-dimensional dual conformal symmetry, one concludes that the regulated $\mathcal{N} = 4$ amplitude will obey the exact symmetry. Assuming cut constructability of the loop amplitudes, which is expected for maximally supersymmetric Yang-Mills, this demonstrates that the dual conformal symmetry is an exact symmetry of the planar amplitude of massively regulated $\mathcal{N} = 4$ theory.

3.2 Dual conformal symmetry

Dual conformal symmetry is a symmetry of the superamplitude that is made manifest by introducing dual (or region) variables subject to the following constraints [9]:

$$\begin{aligned} (x_i - x_j)^{AB} &= \lambda^{Aa}_{\{ij\}} \lambda^{B}_{\{ij\}a}\,, & (x_i - x_j)_{AB} &= \tilde{\lambda}_{\{ij\}A\dot{a}} \tilde{\lambda}^{\dot{a}}_{\{ij\}B}\,, \\ (\theta_i - \theta_j)^{A} &= \lambda^{Aa}_{\{ij\}} \eta_{\{ij\}a}\,, & (\tilde{\theta}_i - \tilde{\theta}_j)_{A} &= \tilde{\lambda}_{\{ij\}A\dot{a}} \tilde{\eta}^{\dot{a}}_{\{ij\}}, \end{aligned} \tag{3.1}$$

where each leg is labeled by the indices $\{ij\}$ of the two adjacent regions, the order of which indicates the direction of momentum flow along the leg (for example, $p^{\mu}_{\{ij\}} = -p^{\mu}_{\{ji\}}$). For tree amplitudes, this notation is redundant since j can always be chosen as $i + 1$. However this prescription does not generalize to loop level, and thus we use a more general notation in anticipation of the multiloop discussion in section 3.4. We will go back and forth between using indices $(i, j, \ldots)$ to label regions and to label legs; the meaning of the indices should be clear from the context. The superamplitude is viewed as a distribution on the full space $(x, \theta, \tilde{\theta}, \lambda, \tilde{\lambda}, \eta, \tilde{\eta})$, with delta function support on the constraint equations (3.1). The cyclic nature of the region variables then automatically enforces momentum and supermomentum conservation.

To obtain the four-dimensional massive amplitudes, we break the six-dimensional spinors

up into four-dimensional representations. Explicit details can be found in refs. [2, 36]. Here we just note that the dual variables should also be broken into four-dimensional pieces and the fifth and sixth dimensional components. With $p_{\{ij\}} = (\check{p}_{\{ij\}}, m_{\{ij\}}, \tilde{m}_{\{ij\}})$, we have:

$$\check{x}_i - \check{x}_j = \check{p}_{\{ij\}}, \quad n_i - n_j = m_{\{ij\}}, \quad \tilde{n}_i - \tilde{n}_j = \tilde{m}_{\{ij\}}\,, \tag{3.2}$$

where we use a check mark over a variable to indicate the components in the four-dimensional subspace. The physical mass squared is then $m^2_{\{ij\}} + \tilde{m}^2_{\{ij\}}$.

The dual conformal boost generator can be expressed as a composition of dual conformal inversions and translations,

$$K^\mu = I\, P_\mu\, I\,, \tag{3.3}$$

so we begin our discussion with the dual conformal inversion operator I. The inversion is defined on the Clifford algebra as

$$I[(\sigma^\mu)_{AB}] \equiv (\tilde{\sigma}_\mu)^{BA}\,, \qquad I[(\tilde{\sigma}^\mu)^{AB}] \equiv (\sigma_\mu)_{BA}\,, \tag{3.4}$$

and on the region variables as

$$I[x_i^\mu] \equiv (x_i^{-1})_\mu = \frac{x_{i\mu}}{x_i^2}\,, \qquad I[\theta_i^A] \equiv (x_i^{-1})_{AB}\theta_i^B\,, \qquad I[\tilde{\theta}_{iA}] \equiv (x_i^{-1})^{AB}\tilde{\theta}_{iB}\,. \tag{3.5}$$

From the inversion of x^μ, we also see that

$$\begin{aligned} I[(x_i - x_j)^{AB}] &= (x_i^{-1})_{AC}(x_i - x_j)^{CD}(x_j^{-1})_{DB} \\ &= (x_j^{-1})_{AC}(x_i - x_j)^{CD}(x_i^{-1})_{DB}\,, \end{aligned} \tag{3.6}$$

and integration measures invert as

$$I[d^6x_i] = (x_i^2)^{-6}d^6x_i\,, \qquad I[d^4\theta_i] = (x_i^2)^2 d^4\theta_i\,, \qquad I[d^4\tilde{\theta}_i] = (x_i^2)^2 d^4\tilde{\theta}_i\,. \tag{3.7}$$

With these definitions in hand, we can deduce the inversion properties of all of the other

variables by requiring the invariance of the constraint equations (3.1) and the definitions of the u and w variables in eqs. (1.13) and (1.15). We leave the proofs of these properties to appendix C and collect the results here:

$$
\begin{aligned}
&I[\lambda^A_{\{ij\}a}] = \frac{x_{iAB}\lambda^{Ba}_{\{ij\}}}{\sqrt{x_i^2 x_j^2}} = \frac{x_{jAB}\lambda^{Ba}_{\{ij\}}}{\sqrt{x_i^2 x_j^2}}\,, && I[\eta_{\{ij\}a}] = -\sqrt{\frac{x_i^2}{x_j^2}}\Big(\eta^a_{\{ij\}} + (x_i^{-1})_{AB}\,\theta_i^A \lambda^{Ba}_{\{ij\}}\Big)\,,\\
&I[\tilde{\lambda}_{\{ij\}A\dot{a}}] = \frac{x_i^{AB}\tilde{\lambda}^{\dot{a}}_{\{ij\}B}}{\sqrt{x_i^2 x_j^2}} = \frac{x_j^{AB}\tilde{\lambda}^{\dot{a}}_{\{ij\}B}}{\sqrt{x_i^2 x_j^2}}\,, && I[\tilde{\eta}^{\dot{a}}_{\{ij\}}] = -\sqrt{\frac{x_i^2}{x_j^2}}\Big(\tilde{\eta}_{\{ij\}\dot{a}} + (x_i^{-1})^{AB}\,\tilde{\theta}_{iA}\tilde{\lambda}_{\{ij\}B\dot{a}}\Big)\,,\\
&I[u_{ia}] = \frac{\beta u_i^a}{\sqrt{x_{i-1}^2}}\,, && I[w_{ia}] = -\frac{1}{\beta}\sqrt{x_{i-1}^2}\,w_i^a\,,\\
&I[\tilde{u}_{i\dot{a}}] = \frac{\tilde{u}_i^{\dot{a}}}{\beta\sqrt{x_{i-1}^2}}\,, && I[\tilde{w}_{i\dot{a}}] = -\beta\sqrt{x_{i-1}^2}\,\tilde{w}_i^{\dot{a}}\,,
\end{aligned}
\tag{3.8}
$$

where β is an unfixed parameter that is irrelevant in our calculations.

Given these inversion rules, one can immediately deduce via eq. (3.3) how each variable transforms under the dual conformal boost generator K^μ. Alternatively, one can deduce the same information by requiring that the dual conformal boost generator respects all of the constraints in eq. (3.1). If we were to use the usual dual conformal boost generator in x space,

$$
K^\mu = \sum_i \left(2\,x_i^\mu x_i^\nu - x_i^2\,\eta^{\mu\nu}\right)\frac{\partial}{\partial x_i^\nu}\,,
\tag{3.9}
$$

the LHS of the definition of the x_i in eq. (3.1) would be nonzero under boosts, while the RHS would vanish. To correct this, we must add derivatives with respect to λ and $\tilde{\lambda}$ to K^μ. These new derivatives in turn would not be compatible with the definition of θ_i, so we must also add θ and η derivatives. Requiring that all of the constraints in eq. (3.1) are consistent

with K^μ then yields

$$\begin{aligned} K^\mu &= \sum_i \left[\left(2\, x_i^\mu x_i^\nu - x_i^2\, \eta^{\mu\nu}\right) \frac{\partial}{\partial x_i^\nu} + \theta_i^A (\sigma^\mu)_{AB} x_i^{BC} \frac{\partial}{\partial \theta_i^C} + \tilde{\theta}_{iA} (\tilde{\sigma}^\mu)^{AB} x_{iBC} \frac{\partial}{\partial \tilde{\theta}_{iC}} \right] \\ &+ \frac{1}{2} \sum_{\{jk\}} \left[\lambda^{Aa}_{\{jk\}} (\sigma^\mu)_{AB} (x_j + x_k)^{BC} \frac{\partial}{\partial \lambda^{Ca}_{\{jk\}}} - (\theta_j + \theta_k)^A (\sigma^\mu)_{AB} \lambda^B_{\{jk\}a} \frac{\partial}{\partial \eta_{\{jk\}a}} \right. \\ &\left. + \tilde{\lambda}_{\{jk\}A\dot{a}} (\tilde{\sigma}^\mu)^{AB} (x_j + x_k)_{BC} \frac{\partial}{\partial \tilde{\lambda}_{\{jk\}C\dot{a}}} - (\tilde{\theta}_j + \tilde{\theta}_k)_A (\tilde{\sigma}^\mu)^{AB} \tilde{\lambda}^{\dot{a}}_{\{jk\}B} \frac{\partial}{\partial \tilde{\eta}^{\dot{a}}_{\{jk\}}} \right] , \end{aligned} \tag{3.10}$$

where i runs over all regions, and $\{jk\}$ runs over all legs. The bosonic part of this generator was given in ref. [2]. One can explicitly check that the infinitesimal transformations generated by this dual conformal boost generator match with those generated by eq. (3.3).

3.3 Dual conformal properties of tree-level amplitudes

In this section, we show that the tree-level amplitudes of six-dimensional maximal sYM exhibit dual conformal covariance. In ref. [2], the four-point tree-level amplitude was shown to be covariant under dual conformal inversion,

$$I[\mathcal{A}_4^{\text{tree}}] = (x_1^2)^2 (x_1^2 x_2^2 x_3^2 x_4^2) \mathcal{A}_4^{\text{tree}}. \tag{3.11}$$

Note that the extra factor $(x_1^2)^2$ relative to the four-dimensional result comes from the mismatch of the degrees of the momentum and supermomentum delta functions in six dimensions. In six dimensions, the momentum conservation delta function is of degree six instead of degree four as in four dimensions. Since the fermionic delta function is still of degree eight, there will be a mismatch in inversion weights of degree two in (x_1^2). After separating out the delta functions from the rest of the amplitude,

$$\mathcal{A}_n^{\text{tree}} = \delta^6 \left(\sum_{i \in \mathcal{E}} p_i \right) \delta^4 \left(\sum_{i \in \mathcal{E}} q_i \right) \delta^4 \left(\sum_{i \in \mathcal{E}} \tilde{q}_i \right) f_n \,, \tag{3.12}$$

it was conjectured that the function f_n, for $n \geq 4$, transforms as

$$I[f_n] = \left(\prod_{i \in \mathcal{E}} x_i^2 \right) f_n \tag{3.13}$$

under dual conformal inversion. We prove this by induction, utilizing the BCFW recursion relations [37]; assuming that all f_m transform as in eq. (3.13) for $4 \leq m < n$, each term in the BCFW recursive construction of f_n will respect eq. (3.13), and hence so will f_n. For the three-point amplitude, due to special kinematics, it is possible to consider the external momenta in a four-dimensional subspace. It is then conceivable that the four-dimensional dual conformal properties carry over to higher dimensions via covariance. However, closer inspection is warranted, because the polarization vectors of the gluons could point outside of the subspace. Furthermore, the six-dimensional three-point amplitude is not proportional to the supermomentum delta function, and hence f_3 cannot be defined.

Given that the function f_n inverts as eq. (3.13), acting with the dual conformal boost generator then gives

$$K^\mu[f_n] = \left(\sum_{i \in \mathcal{E}} 2x_i^\mu \right) f_n. \tag{3.14}$$

The above results can be rewritten for the massive amplitudes. In four-dimensional notation, the conformal inversion acts as

$$I\left[\check{x}^\mu\right] = \frac{\check{x}_\mu}{x^2}\,, \qquad I\left[n\right] = -\frac{n}{x^2}\,, \qquad I\left[\tilde{n}\right] = -\frac{\tilde{n}}{x^2}\,, \tag{3.15}$$

where $x^2 = \check{x}^2 - n^2 - \tilde{n}^2$. The massive amplitude then transforms under the dual conformal boost generators as

$$\check{K}^\mu[f_n] = \left(\sum_{i \in \mathcal{E}} 2\check{x}_i^{\hat{\mu}} \right) f_n\,, \quad K^n[f_n] = \left(\sum_{i \in \mathcal{E}} 2n_i \right) f_n\,, \quad K^{\tilde{n}}[f_n] = \left(\sum_{i \in \mathcal{E}} 2\tilde{n}_i \right) f_n\,. \tag{3.16}$$

The generator $\check{K}^\mu$ is closely related to the dual generator for the massively regulated ampli-

tude [90]. The bosonic dual variable part is

$$\check{K}^\mu = \sum_i \left[2\,\check{x}_i^\mu \left(\check{x}_i^\nu \frac{\partial}{\partial \check{x}_i^\nu} + n_i \frac{\partial}{\partial n_i} + \tilde{n}_i \frac{\partial}{\partial \tilde{n}_i} \right) - x_i^2 \frac{\partial}{\partial \check{x}_{i\mu}} \right] , \tag{3.17}$$

while the bosonic part of the fifth and sixth components of K^μ is

$$\begin{aligned} K^n &= \sum_i \left[2\,n_i \left(\check{x}_i^\nu \frac{\partial}{\partial \check{x}_i^\nu} + n_i \frac{\partial}{\partial n_i} + \tilde{n}_i \frac{\partial}{\partial \tilde{n}_i} \right) + x_i^2 \frac{\partial}{\partial n_i} \right] , \\ K^{\tilde{n}} &= \sum_i \left[2\,\tilde{n}_i \left(\check{x}_i^\nu \frac{\partial}{\partial \check{x}_i^\nu} + n_i \frac{\partial}{\partial n_i} + \tilde{n}_i \frac{\partial}{\partial \tilde{n}_i} \right) + x_i^2 \frac{\partial}{\partial \tilde{n}_i} \right] . \end{aligned} \tag{3.18}$$

Since the massive formulation is obtained straightforwardly from the six-dimensional formalism, from now on we will work with manifest six-dimensional covariance.

3.3.1 The BCFW shift in dual coordinates.

Taking the BCFW shift to be on legs 1 and n, we have

$$\begin{aligned} &p_1(z) = p_1 + zr\,, && q_1(z) = q_1 + zs\,, && \tilde{q}_1(z) = \tilde{q}_1 + z\tilde{s}\,, \\ &p_n(z) = p_n - zr\,, && q_n(z) = q_n - zs\,, && \tilde{q}_n(z) = \tilde{q}_n - z\tilde{s}\,. \end{aligned} \tag{3.19}$$

The precise forms of r, s and $\tilde{s}$ are given in eqs. (1.24) and (1.28). For our purposes, it is sufficient to note that this implies a shift in only the dual coordinates x_1, θ_1 and $\tilde{\theta}_1$,

$$\begin{aligned} &p_1(z) = x_1(z) - x_2\,, && q_1(z) = \theta_1(z) - \theta_2\,, && \tilde{q}_1(z) = \tilde{\theta}_1(z) - \tilde{\theta}_2\,, \\ &p_n(z) = x_n - x_1(z)\,, && q_n(z) = \theta_n - \theta_1(z)\,, && \tilde{\theta}_n(z) = \tilde{\theta}_n - \tilde{\theta}_1(z)\,, \end{aligned} \tag{3.20}$$

where

$$x_1(z) = x_1 + zr\,, \qquad \theta_1(z) = \theta_1 + zs\,, \qquad \tilde{\theta}_1(z) = \tilde{\theta}_1 + z\tilde{s}\,. \tag{3.21}$$

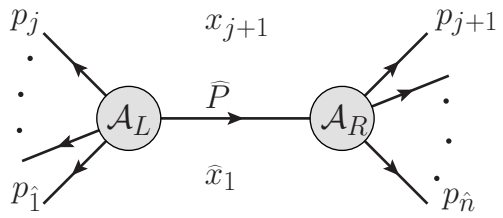

Figure 3.1: A BCFW diagram without three-point subamplitudes.

Thus each BCFW term can be defined in a dual graph with just one shifted dual coordinate. We will denote the legs with shifted momentum by placing hats over the leg labels, while a hat over x and θ is used for shifted regions.

There are two types of BCFW diagrams, characterized by the presence or absence of a three-point subamplitude. We must consider each case separately, due to the fact that we cannot pull out an overall supermomentum conservation delta function from the three-point amplitude, and thus the three-point amplitude does not have the straightforward inversion of eq. (3.13).

3.3.2 BCFW diagrams without three-point subamplitudes

We first consider the case where there is no three-point subamplitude, as in Fig. 3.1. The amplitudes on the left and right can be written as

$$\begin{aligned}
\mathcal{A}_L &= \delta^6\left(\sum_{i\in L} p_i\right)\delta^4\left(\sum_{i\in L} q_i\right)\delta^4\left(\sum_{i\in L}\tilde{q}_i\right) f_L(\hat{1},\cdots,j,\widehat{P})\,, \\
\mathcal{A}_R &= \delta^6\left(\sum_{i\in R} p_i\right)\delta^4\left(\sum_{i\in R} q_i\right)\delta^4\left(\sum_{i\in R}\tilde{q}_i\right) f_R(-\widehat{P},j+1,\cdots,\hat{n})\,.
\end{aligned} \tag{3.22}$$

Each term in the BCFW recursion can then be written as

$$\delta^6\left(\sum_{i\in\mathcal{E}} p_i\right)\delta^4\left(\sum_{i\in\mathcal{E}} q_i\right)\delta^4\left(\sum_{i\in\mathcal{E}}\tilde{q}_i\right) f_n^{(j)}\,, \tag{3.23}$$

where $f_n^{(j)}$ is the contribution to f_n from the BCFW diagram labeled by j,

$$f_n^{(j)} = \frac{i}{P^2}\int d^2\eta_P d^2\tilde{\eta}_P\,\delta^4\left(\sum_{i\in L} q_i\right)\delta^4\left(\sum_{i\in L}\tilde{q}_i\right) f_L f_R\,. \tag{3.24}$$

From the induction step, the functions f_L and f_R invert as

$$\begin{aligned} I\left[f_L\right] &= \left(\widehat{x}_1^2 x_2^2\cdots x_{j+1}^2\right) f_L\,, \\ I\left[f_R\right] &= \left(x_{j+1}^2\cdots x_n^2\widehat{x}_1^2\right) f_R\,. \end{aligned} \tag{3.25}$$

The propagator in $f_n^{(j)}$ has a simple inversion, given by

$$I\left[\frac{1}{P^2}\right] = I\left[\frac{1}{x_{1,j+1}^2}\right] = \frac{x_1^2 x_{j+1}^2}{x_{1,j+1}^2}\,, \tag{3.26}$$

so the only remaining piece of $f_n^{(j)}$ is the fermionic integral. Since the fermionic delta function is of degree eight, the fermionic integral can be completely localized by the delta functions, and the $\eta_P, \tilde{\eta}_P$s in f_L, f_R will be replaced by the solution of the delta functions. The replacement does not affect the inversion properties of f_L, f_R because it simply amounts to the use of supermomentum conservation. The integral was shown in eq. (1.44) to give

$$\begin{aligned} \int d^2\eta_P d^2\tilde{\eta}_P\,\delta^4\left(\sum_{i\in L} q_i\right)\delta^4\left(\sum_{i\in L}\tilde{q}_i\right) &= \left(\widehat{\theta}_1 - \theta_{j+1}\right)^A \tilde{\lambda}_{\widehat{P}A\dot{a}}\tilde{\lambda}^{\dot{a}}_{\widehat{P}B}\left(\widehat{\theta}_1 - \theta_{j+1}\right)^B \\ &\quad\times\left(\widehat{\tilde{\theta}}_1 - \tilde{\theta}_{j+1}\right)_C \lambda^{Ca}_{\widehat{P}}\lambda^D_{\widehat{P}a}\left(\widehat{\tilde{\theta}}_1 - \tilde{\theta}_{j+1}\right)_D\,. \end{aligned} \tag{3.27}$$

Note that we do not write f_L and f_R in the integral because they are independent of $\eta_P, \tilde{\eta}_P$ after the replacement. To see how this expression inverts, we use eqs. (3.5) and (3.8) on each

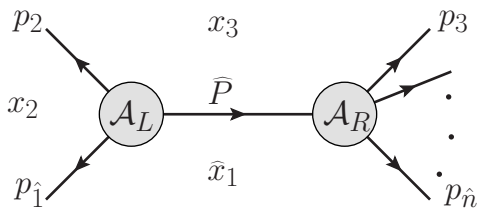

Figure 3.2: A BCFW diagram with a three-point subamplitude.

factor, such as

$$\begin{aligned} I\left[\left(\widehat{\theta}_1-\theta_{j+1}\right)^A\tilde{\lambda}_{\widehat{P}A\dot{a}}\right] &= -\frac{1}{\sqrt{\widehat{x}_1^2x_{j+1}^2}}\left(\widehat{\theta}_1^B(\widehat{x}_1^{-1})_{BA}\widehat{x}_1^{AC}\tilde{\lambda}^{\dot{a}}_{\widehat{P}C}-\theta_{j+1}^B(x_{j+1}^{-1})_{BA}x_{j+1}^{AC}\tilde{\lambda}^{\dot{a}}_{\widehat{P}C}\right) \\ &= -\frac{1}{\sqrt{\widehat{x}_1^2x_{j+1}^2}}\left(\widehat{\theta}_1-\theta_{j+1}\right)^A\tilde{\lambda}^{\dot{a}}_{\widehat{P}A}\,. \end{aligned} \tag{3.28}$$

Doing the same for the other factors, we find

$$\begin{aligned} &I\left[\int d^2\eta_P d^2\tilde{\eta}_P\,\delta^4\left(\sum_{i\in L}q_i\right)\delta^4\left(\sum_{i\in L}\tilde{q}_i\right)\right] \\ &\qquad=\frac{1}{(\widehat{x}_1^2x_{j+1}^2)^2}\int d^2\eta_P d^2\tilde{\eta}_P\,\delta^4\left(\sum_{i\in L}q_i\right)\delta^4\left(\sum_{i\in L}\tilde{q}_i\right) \end{aligned} \tag{3.29}$$

Combining equations (3.25), (3.26) and (3.29), we arrive at the desired result

$$I\left[f_n^{(j)}\right]=\left(\prod_{i\in\mathcal{E}}x_i^2\right)f_n^{(j)}\,. \tag{3.30}$$

3.3.3 BCFW diagrams with a three-point subamplitude

To make a statement about the inversion weight of the entire n-point amplitude, we must also consider the BCFW terms which contain a three-point subamplitude, as shown in Fig. 3.2. It was shown in section 1.5.2 that the contribution of such a diagram is given as,

$$\int d^2\eta_P d^2\tilde{\eta}_P\, \mathcal{A}_3 \frac{i}{P^2} \mathcal{A}_{n-1} \tag{3.31}$$
$$= -\delta^6\left(\sum_{i\in\mathcal{E}} p_i\right)\delta^4\left(\sum_{i\in\mathcal{E}} q_i\right)\delta^4\left(\sum_{i\in\mathcal{E}} \tilde{q}_i\right)(\mathbf{u_2}-\mathbf{u_{\hat{1}}})\,(\tilde{\mathbf{u}}_{\mathbf{2}}-\tilde{\mathbf{u}}_{\hat{\mathbf{1}}})\,\frac{1}{P^2} f_{n-1}\,,$$

where f_{n-1} has been rewritten completely in terms of external leg variables by using the substitutions $q_{\hat{P}} = -q_{\hat{1}} - q_2$ etc. Hence,

$$f_n^{(2)} = -\,(\mathbf{u_2}-\mathbf{u_{\hat{1}}})\,(\tilde{\mathbf{u}}_{\mathbf{2}}-\tilde{\mathbf{u}}_{\hat{\mathbf{1}}})\,\frac{1}{P^2} f_{n-1}\,. \tag{3.32}$$

The inversion of P^2 and f_{n-1} here are straightforward, and we are left with the remaining factors involving $\mathbf{u}$ and $\tilde{\mathbf{u}}$. We consider the inversion of $(\mathbf{u_2}-\mathbf{u_{\hat{1}}})$ in detail. After applying eq. (3.8), we get

$$\begin{aligned} I\left[\mathbf{u_2}-\mathbf{u_{\hat{1}}}\right] &= -\sqrt{\frac{x_2^2}{\widehat{x}_1^2 x_3^2}}\,\beta u_{2a}\left(\eta_2^a + (x_2^{-1})_{AB}\theta_2^A\lambda_2^{Ba}\right) \\ &\quad + \sqrt{\frac{\widehat{x}_1^2}{x_2^2 x_3^2}}\,\beta u_{\hat{1}a}\left(\eta_{\hat{1}}^a + (\widehat{x}_1^{-1})_{AB}\widehat{\theta}_1^A\lambda_{\hat{1}}^{Ba}\right)\,. \end{aligned} \tag{3.33}$$

We can combine the θ-dependent terms in the above equation as

$$\begin{aligned} &\frac{\beta}{\sqrt{\widehat{x}_1^2 x_2^2 x_3^2}}\left(-u_{2a}\,x_{2AB}\,\theta_2^A\lambda_2^{Ba} + u_{\hat{1}a}\,\widehat{x}_{1AB}\,\widehat{\theta}_1^A\lambda_{\hat{1}}^{Ba}\right) \\ &\qquad = \frac{-\beta}{2\sqrt{\widehat{x}_1^2 x_2^2 x_3^2}}\,u_{\hat{1}a}(\widehat{x}_1+x_2)_{AB}(\theta_2^A-\widehat{\theta}_1^A)\lambda_{\hat{1}}^{Ba} \\ &\qquad = \frac{\beta}{2\sqrt{\widehat{x}_1^2 x_2^2 x_3^2}}\,u_{\hat{1}a}(\widehat{x}_1+x_2)_{AB}\lambda_{\hat{1}}^{Ab}\lambda_{\hat{1}}^{Ba}\eta_{\hat{1}b} \\ &\qquad = \frac{-\beta}{4\sqrt{\widehat{x}_1^2 x_2^2 x_3^2}}\,(\widehat{x}_1-x_2)^{AB}\,(\widehat{x}_1+x_2)_{AB}\,\mathbf{u_{\hat{1}}} \\ &\qquad = \beta\,\mathbf{u_{\hat{1}}}\left(\sqrt{\frac{\widehat{\mathbf{x}}_{\mathbf{1}}^{\mathbf{2}}}{\mathbf{x_2^2 x_3^2}}} - \sqrt{\frac{\mathbf{x_2^2}}{\widehat{\mathbf{x}}_{\mathbf{1}}^{\mathbf{2}}\mathbf{x_3^2}}}\right)\,, \end{aligned} \tag{3.34}$$

where in the second line we have used $\widehat{x}_{1AB}\,\lambda_{\hat{1}}^{Ba} = x_{2AB}\,\lambda_{\hat{1}}^{Ba}$ and $u_{\hat{1}a}\lambda_{\hat{1}}^{Ba} = u_{2a}\lambda_2^{Ba}$. Putting this back into eq. (3.33), we arrive at

$$I\left[(\mathbf{u_2} - \mathbf{u_{\hat{1}}})\right] = \beta\sqrt{\frac{x_2^2}{\widehat{x}_1^2 x_3^2}}(\mathbf{u_2} - \mathbf{u_{\hat{1}}})\,. \tag{3.35}$$

The inversion of the antichiral factor $(\tilde{\mathbf{u}}_{\mathbf{2}} - \tilde{\mathbf{u}}_{\hat{\mathbf{1}}})$ behaves in the same way, except that β appears in the denominator. Thus, putting everything together, we have

$$I\left[f_n^{(2)}\right] = \left(\frac{x_2^2}{\widehat{x}_1^2 x_3^2}\right)\left(x_1^2 x_3^2\right)\left(\widehat{x}_1^2 x_3^2 \cdots x_n^2\right) f_n^{(2)} = \left(\prod_{i\in\mathcal{E}} x_i^2\right) f_n^{(2)}. \tag{3.36}$$

This completes the proof of eq. (3.13). In the next section, we turn our attention to planar multiloop amplitudes.

3.4 Loop amplitudes through unitarity cuts

In this section, we will demonstrate that the L–loop planar integrand is covariant under inversion in the following way:

$$I\left[\mathcal{I}_n^L\right] = \left(\prod_{i\in\mathcal{E}} x_i^2\right)\left(\prod_{i=1}^{L}(x_{l_i}^2)^4\right)\mathcal{I}_n^L\,, \tag{3.37}$$

where the integrand is defined with respect to the amplitude as

$$\mathcal{A}_n^L = \delta^6\left(\sum_{i\in\mathcal{E}} p_i\right)\delta^4\left(\sum_{i\in\mathcal{E}} q_i\right)\delta^4\left(\sum_{i\in\mathcal{E}} \tilde{q}_i\right)\int\left(\prod_{i=1}^{L} d^6 x_{l_i}\right)\mathcal{I}_n^L\,. \tag{3.38}$$

Because we are focusing on the integrand itself, there are extra loop region weights $(x_{l_i}^2)^4$. This is the same result as in four dimensions, although in six dimensions the loop integration measure inverts with weight $(x_{l_i}^2)^{-6}$, which does not exactly cancel the weight of the integrand. Therefore, the amplitude after integration will not be covariant unless the integral is restricted to four dimensions, which, as we have discussed, is the case when interpreting the

extra two dimensions as a massive regulator [90].

Our approach to eq. (3.37) is to study the inversion properties of unitarity cuts of the amplitude. In the unitarity method, we are required to perform state sums across the cut propagators, which is achieved by integrating the Grassmann variables $\eta_{l_i}, \tilde{\eta}_{l_i}$ of the cut lines. Since the tree amplitudes contributing to the cuts have definite inversion properties, we only need to understand how the $\eta_{l_i}, \tilde{\eta}_{l_i}$ integration modifies the inversion weight.

To make statements about inversion properties, it is more natural to express everything in terms of dual variables than in terms of η and λ. We therefore trade the supersum η integrals for θ integrals. Suppose a cut not containing any three-point subamplitudes has an internal line between regions i and j. The supersum across this line is expressed as an integral with measure $d^2\eta_{\{ij\}}d^2\tilde{\eta}_{\{ij\}}$. The transformation to dual coordinates is achieved by inserting 1 into the cut in a particular way, given by

$$\begin{aligned}
\mathcal{A}_n^L\Big|_{\text{cut}} &= \int \prod_{\{ij\}} d^2\eta_{\{ij\}}d^2\tilde{\eta}_{\{ij\}} \times \mathcal{A}^{\text{tree}}_{(1)}\mathcal{A}^{\text{tree}}_{(2)}\mathcal{A}^{\text{tree}}_{(3)}\dots\mathcal{A}^{\text{tree}}_{(m)} \\
&= \int \prod_{\{ij\}} d^2\eta_{\{ij\}}d^2\tilde{\eta}_{\{ij\}} \times \prod_{\alpha} \delta^4\left(\sum_{k\in\alpha} q_k\right)\delta^4\left(\sum_{k\in\alpha}\tilde{q}_k\right) f_\alpha \\
&= \int \prod_{\{ij\}} d^2\eta_{\{ij\}}d^2\tilde{\eta}_{\{ij\}} \times \prod_{k} d^4\theta_k d^4\tilde{\theta}_k \times \prod_{\alpha} f_\alpha \\
&\quad \times \prod_{\{rs\}} \delta^4\left(\theta_r^A - \theta_s^A - \lambda^{Aa}_{\{rs\}}\eta_{\{rs\}a}\right)\delta^4\left(\tilde{\theta}_{rB} - \tilde{\theta}_{sB} - \tilde{\lambda}_{\{rs\}B\dot{a}}\tilde{\eta}^{\dot{a}}_{\{rs\}}\right), \qquad (3.39)
\end{aligned}$$

where the product over $\{ij\}$ runs over all internal cut lines, the product over k runs over all regions, the product over $\{rs\}$ runs over all lines, and the product over α runs over the tree subamplitudes. The first two lines of this equality are the definition of the cut, where we have ignored the momentum conservation delta functions on the subamplitudes, because they combine straightforwardly into an overall momentum conservation when cut conditions are relaxed and loop integrals are replaced. Because the integrand in the third and fourth lines has a shift symmetry in the θ variables, the measure $\prod d^4\theta$ is understood to include only $(F-1)$ of the regions, where $F = n + L$ is the total number of regions in the graph.

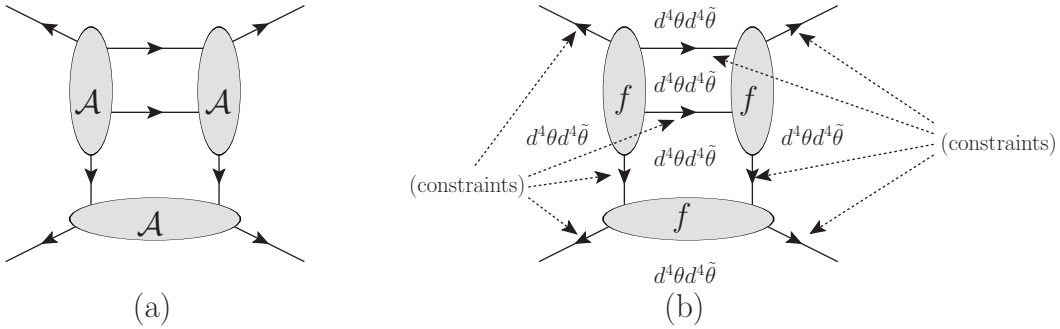

Figure 3.3: A cut of the two-loop four-point amplitude. (a) In the usual expression of the cut, this diagram is dressed with a tree-level amplitude for each blob and a state sum over each internal line. (b) As discussed in the text, for planar cuts this is equivalent to dressing the diagram with an f function for each blob, introducing the dual variable constraints for every line, and integrating over the dual θ variables of every region. Finally, a state sum over each internal line is performed. One can check that the dressing of (b) contains $8 \times 8 = 64$ fermionic delta functions and $5 \times 8 = 40$ integrations over θ (because one of the six regions is fixed by the shift symmetry), leaving 24 unintegrated fermionic delta functions, which are exactly the supermomentum conservation of the subamplitudes in dressing (a).

An explicit example for the two-loop four-point amplitude is given schematically in Fig. 3.3. It does not matter how we fix the symmetry in the measure; our choice will only affect the overall supermomentum delta function, which does not contribute to the conjectured transformation eq. (3.37). We therefore leave this detail implicit.

To see the equality of eq. (3.39), note that we can pull the subamplitude supermomentum delta functions out of the θ delta functions in the fourth line, leaving behind $(P - V)$ delta functions to be used for localizing the θ integrals, where P is the number of lines in the graph, and V is the number of subamplitudes. Because there are $(F - 1)$ of the θ integrals, the leftover delta functions saturate the integral when $F - 1 = P - V$, which is indeed the case for planar graphs.

We can now use the θ delta functions to eliminate all explicit η dependence from each f_α, so that the entire η dependence of the cut appears in the form

$$\int d^2\eta_{\{ij\}} \delta^4 \left(\theta_i^A - \theta_j^A - \lambda_{\{ij\}}^{Aa} \eta_{\{ij\}a}\right) . \tag{3.40}$$

This performs the chiral half of the supersum across the line between regions i and j. The antichiral half of the supersum is completely analogous, so we leave it out. The integration over $\eta_{\{ij\}}$ thus contributes

$$\theta_{ij} \cdot x_{ij} \cdot \theta_{ij} \equiv (\theta_i - \theta_j)^A (x_i - x_j)_{AB} (\theta_i - \theta_j)^B \,. \tag{3.41}$$

We demonstrated in section 3.3.2 that this factor inverts with weight $(x_i^2 x_j^2)^{-1}$.

Returning to the cut in eq. (3.39), the result of doing the η integrals is

$$\begin{aligned} \mathcal{A}_n^L\Big|_{\text{cut}} &= \int \prod_k d^4\theta_k d^4\tilde{\theta}_k \times \prod_\alpha f_\alpha^0 \times \prod_{\{ij\}} (\theta_{ij} \cdot x_{ij} \cdot \theta_{ij})(\tilde{\theta}_{ij} \cdot x_{ij} \cdot \tilde{\theta}_{ij}) \\ &\quad \times \prod_{\{rs\}} \delta^4\left(\theta_r^A - \theta_s^A - \lambda_{\{rs\}}^{Aa} \eta_{\{rs\}a}\right) \delta^4\left(\tilde{\theta}_{rA} - \tilde{\theta}_{sA} - \tilde{\lambda}_{\{rs\}A\dot{a}} \tilde{\eta}_{\{rs\}}^{\dot{a}}\right) \,, \end{aligned} \tag{3.42}$$

where now $\{rs\}$ only runs over the external lines. An overall supermomentum delta function pulls out, leaving $(n-1)$ delta functions of each chirality, which completely saturate the θ integrations over the external regions (this also takes care of the shift symmetry detail). We are finally left with

$$\begin{aligned} \mathcal{A}_n^L\Big|_{\text{cut}} &= \delta^6\left(\sum_{i\in\mathcal{E}} p_i\right) \delta^4\left(\sum_{i\in\mathcal{E}} q_i\right) \delta^4\left(\sum_{i\in\mathcal{E}} \tilde{q}_i\right) \\ &\quad \times \int \left(\prod_k d^4\theta_k d^4\tilde{\theta}_k\right) \left(\prod_{\{ij\}} (\theta_{ij} \cdot x_{ij} \cdot \theta_{ij})(\tilde{\theta}_{ij} \cdot x_{ij} \cdot \tilde{\theta}_{ij})\right) \prod_\alpha f_\alpha \,, \end{aligned} \tag{3.43}$$

where the product over k now runs only over the internal regions, and we have replaced the overall momentum conservation.

We are now in a position to formulate a set of diagrammatic rules for inverting the cut, after restoring the cut propagators. Because each piece of the second line of eq. (3.43) inverts covariantly, the cut inverts to itself multiplied by an overall prefactor (not considering the inversion of the overall delta functions). To calculate the prefactor for a given cut, we have the following rules:

- For every loop region k, the $\theta_k, \tilde{\theta}_k$ measure contributes a factor $(x_k^2)^4$.
- Each internal leg $\{ij\}$ contributes $(x_i^2 x_j^2)^{-1}$, where a factor of $x_i^2 x_j^2$ comes from the cut propagator, and a factor of $(x_i^2 x_j^2)^{-2}$ comes from $(\theta_{ij} \cdot x_{ij} \cdot \theta_{ij})(\tilde{\theta}_{ij} \cdot x_{ij} \cdot \tilde{\theta}_{ij})$
- Each tree-level subamplitude contributes $\prod_i x_i^2$, where i runs over all regions adjacent to the tree.

Given a region i, it is straightforward to invert these rules to figure out what power of x_i^2 appears in the prefactor. If i is an external region, x_i^2 must appear to the power $(\rho_i - \sigma_i)$, where ρ_i and σ_i are the number of tree-level subamplitudes and the number of internal propagators, respectively, adjacent to region i. Each external region necessarily borders one fewer of the internal propagators than the subamplitudes, so the external regions each give x_i^2. If, on the other hand, i is an internal region, then x_i^2 appears to the power $(\rho_i - \sigma_i + 4)$. All internal regions necessarily border the same number of internal propagators as subamplitudes, so the internal regions each give $(x_i^2)^4$. Therefore, we have reached the result that each planar cut with no three-point subamplitudes inverts with the prefactor

$$\left(\prod_{i \in \mathcal{E}} x_i^2\right) \left(\prod_{i=1}^{L} (x_{l_i}^2)^4\right) , \tag{3.44}$$

after the cut propagators have been restored, and not including the overall momentum and supermomentum conservation. It is not difficult to extend this result to cuts involving three-point subamplitudes. The supersum between a three-point subamplitude and another subamplitude in a cut proceeds in the same way as sewing a three-point tree in BCFW. The resulting merged subamplitudes then invert as in eq. (3.36).

Because all cuts invert in exactly the same way, and the correct amplitude must satisfy all generalized unitarity cuts, we conclude that the L–loop integrand inverts as

$$I\left[\mathcal{I}_n^L\right] = \left(\prod_{i \in \mathcal{E}} x_i^2\right) \left(\prod_{i=1}^{L} (x_{l_i}^2)^4\right) \mathcal{I}_n^L \, . \tag{3.45}$$

For a recent discussion of the transition from cuts to the amplitude, see ref. [92]. Note

that bubbles on external lines are not cut detectable, so they potentially violate eq. (3.45). However, because this is the maximally supersymmetric theory, we do not expect these contributions to appear [92].

If we restrict the loop integration measure in eq. (3.38) to a four-dimensional subspace, as when interpreting the two extra dimensions as a massive regulator, the measure will provide an extra inversion weight of $\prod_i (x_{l_i}^2)^{-4}$, which exactly cancels the extra weight of the integrand. The inversion then commutes with the integration, since the infrared singularities have been regulated, and the amplitude obeys an exact dual conformal symmetry to all loops, which we may write as

$$I\left[\int \left(\prod_{i=1}^{L} d^4 x_{l_i}\right) \mathcal{I}_n^L\right] = \left(\prod_{i\in\mathcal{E}} x_i^2\right) \int \left(\prod_{i=1}^{L} d^4 x_{l_i}\right) \mathcal{I}_n^L\,, \qquad \text{(massively regulated } \mathcal{N}=4\text{)}\,. \tag{3.46}$$

3.5 Comments

In this chapter we demonstrated that the six-dimensional maximal sYM tree-level amplitudes and multiloop integrands exhibit dual conformal covariance. While dual conformal symmetry has been shown to exist for theories in $D \neq 4$ [93], it is noteworthy that such a symmetry can be defined for theories which are not invariant under ordinary conformal symmetry [2, 94]. Also, because a massless on-shell particle in six dimensions is equivalent to a massive particle in four dimensions, our six-dimensional result then naturally gives the dual conformal properties of the massively regulated four-dimensional $\mathcal{N}=4$ theory [90].

Part II

BCJ Color-Kinematics Duality and Squaring Relations

CHAPTER 4

Gravity as the Square of Gauge Theory

4.1 Introduction

A key lesson from studies of scattering amplitudes is that weakly coupled gauge and gravity theories have a far simpler and richer structure than is evident from their usual Lagrangians. A striking example of this is Witten's remarkable conjecture that scattering amplitudes in twistor space are supported on curves of a degree controlled by their helicity and loop order [11, 95, 96]. At weak coupling another remarkable structure visible in on-shell tree amplitudes are the Kawai-Lewellen-Tye (KLT) relations, which express gravity tree-level amplitudes as sums of products of gauge-theory amplitudes [74, 97]. These relations were originally formulated in string theory, but hold just as well in field theory. In fact, in many cases, they hold even when no string theory lives above the field theory [98].

The KLT relations have recently been recast into a much simpler form in terms of numerators of diagrams with only three-point vertices. In the new representation the diagrammatic numerators in gravity are simply a product of two corresponding gauge-theory numerators [15]. Underlying these numerator "squaring relations" is a newly discovered duality between kinematic numerators of gauge theory and their associated color factors, by Bern, Carrasco and Johansson (BCJ). The BCJ duality states that gauge-theory amplitudes can be arranged into a form where diagrammatic numerators satisfy a set of identities in one-to-one correspondence to the Jacobi identities obeyed by color factors. The duality appears to hold in large classes of theories including pure Yang-Mills theory and $\mathcal{N} = 4$ super-Yang-Mills. BCJ conjectured that the numerators of gravity diagrams are simply the product of two corresponding gauge-theory numerators that satisfy the duality. These squaring relations

were verified in ref. [15] at tree level up to eight points. Interestingly, the duality also leads to a set of non-trivial relations between gauge-theory amplitudes [15], which are now well understood in string theory [99]. The numerator duality relations have also been understood from the vantage point of string theory [100, 101, 102]. In particular, the heterotic string offers important insight into these relations, because of the parallel treatment of color and kinematics [101].

The unitarity method [41] immediately implies that gravity loop amplitudes must have the double-copy property, if the corresponding gauge-theory loop amplitudes can be put in a form that satisfies the BCJ duality, as does indeed appear to be the case [103]. The squaring relations then apply to gravity numerators for *any* value of loop momenta, *i.e.* with no cut conditions applied. This is to be contrasted with the KLT relations, which are valid only at tree level, and can be applied at loop level only on unitarity cuts that decompose loop amplitudes into tree amplitudes [69]. The KLT relations take a different functional form for every cut of a given amplitude, depending on the precise tree-amplitude factors involved in the cut. The squaring relations, on the other hand, take a simple universal form for any choice of loop momenta.

In our approach to understand the color-kinematics duality, we use a more traditional Lagrangian viewpoint. A natural question is: what Lagrangian generates diagrams that automatically satisfy the BCJ duality? We shall describe such a Lagrangian here, and present its explicit form up to five points. We have also worked out the six-point Lagrangian and outline its structure, and make comments about the all-orders form of the Lagrangian. We find that a covariant Lagrangian whose diagrams satisfy the duality is necessarily non-local. We can make this Lagrangian local by introducing auxiliary fields. Remarkably we find that, at least through six points, the Lagrangian differs from ordinary Feynman gauge simply by the addition of an appropriate zero, namely terms that vanish by the color Jacobi identity. Although the additional terms vanish when summed, they appear in diagrams in just the right way so that the BCJ duality is satisfied. Based on the structures we find, it seems likely that any covariant Lagrangian where diagrams with an arbitrary number of external legs satisfy the duality must have an infinite number of interactions.

In ref. [104], the problem was posed of how to construct a Lagrangian that reflects the double-copy property of gravity. That reference carried out some initial steps, showing that one can factorize the graviton indices into "left" and "right" classes consistent with the factorization observed in the KLT relations. (See also ref. [105].) Unfortunately, beyond three points the relationship of the constructed gravity Lagrangian to gauge theory was rather obscure. As it turns out, a key ingredient was missing: the duality between color and kinematics, which was discovered much later [15]. Using the modified local version of the gauge-theory Lagrangian whose Feynman diagrams respect the BCJ duality, we construct a Lagrangian for gravity valid through five points, as a double copy of the gauge-theory one. The likely appearance of an infinite number of interactions in the modified gauge-theory Lagrangian is perhaps natural, because we expect any covariant gravity Lagrangian to also have an infinite number of terms.

We present a simple application of the BCJ duality. Since the BCJ duality states that diagrammatic numerators have the same algebraic structure as color factors, we can immediately make use of different known color representations of amplitudes to write dual formulas where color and kinematic numerators are swapped. In particular, Del Duca, Dixon and Maltoni [106] have given a color decomposition of tree amplitudes using adjoint-representation color matrices. They derived this color decomposition using the color Jacobi identity and Kleiss-Kuijf relations [107]. By swapping color and numerator factors in their derivation, we immediately obtain novel forms of both gauge-theory and gravity tree amplitudes.

4.2 Review of BCJ duality

4.2.1 General Considerations

Consider a gauge-theory amplitude, which we write in a diagrammatic form,

$$\frac{1}{g^{n-2}}\,\mathcal{A}_n^{\text{tree}}(1,2,3,\ldots,n) \;=\; \sum_{\text{diags. } i} \frac{n_i c_i}{\prod_{\alpha_i} s_{\alpha_i}}\,, \tag{4.1}$$

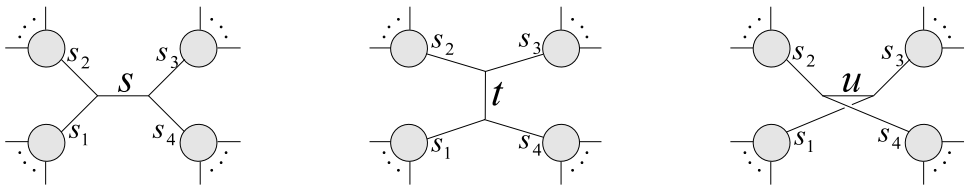

Figure 4.1: A Jacobi relation between color factors of diagrams. According to the BCJ duality the diagrammatic numerators of amplitudes can be arranged in a way that they satisfy relations in one-to-one correspondence to the color Jacobi identities.

where the sum runs over all diagrams i with only three-point vertices, the c_i are color factors, the n_i are kinematic numerators, and the s_{α_i} are the inverse propagators associated with the channels α_i of the diagram i. Any gauge-theory amplitude can be put into this form by replacing contact terms with numerator factors canceling propagators, *i.e.,* s_α/s_α and assigning the contribution to the proper diagram according to the color factor. The value of the color coefficient c_i of each term is obtained from the diagram i by dressing each three-point vertex with a structure constant $\tilde{f}^{abc}$, where

$$\tilde{f}^{abc} \equiv i\sqrt{2} f^{abc} = \mathrm{Tr}\big([T^a, T^b]\, T^c\big), \tag{4.2}$$

and dressing each internal line with δ^{ab}.

A key property of the $\tilde{f}^{abc}$ is that they satisfy the Jacobi identity. Consider, for example, the color factors of the three diagrams illustrated in Fig. 4.1. They take the schematic form,

$$c_s \equiv \ldots \tilde{f}^{a_1 a_2 b} \tilde{f}^{b a_3 a_4} \ldots\,, \qquad c_t \equiv \ldots \tilde{f}^{a_1 a_4 b} \tilde{f}^{b a_2 a_3} \ldots\,, \qquad c_u \equiv \ldots \tilde{f}^{a_1 a_3 b} \tilde{f}^{b a_4 a_2} \ldots\,, \tag{4.3}$$

where the '$\ldots$' signify factors common to all three diagrams. The color factors then, of course, satisfy the Jacobi identity

$$c_s + c_t + c_u = 0\,. \tag{4.4}$$

Here we have chosen a sign convention[1] that differs from ref. [15].

The BCJ conjecture states that numerators n_i can always be found that satisfy Jacobi relations in one-to-one correspondence with the color Jacobi identities,

$$c_i + c_j + c_k = 0 \qquad \Rightarrow \qquad n_i + n_j + n_k = 0\,, \tag{4.5}$$

where i, j and k label diagrams whose color factors are related by a Jacobi identity. (In general the relative signs between the color factors in all Jacobi identities cannot be taken to be globally positive, but according to the BCJ conjecture the relative signs always match between the color and kinematic identities.) In addition, BCJ duality also requires that the n_i satisfy the same self-anti-symmetry relations as the c_i. That is, if a color factor is anti-symmetric under an interchange of two legs, the corresponding numerator satisfies the same antisymmetry relations,

$$c_i \to -c_i \qquad \Rightarrow \qquad n_i \to -n_i\,. \tag{4.6}$$

We note that when the color-ordered partial amplitudes are expressed in terms of numerators satisfying these self-anti-symmetry relations, they automatically satisfy the Kleiss-Kuijf relations [107, 106] between color-ordered partial amplitudes [15].

4.2.2 Five-point example and generalized Jacobi-like structures

Consider the five-point case as a simple example, discussed already in some detail from various viewpoints in refs. [15, 100, 101, 102]. At five points there are 15 numerators and 9 independent duality relations, leaving 6 numerators. Of these remaining numerators, 4 can be chosen arbitrarily due to a "generalized gauge invariance". By choosing the remaining two n_i to correctly give two of the partial amplitudes, non-trivial relations between color-ordered amplitudes can be derived from the condition that the remaining partial amplitudes

[1] In any given Jacobi relation the relative signs are arbitrary since they always can be moved between color factors and kinematic numerators.

are also reproduced correctly. For example,

$$s_{35}A_5^{\rm tree}(1,2,4,3,5) - (s_{13}+s_{23})A_5^{\rm tree}(1,2,3,4,5) - s_{13}A_5^{\rm tree}(1,3,2,4,5) = 0\,. \tag{4.7}$$

This relation has generalizations for an arbitrary number of external legs [15], which have been derived using string theory [99].

As discussed in refs. [101, 102], eq. (4.7) is equivalent to a relation that exhibits a Jacobi-like structure,

$$\frac{n_4 - n_1 + n_{15}}{s_{45}} - \frac{n_{10} - n_{11} + n_{13}}{s_{24}} - \frac{n_3 - n_1 + n_{12}}{s_{12}} - \frac{n_5 - n_2 + n_{11}}{s_{51}} = 0\,, \tag{4.8}$$

where only the sum over terms is required to vanish. In this equation, the Jacobi-like structure involves additional minus signs because we follow the sign conventions given in ref. [15] for the expansion of the five-point amplitude,

$$\begin{aligned}
A_5^{\rm tree}(1,2,3,4,5) &\equiv \frac{n_1}{s_{12}s_{45}} + \frac{n_2}{s_{23}s_{51}} + \frac{n_3}{s_{34}s_{12}} + \frac{n_4}{s_{45}s_{23}} + \frac{n_5}{s_{51}s_{34}}\,,\\
A_5^{\rm tree}(1,2,4,3,5) &\equiv \frac{n_{12}}{s_{12}s_{35}} + \frac{n_{11}}{s_{24}s_{51}} - \frac{n_3}{s_{43}s_{12}} + \frac{n_{13}}{s_{35}s_{24}} - \frac{n_5}{s_{51}s_{43}},\\
A_5^{\rm tree}(1,3,2,4,5) &= \frac{n_{15}}{s_{13}s_{45}} - \frac{n_2}{s_{23}s_{51}} - \frac{n_{10}}{s_{24}s_{13}} - \frac{n_4}{s_{45}s_{23}} - \frac{n_{11}}{s_{51}s_{24}}\,.
\end{aligned} \tag{4.9}$$

As explained in ref. [101, 102], relations of the form (4.8) are the natural gauge-invariant numerator identities that emerge from string theory. Because of the generalized gauge invariance, these relations are less stringent than the BCJ duality. Indeed, the individual terms in eq. (4.8) are not required to vanish, but only their sum. We note that the heterotic string offers some important insight into the BCJ duality (4.5): in the heterotic string both color and kinematics arise from world-sheet fields, making the duality more natural [101]. Identities of the form (4.8), though interesting, will not play a role in the analysis below. In the remainder of this paper we will only be concerned with numerators n_i that satisfy the more stringent BCJ-duality requirements of eq. (4.5).

4.2.3 Gravity squaring relations

Another conjecture in ref. [15] is that gravity tree amplitudes can be constructed directly from the n_i through "squaring relations". Consider two gauge-theory amplitudes,

$$\begin{aligned} \frac{1}{g^{n-2}} \mathcal{A}_n^{\text{tree}}(1,2,3,\ldots,n) &= \sum_{\text{diags. } i} \frac{n_i c_i}{\prod_{\alpha_i} s_{\alpha_i}}\,, \\ \frac{1}{\tilde{g}^{n-2}} \widetilde{\mathcal{A}}_n^{\text{tree}}(1,2,3,\ldots,n) &= \sum_{\text{diags. } i} \frac{\tilde{n}_i \tilde{c}_i}{\prod_{\alpha_i} s_{\alpha_i}}\,. \end{aligned} \tag{4.10}$$

These two amplitudes do not have to be from the same theory, and can have differing gauge groups and particle contents. In ref. [15] the requirement that *both* the n_i and the $\tilde{n}_i$ satisfy the BCJ duality was imposed, *i.e.* they satisfy all duality conditions $n_i + n_j + n_k = 0$ and $\tilde{n}_i + \tilde{n}_j + \tilde{n}_k = 0$. The conjectured squaring relations state that gravity amplitudes are given simply by

$$\frac{-i}{(\kappa/2)^{n-2}} \mathcal{M}_n^{\text{tree}}(1,2,3,\ldots,n) = \sum_{\text{diags. } i} \frac{n_i \tilde{n}_i}{\prod_j s_{\alpha_i}}\,, \tag{4.11}$$

where the sum runs over the same set of diagrams as in eq. (4.10). The states appearing in the gravity theory are just direct products of gauge-theory states, and their interactions are dictated by the product of the gauge-theory momentum-space three-point vertices. The squaring relations (4.11) were explicitly checked through eight points and have recently been understood from the KLT relations in heterotic string theory [101].

Using standard factorization arguments it is simple to see why one would expect the BCJ duality to imply that gravity numerators are a double copy of gauge-theory numerators. Let us assume that the numerators of all n-point gauge-theory amplitudes (4.1) satisfy the BCJ duality (4.5). Let us also assume that we have already proven that the squaring relations (4.11) hold for amplitudes with fewer legs. Consider an ansatz for the n-point graviton amplitude given in terms of diagrams by the double-copy formula (4.11). We now step through all possible factorization channels using real momenta. By general field-theory considerations we know that in each channel the diagrams break up into products of lower-

point diagrams. The sum over diagrams on each side of the factorization pole forms a lower-point amplitude. Since each numerator factor of the n-point expression satisfies the duality condition, we expect the lower-point tree diagrams on each side of the factorized propagator to inherit this property when we choose special kinematics to factorize a diagram. Thus on each side of the pole we have a correct set of double-copy numerators for the lower-point gravity amplitudes. Stepping through all factorization channels we see that we have correct diagram-by-diagram factorizations in all channels. This provides a strong indication that the double-copy property follows from BCJ duality.

4.3 A Lagrangian generating diagrams with BCJ duality

We now turn to the question of finding a Lagrangian which generates amplitudes with numerators that manifestly satisfy the BCJ duality. If a local Lagrangian of this type could be found, it would enable us to construct a corresponding gravity Lagrangian whose squaring relations with Yang-Mills theory are manifest. We show that such a construction is indeed possible, and we present the explicit form of a Yang-Mills Lagrangian which generates diagrams that respect the BCJ duality up to five points. We use it to construct the corresponding Lagrangian for gravity. We also outline the structure of Lagrangians that preserve the duality in higher-point diagrams.

4.3.1 General strategy of the construction

A Yang-Mills Lagrangian with manifest BCJ duality can only differ from the conventional Yang-Mills Lagrangian by terms that do not affect the amplitudes. The amplitudes are unaffected, for example, by adding total derivative terms or by carrying out field redefinitions. In fact, the MHV Lagrangian [108] for the CSW [12] expansion is an example where identities or structures of tree-level amplitudes can be derived through a field redefinition of the original Lagrangian. Such a construction has the additional complication that a Jacobian can appear at loop level. Surprisingly, we find that not only does a Lagrangian with manifest BCJ duality exist, it differs from the conventional Lagrangian by terms whose sum is identically zero by

the color Jacobi identity! Although the sum over added terms vanishes, they cause the necessary rearrangements so that the BCJ duality holds. Another curious property is that the additional terms are necessarily non-local, at least if we want a covariant Lagrangian without auxiliary fields.

For example, consider five-gluon tree amplitudes. To obtain diagrams that satisfy the BCJ duality one is required to add terms to the Lagrangian of the form

$$\mathcal{L}_5' \sim \mathrm{Tr}\,[A^\nu, A^\rho]\frac{1}{\Box}\big([[\partial_\mu A_\nu, A_\rho], A^\mu] + [[A_\rho, A^\mu], \partial_\mu A_\nu] + [[A^\mu, \partial_\mu A_\nu], A_\rho]\big), \tag{4.12}$$

along with other contractions. If we expand the commutators, the added terms immediately vanish by the color Jacobi identity. If, however, the commutators are re-expressed in terms of group-theory structure constants, they generate terms that get distributed across different diagrams and color factors. We find similar results up to six points, suggesting that it is a general feature for any number of points.

Since the BCJ duality relates the structure of kinematic numerators and color factors of diagrams with only three-point vertices, the desired Lagrangian should contain only three-point interactions. To achieve this we introduce auxiliary fields. The auxiliary fields not only reduce the interactions down to only three points, they also convert the newly introduced non-local terms into local interactions. This procedure introduces a large set of auxiliary fields into the Lagrangian. This is not surprising since we want a double copy of this Lagrangian to describe gravity. The ordinary gravity Lagrangian contains an infinite set of contact terms; if we were to write it in terms of three-point interactions we would need to introduce a new set of auxiliary fields for each new contact term in the expansion. Since in our approach the gravity Lagrangian is simply the square of the Yang-Mills Lagrangian, it is natural to expect that the desired Lagrangian contains a large (perhaps infinite) number of auxiliary fields. We now begin our construction of a Yang-Mills Lagrangian with manifest BCJ duality.

4.3.2 The Yang-Mills Lagrangian through five points

We write the Yang-Mills Lagrangian as

$$\mathcal{L}_{YM} = \mathcal{L} + \mathcal{L}'_5 + \mathcal{L}'_6 + \dots \tag{4.13}$$

where $\mathcal{L}$ is the conventional Yang-Mills Lagrangian and $\mathcal{L}'_n$, $n > 4$ are the additional terms required to satisfy the BCJ duality. At four points, the BCJ duality is trivially satisfied in any gauge [15], so $\mathcal{L}$ by itself will generate diagrams whose numerators satisfy eq. (4.5). For simplicity we choose Feynman gauge for $\mathcal{L}$,[2] though similar conclusions hold for other gauges. All contact terms are uniquely assigned to the three-vertex diagram carrying the corresponding color factor. The $\mathcal{L}'_n$ are required to leave scattering amplitudes invariant, and they must rearrange the numerators of diagrams in a way so that the BCJ duality is satisfied. It turns out that the set of terms with the desired properties is not unique. Indeed, "self-BCJ" terms that satisfy the BCJ duality by themselves can also be added. This ambiguity is related to the residual "gauge invariance" that remains after solving the duality identities [15, 101].

By imposing the constraint that the generated five-point diagrams satisfy the BCJ duality (4.5), we find the following Lagrangian:

$$\begin{aligned}
\mathcal{L} &= \tfrac{1}{2} A^a_\mu \Box A^{a\mu} - g f^{a_1 a_2 a_3} \partial_\mu A^{a_1}_\nu A^{a_2 \mu} A^{a_3 \nu} - \tfrac{1}{4} g^2 f^{a_1 a_2 b} f^{b a_3 a_4} A^{a_1}_\mu A^{a_2}_\nu A^{a_3 \mu} A^{a_4 \nu} \\
\mathcal{L}'_5 &= -\tfrac{1}{2} g^3 f^{a_1 a_2 b} f^{b a_3 c} f^{c a_4 a_5} \\
&\quad \times \left(\partial_{[\mu} A^{a_1}_{\nu]} A^{a_2}_\rho A^{a_3 \mu} + \partial_{[\mu} A^{a_2}_{\nu]} A^{a_3}_\rho A^{a_1 \mu} + \partial_{[\mu} A^{a_3}_{\nu]} A^{a_1}_\rho A^{a_2 \mu} \right) \frac{1}{\Box} (A^{a_4 \nu} A^{a_5 \rho}) \,.
\end{aligned} \tag{4.14}$$

The numerators n_i are derived from this action by first computing the contribution from the three-point vertices, which gives a set of three-vertex diagrams with unique numerators. Then the contributions from the four- and five-point interaction terms are assigned to the various diagrams with only three-point vertices according to their color factors. Since these terms will contain fewer propagators than those obtained by using only three-point vertices,

[2] We are considering only tree level at this point. Therefore we ignore ghost terms.

their contributions to the numerators contain inverse propagators. Finally, we combine all diagrams with the same color factor, however they arose in the procedure above, into a single diagram. Its kinematic coefficient is the desired numerator that satisfies the BCJ duality. In this light, the purpose of $\mathcal{L}_5'$ is to restore the BCJ duality (4.5) violated by the interaction terms of $\mathcal{L}$.

Although $\mathcal{L}_5'$ is not explicitly local, as we mentioned, we can make it local by the introduction of auxiliary fields. It turns out that without auxiliary fields there is no solution for a local Lagrangian in any covariant gauge that generates numerators satisfying the BCJ duality. The non-locality explains the difficulty of stumbling onto this Lagrangian without knowing its desired property ahead of time.

As previously mentioned, $\mathcal{L}_5'$ is identically zero by the color Jacobi identity. To see this we can relabel color indices to obtain

$$\begin{aligned}\mathcal{L}_5' = &-\tfrac{1}{2}g^3(f^{a_1a_2b}f^{ba_3c} + f^{a_2a_3b}f^{ba_1c} + f^{a_3a_1b}f^{ba_2c})f^{ca_4a_5} \\ &\times \partial_{[\mu}A^{a_1}_{\nu]}A^{a_2}_{\rho}A^{a_3\mu}\frac{1}{\Box}(A^{a_4\nu}A^{a_5\rho})\,. \end{aligned} \tag{4.15}$$

As apparent in (4.15), the canceling terms have different color factors and thus appear in different channels. For the individual diagrams these terms are non-vanishing. Furthermore, they alter the numerators of the individual diagrams such that the BCJ duality (4.5) is satisfied.

It is interesting to note that there is one other term that can be added to Yang-Mills at five points which preserves the relation (4.5):

$$\begin{aligned}\mathcal{D}_5 = &\tfrac{-\beta}{2}g^3 f^{a_1a_2b}f^{ba_3c}f^{ca_4a_5} \\ &\times \left(\partial_{(\mu}A^{a_1}_{\nu)}A^{a_2}_{\rho}A^{a_3\mu} + \partial_{(\mu}A^{a_2}_{\nu)}A^{a_3}_{\rho}A^{a_1\mu} + \partial_{(\mu}A^{a_3}_{\nu)}A^{a_1}_{\rho}A^{a_2\mu}\right)\frac{1}{\Box}(A^{a_4\nu}A^{a_5\rho})\,, \end{aligned} \tag{4.16}$$

where β is an arbitrary parameter. $\mathcal{D}_5$ also vanishes identically by the color Jacobi identity. Since $\mathcal{D}_5$ does not serve to correct lower-point contributions to make the BCJ duality relations hold through five points, we do not need to include it. It does however show that there are

families of Lagrangians with the desired properties.

4.3.3 Towards gravity

Now that we have a Lagrangian that gives the desired numerators n_i for gauge theory (4.10), we use it to construct the tree-level gravity Lagrangian by demanding that it gives diagrams whose numerators are a double copy of the gauge-theory numerators, as in eq. (4.11). However, as explained above, we need to first bring the Yang-Mills Lagrangian into a cubic form to achieve this. We can do so by introducing an auxiliary field $B^a_{\mu\nu}$:

$$\mathcal{L}_{YM} = \tfrac{1}{2} A^{a\mu} \Box A^a_\mu + B^{a\mu\nu} B^a_{\mu\nu} - g f^{abc} (\partial_\mu A^a_\nu + B^a_{\mu\nu}) A^{b\mu} A^{c\nu} \,. \tag{4.17}$$

This is equivalent to the ordinary Yang-Mills Lagrangian as we can immediately verify by integrating out $B^a_{\mu\nu}$, *i.e.* by substituting the equation of motion of $B^a_{\mu\nu}$,

$$B^a_{\mu\nu} = \frac{g}{2} f^{abc} (A^b_\mu A^c_\nu) \,. \tag{4.18}$$

Since the BCJ duality is trivially satisfied through four points, naively one would take the square of this action to obtain a tree-level action for gravity valid through four points. However, since the squaring is with respect to the numerators n_i and not numerator over propagator, n_i/s_α, we need the auxiliary fields to generate the numerators with the inverse propagators directly, instead of multiplying and dividing by inverse propagators afterwards. This implies that the auxiliary fields must become dynamical (to generate the required propagator) and that their interactions must contain additional derivatives to produce the inverse propagator necessary to cancel the propagator. At four points this leads to the Lagrangian:

$$\mathcal{L}_{YM} = \tfrac{1}{2} A^{a\mu} \Box A^a_\mu - B^{a\mu\nu\rho} \Box B^a_{\mu\nu\rho} - g f^{abc} (\partial_\mu A^a_\nu + \partial^\rho B^a_{\rho\mu\nu}) A^{b\mu} A^{c\nu} \,, \tag{4.19}$$

where the equation of motion for the auxiliary field $B^a_{\mu\nu\rho}$ becomes

$$\Box B^a_{\mu\nu\rho} = \frac{g}{2} f^{abc} \partial_\mu (A^b_\nu A^c_\rho) \,. \tag{4.20}$$

We are now ready to construct a gravity action that gives the correct four-point amplitude. We begin in momentum space, where the identification

$$A_\mu(k)\tilde{A}_\nu(k) \to h_{\mu\nu}(k) \tag{4.21}$$

can be trivially implemented. We first demonstrate how the gravity action can be derived from the four-point Yang-Mills Lagrangian. We write the Yang-Mills Lagrangian in momentum space. Since gravity does not have any color indices, we encode the information of the structure constants in the anti-symmetrization and cyclicity of the interaction terms. We drop the coupling constant for now; it can easily be restored in the final gravity action. We also neglect factors of 2π in the measure for convenience. We arrive at

$$\begin{aligned} \mathcal{S}_{YM} \sim \frac{1}{2} \int d^D k_1 d^D k_2 \, \delta^D(k_1 + k_2) k_2^2 \Big[A^\mu(k_1) A_\mu(k_2) - 2 B^{\mu\nu\rho}(k_1) B_{\mu\nu\rho}(k_2) \Big] \,, \\ + \int d^D k_1 d^D k_2 d^D k_3 \, \delta^D(k_1 + k_2 + k_3) \\ \times P_6 \Big\{ \big[k_{1\mu} A_\nu(k_1) + k_1^\rho B_{\rho\mu\nu}(k_1) \big] A^\mu(k_2) A^\nu(k_3) \Big\} \,, \end{aligned} \tag{4.22}$$

where P_6 indicates a sum over all permutations of $\{k_1, k_2, k_3\}$ with the anti-symmetrization signs included. From here, we can read off a gravity action valid through four points:

$$\mathcal{S}_{\text{grav}} = \mathcal{S}_{\text{kin}} + \mathcal{S}_{\text{int}} \,, \tag{4.23}$$

with

$$\begin{aligned}
\mathcal{S}_{\rm kin} \sim & \frac{1}{4}\int d^D k_1 d^D k_2 \delta^D(k_1+k_2) k_2^2 \\
& \times \Big[A^\mu(k_1)A_\mu(k_2) - 2B^{\mu\nu\rho}(k_1)B_{\mu\nu\rho}(k_2)\Big] \\
& \times \Big[\tilde{A}^\sigma(k_1)\tilde{A}_\sigma(k_2) - 2\tilde{B}^{\sigma\tau\lambda}(k_1)\tilde{B}_{\sigma\tau\lambda}(k_2)\Big] , \\
\mathcal{S}_{\rm int} \sim & \int d^D k_1 d^D k_2 d^D k_3 \delta^D(k_1+k_2+k_3) \\
& \times P_6\Big\{\big[k_{1\mu}A_\nu(k_1) + k_1^\rho B_{\rho\mu\nu}(k_1)\big]A^\mu(k_2)A^\nu(k_3)\Big\} \\
& \times P_6\Big\{\big[k_{1\lambda}\tilde{A}_\sigma(k_1) + k_1^\tau \tilde{B}_{\tau\lambda\sigma}(k_1)\big]\tilde{A}^\lambda(k_2)\tilde{A}^\sigma(k_3)\Big\} .
\end{aligned} \tag{4.24}$$

In extracting the Feynman rules from this action the "left" and "right" fields each contract independently. For example, for the propagators we have,

$$\begin{aligned}
\langle A_\mu(k_1)\tilde{A}_\rho(k_1)A_\nu(k_2)\tilde{A}_\sigma(k_2)\rangle &= \frac{i\eta_{\mu\nu}\eta_{\rho\sigma}}{k_1^2}\delta^4(k_1+k_2) , \\
\langle A_\mu(k_1)\tilde{B}_{\rho\sigma\tau}(k_1)A_\nu(k_2)\tilde{B}_{\eta\kappa\lambda}(k_2)\rangle &= -\frac{i\eta_{\mu\nu}\eta_{\rho\eta}\eta_{\sigma\kappa}\eta_{\tau\lambda}}{2k_1^2}\delta^4(k_1+k_2) .
\end{aligned} \tag{4.25}$$

By construction, this action will give the correct three- and four-graviton tree-level amplitudes.

We note that one can construct the coordinate-space action by combining the left-right fields as

$$\begin{aligned}
A^\mu\tilde{A}^\nu &\rightarrow h^{\mu\nu} , \\
A^\mu\tilde{B}^{\nu\rho\sigma} &\rightarrow g^{\mu\nu\rho\sigma} , \\
B^{\mu\rho\sigma}\tilde{A}^\nu &\rightarrow \tilde{g}^{\mu\rho\sigma\nu} , \\
B^{\mu\rho\sigma}\tilde{B}^{\nu\tau\lambda} &\rightarrow f^{\mu\rho\sigma\nu\tau\lambda} ,
\end{aligned} \tag{4.26}$$

where $h^{\mu\nu}$ is the physical field, which includes the graviton, anti-symmetric tensor, and

dilaton. The kinetic terms in x space take the form

$$\mathcal{S}_{\rm kin} = -\frac{1}{2}\int d^D x \Big[h^{\mu\nu}\Box h_{\mu\nu} - 2g^{\mu\nu\rho\sigma}\Box g_{\mu\nu\rho\sigma} - 2\tilde{g}^{\mu\nu\rho\sigma}\Box\tilde{g}_{\mu\nu\rho\sigma} + 4f^{\mu\nu\rho\sigma\tau\lambda}\Box f_{\mu\nu\rho\sigma\tau\lambda}\Big] . \quad (4.27)$$

The interaction terms can similarly be constructed, but we do not display them here as there are 144 of them.

To move on to five points, we need to introduce a new set of auxiliary fields to rewrite the non-local terms in a local and cubic form. We simply give the result:

$$\begin{aligned}\mathcal{L}_5' \to\ & Y^{a\mu\nu}\Box X^a_{\mu\nu} + D^{a\mu\nu\rho}_{(3)}\Box C^a_{(3)\ \mu\nu\rho} + D^{a\mu\nu\rho\sigma}_{(4)}\Box C^a_{(4)\ \mu\nu\rho\sigma} \\ & + g f^{abc}\left(Y^{a\mu\nu}A^b_\mu A^c_\nu + \partial_\mu D^{a\mu\nu\rho}_{(3)}A^b_\nu A^c_\rho - \tfrac{1}{2}\partial_\mu D^{a\mu\nu\rho\sigma}_{(4)}\partial_{[\nu}A^b_{\rho]}A^c_\sigma\right) \\ & + g f^{abc}X^{a\mu\nu}\left(\tfrac{1}{2}\partial_\rho C^{b\rho\sigma}_{(3)\ \mu}\partial_{[\sigma}A^c_{\nu]} + \partial_\rho C^{b\rho\sigma}_{(4)\ \nu[\mu}A^c_{\sigma]}\right) . \end{aligned} \quad (4.28)$$

Note that these new auxiliary fields do not couple to $B^{\mu\nu\rho}$. It is now straight-forward to transform (4.28) to momentum space and, through the squaring process, obtain a gravity Lagrangian that is valid through five points.

4.3.4 Beyond five points

As we increase the number of legs we find new violations of manifest BCJ duality, so we need to add further terms. We have constructed a six-point correction to the interactions so that the Lagrangian generates numerators with manifest BCJ duality.

The general structure of $\mathcal{L}_6'$ is similar to that of $\mathcal{L}_5'$; after relabeling color indices, we can arrange $\mathcal{L}_6'$ to vanish by two Jacobi identities:

$$\begin{aligned} 0 &= \left(f^{a_1a_2b}f^{ba_3c} + f^{a_2a_3b}f^{ba_1c} + f^{a_3a_1b}f^{ba_2c}\right)f^{cda_6}f^{da_4a_5}\,, \\ 0 &= f^{a_1a_2b}\left(f^{ba_3c}f^{cda_6} + f^{bdc}f^{ca_6a_3} + f^{ba_6c}f^{ca_3d}\right)f^{da_4a_5}. \end{aligned} \quad (4.29)$$

The first of these two color factors is contracted with 59 different terms having a schematic

form[3]

$$\frac{1}{\Box}(A^{a_1}A^{a_2}A^{a_3})\frac{1}{\Box}(A^{a_4}A^{a_5})A^{a_6}\,, \tag{4.30}$$

where the parenthesis indicate which fields the $\frac{1}{\Box}$ acts on. The second color factor contracts with 49 terms of the form

$$\frac{1}{\Box}(A^{a_1}A^{a_2})A^{a_3}\frac{1}{\Box}(A^{a_4}A^{a_5})A^{a_6}\,. \tag{4.31}$$

In each term, there are an additional two partial derivatives in the numerator acting on the gauge fields. The large number of terms arises from the many different ways to contract the 8 Lorentz indices. We have found that the coefficients of these 108 terms depend on 30 distinct free parameters, in addition to the β that showed up at five points (4.16). Thus, there is a 30-parameter family of self-BCJ six-point interactions.

We anticipate that this structure continues to higher orders, with the addition of new vanishing combinations of terms. We have seen no indication that the Lagrangian will terminate; for each extra leg that we add to an amplitude, we will likely need to add more terms to the action to ensure that the diagrams satisfy the BCJ duality. A key outstanding problem is to find a pattern or symmetry that would enable us to write down the all-order BCJ-corrected action without having to analyze each n-point level at a time.

If the construction of a Lagrangian to all orders succeeds, it would be a fully off-shell realization of the BCJ duality at the classical level. It would be interesting to then study non-perturbative phenomena such as instantons using this Lagrangian to see whether BCJ duality and the squaring relations can elucidate physics beyond the regime of scattering amplitudes. Our off-shell construction suggests that BCJ duality may also work at loop level. Of course, one would need to account for the ghost structure and, more importantly, demonstrate that the loop amplitudes so constructed do indeed have the desired duality properties manifest.

[3]Momentum conservation can alter these counts but we give them as an indication of the number of terms involved.

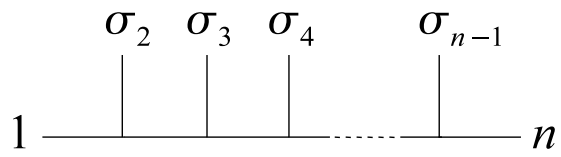

Figure 4.2: A graphical representation of the color basis $c_{1,\sigma_2,\ldots,\sigma_{n-1},n}$ introduced in ref. [106]. Each vertex represents a structure constant $\tilde{f}^{abc}$, while each bond indicates contracted indices between the $\tilde{f}^{abc}$. This is also precisely the diagram associated with the kinematic numerator $n_{1,\sigma_2,\ldots,\sigma_{n-1},n}$.

4.4 A few simple implications

In this short section, we point out that the BCJ duality immediately leads to some novel forms of gauge and gravity amplitudes. Del Duca, Dixon and Maltoni [106] presented an alternative color decomposition from the usual one,

$$\mathcal{A}_n^{\text{tree}}(1,2,\ldots,n) = g^{n-2} \sum_{\sigma\in S_{n-2}} c_{1,\sigma_2,\ldots,\sigma_{n-1},n} A_n^{\text{tree}}(1,\sigma_2,\ldots,\sigma_{n-1},n)\,, \tag{4.32}$$

where $\mathcal{A}_n^{\text{tree}}$ is the full color-dressed n-gluon amplitude, and the A_n^{tree} are the usual color-ordered partial gauge-theory amplitudes. The sum runs over all permutations of $n-2$ legs. The color factors are

$$c_{1,\sigma_2,\ldots,\sigma_{n-1},n} \equiv \tilde{f}^{a_1 a_{\sigma_2} x_1}\tilde{f}^{x_1 a_{\sigma_3} x_2}\cdots\tilde{f}^{x_{n-3} a_{\sigma_{n-1}} a_n}\,. \tag{4.33}$$

Diagrammatically, this color factor is associated with Fig. 4.2. This form is derived starting from eq. (4.1) and using color Jacobi identities along with the Kleiss-Kuijf relations, which are equivalent to the self-anti-symmetry of the diagrammatic numerator factors.

A simple observation is that when diagram numerators are chosen to satisfy the BCJ duality, they have precisely the same algebraic structure as color factors. Thus, we can immediately write a dual formula decomposing the full amplitude into numerators instead of color factors:

$$\mathcal{A}_n^{\text{tree}}(1,2,\ldots,n) = g^{n-2} \sum_{\sigma\in S_{n-2}} n_{1,\sigma_2,\ldots,\sigma_{n-1},n}\, A_n^{\text{scalar}}(1,\sigma_2,\ldots,\sigma_{n-1},n)\,, \tag{4.34}$$

where A_n^{scalar} is a dual partial scalar amplitude with ordered legs obtained by replacing the gauge-theory numerator factors with group-theory color factors. The numerator factors $n_{1,\sigma_2,\ldots,\sigma_{n-1},n}$ are the numerators of the diagrams displayed in Fig. 4.2. Note that all other numerators can be expressed as linear combinations of the $n_{1,\sigma_2,\ldots,\sigma_{n-1},n}$ through the duality relations, and the form (4.34) for the gauge-theory amplitude makes this property manifest. This form is related to an unusual color decomposition of gauge-theory amplitudes which follows from applying KLT relations to the low-energy limit of heterotic strings [98].

Similarly, this immediately gives us a new representation for graviton amplitudes in terms of gauge-theory amplitudes,

$$\mathcal{M}_n^{\text{tree}}(1,2,\ldots,n) = i\kappa^{n-2} \sum_{\sigma\in S_{n-2}} n_{1,\sigma_2,\ldots,\sigma_{n-1},n}\, A_n^{\text{tree}}(1,\sigma_2,\ldots,\sigma_{n-1},n)\,, \tag{4.35}$$

where A_n^{tree} is the usual gauge-theory color-ordered amplitude.

CHAPTER 5

A Color Dual Form for Gauge-Theory Amplitudes

How far does the analogy between color and kinematics extend? We know that in SU(N_c) gauge theory, useful trace representations of the color factors exist. In this chapter, we show that the analogy between color and kinematics is sufficiently robust that a representation of the kinematic numerators exists which shares the same algebraic properties as color traces. Moreover we will show that additional interesting constraints can be imposed which uniquely determine the kinematic trace-like representation in terms of kinematic numerators satisfying the duality.

At tree level, the well-known trace-based color decomposition of gluon amplitudes is [56],

$$\mathcal{A}_m^{\rm tree} = g^{m-2} \sum_\sigma {\rm Tr}[T^{a_1} \cdots T^{a_m}] A_m^{\rm tree}(1,2,\ldots,m)\,, \tag{5.1}$$

where g is the gauge coupling, $A_m^{\rm tree}$ is a partial amplitude stripped of color factors, and the T^{a_i} are fundamental-representation matrices of an SU(N_c) Lie group. The sum runs over all non-cyclic permutations of external legs. The labels on momenta, polarizations or spinors, implicit in eq. (5.1), are also to be permuted in the sum. The color-stripped partial amplitudes can be expressed as a subset of diagrams following the same ordering of legs as in the partial amplitudes, but with no color factors. (For example, see eq. (4.5) of ref. [15].)

We propose that a dual description exists where we can swap the role of color and kinematics in the trace-based color decomposition, in particular by rewriting eq. (5.1) in a dual form,

$$\mathcal{A}_m^{\rm tree} \;=\; g^{m-2} \sum_\sigma \tau_{(12\ldots m)} A_m^{\rm dual}(1,2,\ldots,m)\,, \tag{5.2}$$

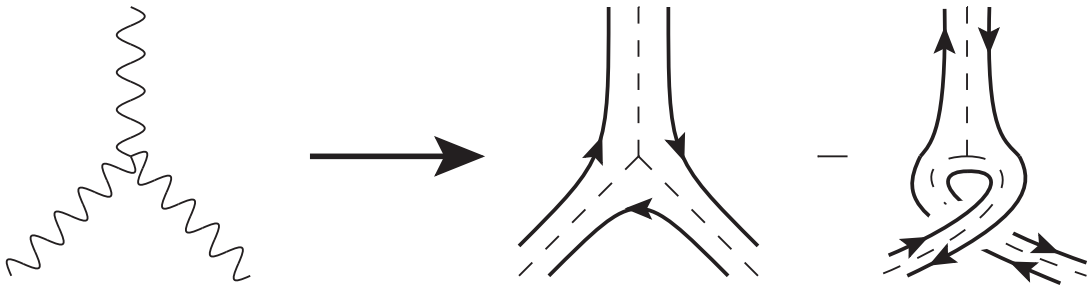

Figure 5.1: An antisymmetric vertex in a cubic graph is replaced by a difference of two double-line vertices.

where the $\tau_{(12\ldots m)}$ are kinematic prefactors satisfying the same cyclic properties as color traces. $A_m^{\rm dual}$ is a dual amplitude defined by replacing all kinematic numerators with color factors. That is, they can be generated by the same color-ordered graphs that generate $A_m^{\rm tree}$, except instead of a kinematic factor at every vertex, we simply have an $\tilde{f}^{abc}$. The dual amplitudes are not gauge-theory amplitudes, but amplitudes in a ϕ^3 theory dressed with group-theory factors.

If we assume that the duality (4.5) holds, then gravity amplitudes can be obtained directly from Yang-Mills numerators by replacing the color factors with another copy of the kinematic numerators [15], as proven at tree level [4] and conjectured to hold to all loop orders [103]. Since the kinematic numerators share the same algebraic properties as color factors, it is then straightforward to rearrange gravity amplitudes into a form analogous to the gauge-theory dual form (5.2),

$$\mathcal{M}_m^{\rm tree} \;=\; i\left(\frac{\kappa}{2}\right)^{m-2} \sum_\sigma \tau_{(12\ldots m)} A_m^{\rm tree}(1,2,\ldots,m)\,,$$

Here κ is the gravitational coupling, $A_m^{\rm tree}$ are partial amplitudes of Yang-Mills theory and τ is exactly the same kinematic prefactor as in eq. (5.2).

The τ's are generated by expressing each numerator in terms of a set of objects which satisfy the cyclic symmetry of color traces. For example, at the three-point level we demand

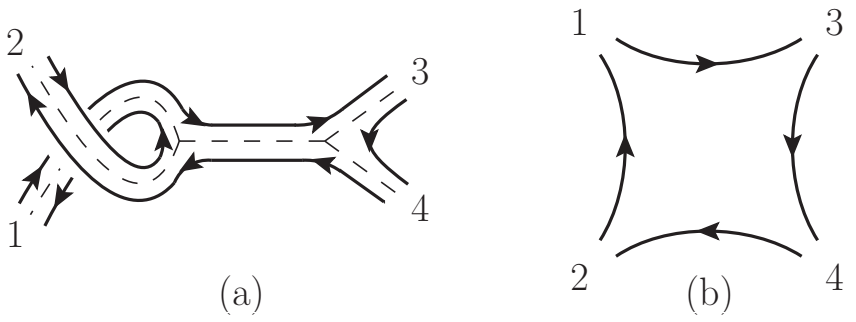

Figure 5.2: Sewing of two vertices in a double-line graph (a). The ordering of the external legs follows the arrow around the graph. This graph corresponds with the kinematic quantity $\tau_{(1342)}$. The same double-line graph is displayed in (b) in a form emphasizing that it is the same quantity whether we sew the two three-point τ's in the 12 channel or 13 channel.

that,

$$n_{123} = \tau_{(123)} - \tau_{(132)} \,,$$

where n_{123} is just the three vertex, as illustrated in Fig. 5.1. In general, we will use parentheses around the subscript labels on the τ's to indicate which color trace the quantity is analogous to. In particular, $\tau_{(123)}$ is analogous to $\mathrm{Tr}[T^{a_1}T^{a_2}T^{a_3}]$.

For any number of legs, we can associate diagrams to the τ's in a manner completely parallel to the standard 't Hooft double-line formalism for color. Just as the color traces "trivialize" the color Jacobi identities, the τ's will do the same for the kinematic numerator factors, emphasizing the parallelism between color and kinematics. For example, in Fig. 5.2(a) we display the double-line diagram for $\tau_{(1324)}$ obtained by sewing together two double-line three-point graphs. For the duality (4.5) to hold, the kinematic expression associated with each double-line graph should depend on only the topological structure of the graph, rather than on the detailed structure of vertices and internal lines in the underlying cubic graph. That is, a more appropriate way to draw the graph in Fig. 5.2(a) is shown in Fig. 5.2(b). In much the same way as single traces used in the tree-level color decomposition depend on only the cyclic ordering of legs, we demand that the τ's also depend on only the ordering. The property that one should obtain the same object when sewing in either

channel is of course reminiscent of a key feature of string theory. However, at present we take the diagrams only as guides, since we do not have rules for directly combining lower-point τ's into higher-point ones.

To be more explicit, consider some examples. At four points there are three graphs contributing to eq. (4.1). These numerators are expressed in terms of τ via

$$n_{12(34)} = \tau_{(1[2,[3,4]])} \,, \tag{5.3}$$

where the parenthesis on the indices of n indicates the associated propagators, *i.e.* in this case we have one, $i/(k_3 + k_4)^2$. For τ the brackets signify an antisymmetric combination, *i.e.* $\tau_{(12[3,4])} \equiv \tau_{(1234)} - \tau_{(1243)}$. The two other channels at four points are just relabelings of this channel. We note that by expressing the n_j in terms of τ, the Jacobi-like equation $n_{12(34)} - n_{23(41)} - n_{42(31)} = 0$ holds automatically.

Can we find an explicit form of τ with the desired cyclicity? It is not difficult to check at four points that

$$\tau_{(1234)} \;\; = \;\; \frac{1}{6}(n_{12(34)} + n_{23(41)})$$

indeed satisfies cyclicity and after using the duality relations (4.5) returns the numerators when combined as in eq. (5.3). The other τ's are given by relabelings. Interestingly, this solution satisfies some additional properties, namely invariance under a reversal of arguments and also an identity reminiscent of the U(1) decoupling identity for amplitudes,

$$\tau_{(1234)} + \tau_{(1342)} + \tau_{(1423)} = 0 \,.$$

More generally, our ability to express the τ's directly in terms of the graph numerators n_j is precisely dependent on having τ satisfying identities of the same form as Kleiss-Kuijf

identities,

$$\tau_{(1\{\alpha\}m\{\beta\})} \;=\; (-1)^{|\beta|} \sum_{\{\sigma\}} \tau_{(1\{\sigma\}m)}, \tag{5.4}$$

where the sum is over the "ordered permutations" $\{\sigma\} \in \mathrm{OP}(\{\alpha\}, \{\beta^T\})$, that is, all permutations of $\{\alpha\} \bigcup \{\beta^T\}$ that maintain the order of the individual elements belonging to each set within the joint set. The notation $\{\beta^T\}$ represents the set $\{\beta\}$ with the ordering reversed, and $|\beta|$ is the number of elements in $\{\beta\}$. For gauge-theory partial amplitudes, these relations were conjectured in ref. [109] and proven in ref. [110]. They are a consequence of the antisymmetric nature of the vertices describing the n_j, as noted in ref. [15]. Indeed, any cyclic object, such as τ, that can be expressed as a linear combination of the n_j with prefactors that respect the symmetry and relabeling properties of the n_j automatically will satisfy the Kleiss-Kuijf relations.

At five points we have

$$\begin{aligned} n_{12(3(45))} &= \tau_{(1[2,[3,[4,5]]])}\,, \\ \tau_{(12345)} &= \frac{1}{20} \sum_{\sigma} n_{12(3(45))}\,, \end{aligned}$$

where the sum runs over cyclic permutations. The numerator $n_{12(3(45))}$ is the graph with Feynman propagators $i/(k_1 + k_2)^2$ and $i/(k_4 + k_5)^2$. One can straightforwardly verify that this τ satisfies the relations (5.4).

At six points we can express the numerators of the two contributing diagrams in terms of the τ via

$$\begin{aligned} n_{12(3(4(56)))} &= \tau_{(1[2,[3,[4,[5,6]]]])}\,, \\ n_{(12)(34)(56)} &= n_{12(3(4(56)))} - n_{12(4(3(56)))}\,. \end{aligned}$$

The decomposition of τ in terms of the numerators is more complicated, in part because

non-trivial rearrangements are possible using the duality (4.5). One such solution is

$$\begin{aligned}\tau_{(1\ldots6)} \;=\; & \tfrac{1}{1890}\sum_{\sigma}\Big(32n_{12(3(4(56)))} - 3n_{12(4(3(56)))} \\ & - \tfrac{31}{2}n_{12(3(6(45)))} - \tfrac{31}{2}n_{12(6(3(45)))} + 2n_{36(1(2(45)))} \\ & + 2n_{36(2(1(45)))} + 2n_{36(4(1(25)))} - n_{26(1(4(35)))} \\ & - n_{26(4(1(35)))} - n_{35(1(2(46)))} - n_{35(2(1(46)))} \\ & + n_{24(1(3(56)))} + n_{24(3(1(56)))} - n_{26(1(3(45)))} \\ & - n_{26(3(1(45)))}\Big)\,, \end{aligned} \tag{5.5}$$

where here the sum runs over the cyclic permutations of labels. The reader may also verify that $\tau_{(1\ldots6)}$ satisfies the Kleiss-Kuijf relations (5.4), given the algebraic properties of the kinematic numerators.

We have explicitly verified through nine points that an expression for τ in terms of kinematic numerators (as in eq. (5.5)) exists and that it automatically satisfies the Kleiss-Kuijf-like relations (5.4). The explicit expression for τ at $m = 7$ contains more than 600 numerators and grows rapidly as the number of legs increases. Generally, it is better to think of the n_j numerators as functions of the τ. A general solution is

$$n_{12(3(\ldots m))\cdots)} = \tau_{(1[2,[3,[\ldots m]]\cdots])}\,.$$

The remaining numerators can be obtained by solving the duality relations (4.5), which must automatically hold for numerators expressed in terms of the τ's.

An interesting consequence of the above is that we can define an alternative color decomposition in place of eq. (5.1), where instead of color traces we use objects that satisfy Kleiss-Kuijf relations as well. These objects are given by taking the above equations for the τ in terms of the numerators n_j and replacing them with color factors c_j. This gives a valid set of objects to use in place of color traces in eq. (5.1). Using the explicit formulas given above, it is straightforward to confirm though six points that the amplitude in eq. (5.1) is

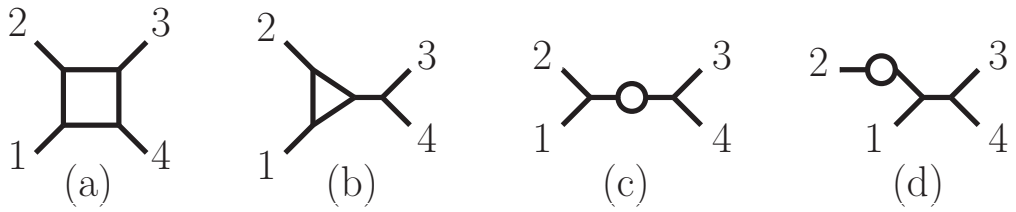

Figure 5.3: Cubic diagrams appearing in one-loop four-point amplitudes.

unchanged under this substitution.

Can this construction be extended to loop level? As an initial peek at this question, we turn to the simple case of a one-loop four-point $\mathcal{N} = 4$ super-Yang-Mills amplitude, first obtained in ref. [111]. We follow the same diagrammatic double-line formalism as at tree level.

The four types of cubic diagrams contributing to the four-point one-loop amplitude are shown in Fig. 5.3. The numerators associated with these diagrams in the BCJ representation are

$$n_{(\mathrm{a})} = stA^{\mathrm{tree}}\,, \qquad n_{(\mathrm{b})} = n_{(\mathrm{c})} = n_{(\mathrm{d})} = 0\,,$$

where s and t are standard four-point Mandelstam invariants. Although this seems like a trivial state of affairs, expanding each numerator in terms of the double-line graphs reveals unexpected structure. In this expansion, there are multiple lines flowing around the double-line graphs, and we indicate the external legs attached to each line with a $(12\ldots)$ in the subscript of τ. Since each one-loop graph carries two independent lines, each τ will have two sets of parentheses in the subscripts. The graphs that appear in the expansion of the present example are $\tau_{(1)(234)}$, $\tau_{(12)(34)}$ and $\tau_{(1234)()}$, along with relabelings of these. The decomposition of the four numerators in terms of the τ's is straightforward and closely parallels a $\mathrm{U}(N_c)$ color decomposition.

One immediate solution to the decomposition can be obtained by setting $\tau_{(1234)()}$ proportional to the box numerator, and the other two τ functions to zero. A similar construction

also works for the five-point amplitude [41] of $\mathcal{N}=4$ super-Yang-Mills theory. In this case $\tau_{(12345)()}$ are set proportional to the pentagon numerator given in ref. [112].[1]

A more interesting solution to the four-point decomposition is

$$\begin{aligned}\tau_{(1234)()} &= \frac{1}{62} stA^{\text{tree}}\,, \qquad \tau_{(12)(34)} = \frac{3}{31} stA^{\text{tree}}\,,\\ \tau_{(1)(234)} &= -\frac{3}{62} stA^{\text{tree}}\,.\end{aligned}$$

With this solution the τ functions satisfy the same identities as the color-ordered partial amplitudes, namely,

$$\tau_{(\{\alpha\})(\{\beta\})} = (-1)^{|\beta|} \sum_{\{\sigma\}} \tau_{(\{\sigma\})()}\,,$$

where the sum is over the "cyclically ordered permutations" $\text{COP}(\{\alpha\},\{\beta^T\})$, that is, all permutations of $\{\alpha\}\bigcup\{\beta^T\}$ that maintain the cyclic orderings of $\{\alpha\}$ and $\{\beta^T\}$ separately, and with one leg fixed (see ref. [41]).

To go beyond these simple examples, one needs a self-consistent assignment of loop momentum labels, with an understanding of the proper way to associate kinematic information with the double-line graphs. At tree and one-loop level, each double-line graph can be interpreted as defining an embedding of the underlying cubic graph in a plane, while at higher loops, non-planar embeddings also appear, introducing a topological hierarchy to the graphs analogous to the $1/N_c$ expansion of Yang-Mills. We leave the study of loop level to future work.

There are also a number of other interesting open questions. For example, it would be very useful to find a direct recursive procedure for building the τ's. Such a construction would automatically produce numerators that satisfy the color-kinematics duality. We also note that the double-line graphs describing the kinematic trace representation are reminiscent of open string diagrams. This brings up the interesting question of whether the properties

[1] We thank J. J. M. Carrasco and H. Johansson for pointing out that the color-kinematics duality holds with this form.

we have described here can be unraveled in string theory. More generally, the trace-like representation described here emphasizes a group-theoretic origin for the duality. Because the same kinematic numerators appear in gravity theories, the same underlying group theory should carry over to gravity. It remains an important challenge to understand the origin of this duality and to fully map out its implications.

CHAPTER 6

Absence of Three-Loop Four-Point Ultraviolet Divergences in $\mathcal{N} = 4$ Supergravity

Recent years have seen a resurgence of interest in the possibility that certain supergravity theories may be ultraviolet finite. This question had been carefully studied in the late 70's and early 80's in the hope of using supergravity to construct fundamental theories of gravity. The conclusion of these early studies was that nonrenormalizable ultraviolet divergences would almost certainly appear at a sufficiently large number of quantum loops, though this remains unproven. Although supersymmetry tends to tame the ultraviolet divergences, it does not appear to be sufficient to overcome the increasingly poor ultraviolet behavior of gravity theories stemming from the two-derivative coupling. The consensus opinion from that era was that all pure supergravity theories would likely diverge at three loops (see e.g. ref. [113]), though with assumptions, certain divergences are perhaps delayed a few extra loop orders [114].

More recently, direct calculations of divergences in supergravity theories have been carried out [69, 70, 71, 115], shedding new light on this issue. From these studies we now know that through four loops maximally supersymmetric $\mathcal{N} = 8$ supergravity is finite in space-time dimensions, $D < 6/L + 4$ for $L = 2, 3, 4$ loops. These calculations also tell us that the bound is saturated. In $D = 4$, $E_{7(7)}$ duality symmetry [116] has recently been used to imply ultraviolet finiteness below seven loops [117], also explaining the observed lack of divergences. In a parallel development, string theory and a first quantized formalism use supersymmetry considerations to arrive at similar conclusions [118]. The latter approach leads to D-dimensional results consistent with the explicit calculations through four loops,

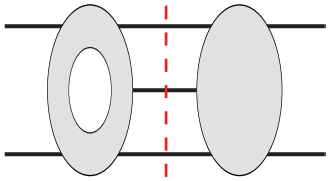

Figure 6.1: A sample cut at three loops displaying cancellations in $\mathcal{N} = 4$ supergravity special to four dimensions.

but predicts a worse behavior starting at $L = 5$. At seven loops, the potential four-graviton counterterm of $\mathcal{N} = 8$ supergravity [119] appears to be consistent with all known symmetries [117, 120]. (See ref. [121] for a more optimistic opinion.) More generally, $1/\mathcal{N}$-BPS operators serve as potential counterterms for $\mathcal{N} = 4, 5, 6, 8$ supergravity at $L = 3, 4, 5, 7$ loops, respectively, suggesting that in $D = 4$ ultraviolet divergences will occur at these loop orders in these theories [120]. It therefore might seem safe to conclude that $\mathcal{N} = 4$ supergravity [122] in particular will diverge at three loops.

On the other hand, studies of scattering amplitudes suggest that additional ultraviolet cancellations will be found beyond these. We know that even pure Einstein gravity at one loop exhibits remarkable cancellations as the number of external legs increases [123]. Through unitarity, such cancellations feed into nontrivial ultraviolet cancellations at *all* loop orders [124]. In addition, the proposed double-copy structure of gravity loop amplitudes [103] suggests that gravity amplitudes are more constrained than symmetry considerations suggest. In this chapter we show that the ultraviolet properties of $\mathcal{N} = 4$ supergravity are indeed better than had been anticipated.

To motivate the possibility of hidden cancellations in $\mathcal{N} = 4$ supergravity, consider the unitarity cut displayed in Fig. 6.1 isolating a one-loop subamplitude in a three-loop amplitude. As noted in refs. [123, 125], at one loop a five-point diagram in an $\mathcal{N} = 4$ supergravity amplitude effectively can have up to five powers of loop momenta in the numerator, similar to the power counting of pure Yang-Mills theory. There are also three additional powers of numerator loop momentum coming from the tree amplitude on the right-hand side of the cut, giving a total of at least eight powers of numerator loop momentum. Taking into

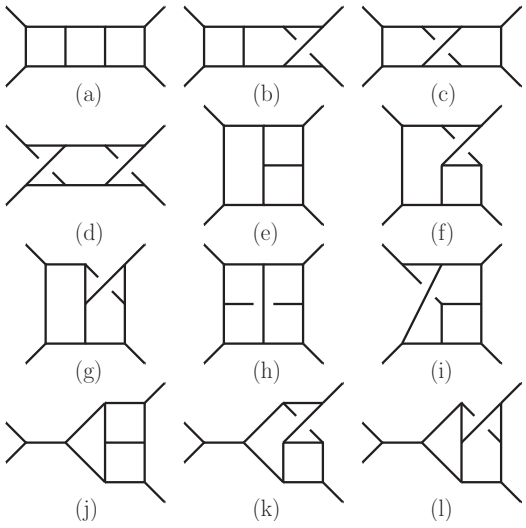

Figure 6.2: The twelve graphs appearing in the three-loop $\mathcal{N} = 4$ sYM amplitude [103] and in gravity amplitudes obtained from these using the double-copy formula.

account three loop integrals and ten propagators suggests that this amplitude should diverge at least logarithmically in $D = 4$. (The power counting analysis of this cut performed in ref. [125] assumed that additional powers of numerator loop momenta coming from the tree amplitude in the cut can be ignored, contrary to our analysis.)

However, this type of power counting is too naïve and does not account for the special property that no one- and two-loop ultraviolet divergences are present in $D = 4$ [126]. Thus in $D = 4$ there are additional cancellations of the loop momenta in one-loop subdiagrams, effectively removing powers of loop momenta from the numerators of the loop integrands once all pieces have been combined and integrated. These additional cancellations can affect the higher-loop effective overall power counting. We show this occurs by computing the coefficient of the potential three-loop four-point divergences in $\mathcal{N} = 4$ supergravity.

To make the calculation of the potential three-loop divergence feasible, we use the duality between color and kinematics uncovered by Bern, Carrasco and Johansson (BCJ) [15, 103]. According to this conjecture, we can reorganize a (super) Yang-Mills amplitude into graphs where the numerators satisfy identities in one-to-one correspondence with color Jacobi identities. Whenever this is accomplished, we obtain corresponding gravity amplitudes simply by replacing color factors with kinematic numerators of a corresponding second gauge-theory

amplitude. That is, gravity loop amplitudes are given by [103],

$$\frac{(-i)^{L+1}}{(\kappa/2)^{n-2+2L}}\mathcal{M}_n^{\rm loop} = \sum_j \int \prod_{l=1}^{L} \frac{d^D p_l}{(2\pi)^D} \frac{1}{S_j} \frac{n_j \tilde{n}_j}{\prod_{\alpha_j} p_{\alpha_j}^2}\,, \tag{6.1}$$

where n_j and $\tilde{n}_j$ are kinematic numerator factors from gauge-theory amplitudes and κ is the gravitational coupling. The factors S_j are the usual combinatoric factors associated with the symmetries of the graphs. The sum runs over all distinct graphs with cubic vertices, such as the ones appearing in Fig. 6.2. The propagators appearing in eq. (6.1) are the ordinary propagators corresponding to the internal lines of the graphs. Depending on the particular theory under consideration, we use different component gauge-theory numerators in eq. (6.1).

In our study of pure $\mathcal{N} = 4$ supergravity with no matter multiplets [122], we take one component gauge theory to be $\mathcal{N} = 4$ super-Yang-Mills (sYM) theory and the second component to be nonsupersymmetric pure Yang-Mills theory. This construction was used in earlier one- and two-loop studies of $\mathcal{N} \geq 4$ supergravity amplitudes [127]. The main differences in our case are that integrated gauge-theory expressions are not known and that the $\mathcal{N} = 4$ sYM numerators are not all independent of loop momenta.

As explained in refs. [103, 4], only one of the two component gauge-theory amplitudes needs to be in a form manifestly satisfying the duality for the double-copy property (6.1) to hold. The other gauge-theory amplitude can be any convenient representation arranged into diagrams with only cubic vertices. We note that our construction applies immediately to all four-point amplitudes of pure $\mathcal{N} = 4$ supergravity, since these are constructed simply by considering all possible external states on the $\mathcal{N} = 4$ sYM side of the double copy; at four-points this information is entirely encoded in an overall prefactor of the tree amplitude. At three loops, we take the $\mathcal{N} = 4$ sYM copy from ref. [103], since it has BCJ duality manifest. This representation of the $\mathcal{N} = 4$ sYM amplitude is described by the 12 graphs in Fig. 6.2. For the pure Yang-Mills copy, we use ordinary Feynman diagrams in Feynman gauge, including ghost contributions. The contact contributions are assigned to diagrams with only cubic vertices according to their color factor. In this construction, most Feynman diagrams are irrelevant because in the double-copy formula they get multiplied by vanishing

$\mathcal{N} = 4$ sYM diagram numerators. This construction gives the complete three-loop four-point integrand of $\mathcal{N} = 4$ supergravity. We have also applied these ideas to reproduce the absence of one- and two-loop divergences in pure $\mathcal{N} = 4$ supergravity, starting from the one- and two-loop four-point sYM amplitudes [111, 66].

To prove the correctness of our construction, we use the unitarity method [41, 69]. The generalized unitarity cuts decompose the constructed integrand into sums of products of tree amplitudes, which match against the values obtained using the double-copy property at tree level [103, 4]. Since all cuts automatically have the proper values in D dimensions, the amplitude so constructed is correct.

Inserting the numerators of pure Yang-Mills amplitudes generated by the Feynman rules into the double-copy formula (6.1) leads to tens of thousands of high-rank tensor integrals, from which we must extract the ultraviolet divergences. We do so by expanding in small external momenta. This gives vacuum diagrams containing both infrared and ultraviolet divergences. To deal with ultraviolet divergences, we use the four-dimensional-helicity regularization scheme [128], since it preserves supersymmetry and has been used successfully in analogous multiloop pure gluon and supersymmetric amplitudes. In this scheme, the number of states remain at their four-dimensional values. Then at the level of the vacuum integrals, we introduce a uniform mass m to separate the infrared divergences from the ultraviolet ones. Although ultimately there are no one- and two-loop ultraviolet divergences in $\mathcal{N} = 4$ supergravity, individual integrals generally do contain subdivergences due to their poor power counting. To deal with this, we make extensive use of the observations of Marcus and Sagnotti [129] to subtract subdivergences integral by integral. Extractions of ultraviolet divergences in higher-dimensional $\mathcal{N} = 8$ supergravity were discussed recently in refs. [130, 115].

At two or higher loops, the introduced mass regulator induces unphysical regulator dependence in individual integrals. However, at least for logarithmically divergent integrals, the regulator dependence comes entirely from subdivergences, which we systematically subtract [129]. We therefore introduce the mass regulator before subtracting subdivergences,

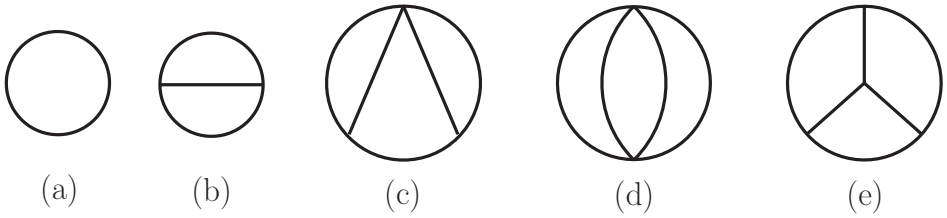

Figure 6.3: The basis of vacuum integrals for one through three loops.

but after reducing all integrals to logarithmic by series expansion in small external momenta. To implement the subtractions, we recursively define the subtracted divergence $\mathcal{S}[\ldots]$ of an integral,

$$\mathcal{S}\left[\int \prod_{i=1}^{L} dp_i\, I\right] \equiv \mathrm{Div}\left[\int \prod_{i=1}^{L} dp_i\, I\right] - \sum_{l=1}^{L-1} \sum_{\substack{l-\text{loop} \\ \text{subloops}}} \mathrm{Div}\left[\int \prod_{j=l+1}^{L} dp'_j\, \mathcal{S}\left[\int \prod_{i=1}^{l} dp'_i\, I\right]\right], \quad (6.2)$$

where Div[...] is the complete divergence of an integral, I is the integrand, and dp_i is shorthand for $d^D p_i/(2\pi)^D$. The sum over subloops must include *all* subloops of the diagram where a subdivergence could occur — not just the loops that are manifestly parametrized by p_i — and here we have indicated this by changing variables to p'_i in each subtraction, such that the $l-$loop subintegral under consideration is parametrized by $p'_1, \ldots, p'_l$. For example, graph (e) in Fig. 6.2 has seven one-loop subintegrals and six two-loop subintegrals to consider, and each two-loop subintegral has three one-loop subintegrals of its own.

By the time we apply eq. (6.2), each integral has a single scale given by the mass regulator m. We are left with the task of calculating the divergences Div[...] of single-scale vacuum integrals. To evaluate these integrals, we first eliminate tensors composed of loop momenta from the numerators by noticing that the integrals must be linear combinations of products of metric tensors $\eta^{\mu\nu}$. (See ref. [115] for a recent discussion of evaluating tensor vacuum integrals.) Then we reduce the resulting scalar integrals to a basis using integration by parts, as implemented in FIRE [131]. The resulting basis is given by the scalar vacuum integrals shown in Fig. 6.3 (along with products of lower-loop integrals), with a single massive propagator corresponding to each line. As cross checks we also used MB [132] and FIESTA [133].

Graph	(divergence)/$(\langle 12\rangle^2[34]^2 s t A^{\rm tree}(\frac{\kappa}{2})^8)$
(a)-(d)	0
(e)	$\frac{263}{768}\frac{1}{\epsilon^3} + \frac{205}{27648}\frac{1}{\epsilon^2} + \left(-\frac{5551}{768}\zeta_3 + \frac{326317}{110592}\right)\frac{1}{\epsilon}$
(f)	$-\frac{175}{2304}\frac{1}{\epsilon^3} - \frac{1}{4}\frac{1}{\epsilon^2} + \left(\frac{593}{288}\zeta_3 - \frac{217571}{165888}\right)\frac{1}{\epsilon}$
(g)	$-\frac{11}{36}\frac{1}{\epsilon^3} + \frac{2057}{6912}\frac{1}{\epsilon^2} + \left(\frac{10769}{2304}\zeta_3 - \frac{226201}{165888}\right)\frac{1}{\epsilon}$
(h)	$-\frac{3}{32}\frac{1}{\epsilon^3} - \frac{41}{1536}\frac{1}{\epsilon^2} + \left(\frac{3227}{2304}\zeta_3 - \frac{3329}{18432}\right)\frac{1}{\epsilon}$
(i)	$\frac{17}{128}\frac{1}{\epsilon^3} - \frac{29}{1024}\frac{1}{\epsilon^2} + \left(-\frac{2087}{2304}\zeta_3 - \frac{10495}{110592}\right)\frac{1}{\epsilon}$
(j)	$-\frac{15}{32}\frac{1}{\epsilon^3} + \frac{9}{64}\frac{1}{\epsilon^2} + \left(\frac{101}{12}\zeta_3 - \frac{3227}{1152}\right)\frac{1}{\epsilon}$
(k)	$\frac{5}{64}\frac{1}{\epsilon^3} + \frac{89}{1152}\frac{1}{\epsilon^2} + \left(-\frac{377}{144}\zeta_3 + \frac{287}{432}\right)\frac{1}{\epsilon}$
(l)	$\frac{25}{64}\frac{1}{\epsilon^3} - \frac{251}{1152}\frac{1}{\epsilon^2} + \left(-\frac{835}{144}\zeta_3 + \frac{7385}{3456}\right)\frac{1}{\epsilon}$

Table 6.1: The graph-by-graph divergences for the four-graviton amplitude with helicities $(1^-2^-3^+4^+)$ (up to an overall normalization). Each expression includes a permutation sum over external legs, with the symmetry factor appropriate to the graph. These quantities are not individually gauge-invariant, and here we use spinor helicity with the choice of reference momenta $q_1 = q_2 = k_3$ and $q_3 = q_4 = k_1$. The sum over the diagram contributions vanishes.

We evaluated all but the last of these integrals to the required order in ϵ by Mellin-Barnes integration with resummation of residues using the methods presented in ref. [134]. The last integral can be evaluated by making a two-loop subintegral massless and integrating it first. This does not affect the ultraviolet divergence because there are no subdivergences in this case. (The value of the two-loop subintegral can be found in ref. [135].) The results are rational linear combinations of the transcendental numbers ζ_2, ζ_3, and $\sqrt{3}\,\mathrm{Im}\left(\mathrm{Li}_2\left(e^{i\pi/3}\right)\right)$.

At two loops only the first two integrals shown in Fig. 6.3 are needed. Adding together the contributions reproduces the fact that there are no two-loop divergences in pure supergravity theories. At three loops all vacuum integrals in Fig. 6.3 contribute. In Table 6.1, we have collected the derived divergences of the three-loop four-graviton amplitude for each graph in Fig. 6.2. The results shown in the table are summed over the independent permutations including symmetry factors. The individual graphs are not gauge invariant and are valid only for the indicated choice of spinor-helicity reference momenta (see e.g. ref. [56]). We have divided out a prefactor depending on the four-point color-ordered super-Yang-Mills tree amplitude, spinor inner products and the usual Mandelstam invariants s and t. We note that the transcendental numbers except ζ_3 cancel within each graph.

In the sum over all contributions (obtained by adding the rows in the table 6.1), not only

do the $1/\epsilon^3$ and $1/\epsilon^2$ divergences cancel, as required because there are no divergent subamplitudes, but the $1/\epsilon$ singularity also cancels. This proves that the three-loop amplitude is ultraviolet finite. As a rather nontrivial check, we confirmed that the sum over all contributions is independent of reference momentum choices. As another nontrivial confirmation, we found that by introducing a uniform mass in the amplitude at the start of the calculation, all ultraviolet divergences cancel without the need for subdivergence subtraction. This matches expectations that all ultraviolet subdivergences should cancel out from the total amplitude (although there may be potential regulator dependence issues with this approach). Since all nonvanishing four-point amplitudes in the theory are proportional to four-graviton ones, our calculation demonstrates that there are no divergences in any three-loop four-point amplitude of the theory.

In summary, we used the recently uncovered duality between color and kinematics to streamline the calculation of the coefficient of the potential three-loop ultraviolet divergence of $\mathcal{N} = 4$ supergravity, proving that it vanishes. Might cancellations persist beyond this? It is interesting to note that the $D = 4$ cancellations found in one- and two-loop subamplitudes and used to motivate our three-loop computation can be used just as well to argue for higher-loop cancellations. Moreover, the double-copy property of gravity amplitudes shows there is more structure than captured by the known symmetries. Our three-loop calculation provides a concrete example showing that power counting based on known symmetries can be misleading. The results of this calculation strongly motivate further high-loop explorations of the ultraviolet divergence structure of supergravity theories. In particular, they emphasize the importance of explicitly computing the ultraviolet properties of $\mathcal{N} = 8$ supergravity at five loops.

APPENDIX A

Clifford algebra conventions

Here we follow the conventions of [33]. The Clifford algebra is given as,

$$\sigma^{\mu}_{AB}\tilde{\sigma}^{\nu BC} + \sigma^{\nu}_{AB}\tilde{\sigma}^{\mu BC} = 2\eta^{\mu\nu}\delta^{C}_{A}\,. \tag{A.1}$$

The explicit forms of the matrices $\sigma, \tilde{\sigma}$ are given in [33]. They satisfy the following identities:

$$\begin{aligned}
&\sigma^{\mu}_{AB}\sigma_{\mu CD} = -2\epsilon_{ABCD}\,,\\
&\tilde{\sigma}^{\mu AB}\tilde{\sigma}^{CD}_{\mu} = -2\epsilon^{ABCD}\,,\\
&\tilde{\sigma}^{\mu AB}\sigma_{\mu CD} = -2\left(\delta^{[A}_{C}\delta^{B]}_{D}\right)\,,\\
&tr(\sigma^{\mu}\tilde{\sigma}_{\nu}) = \sigma^{\mu}_{AB}\tilde{\sigma}^{\nu BA} = 4\eta^{\mu\nu}\,.
\end{aligned} \tag{A.2}$$

From the above, one can deduce,

$$\begin{aligned}
&x^{\mu} = \frac{1}{4}(\tilde{\sigma}^{\mu})^{BA}x_{AB} = \frac{1}{4}(\sigma^{\mu})_{BA}x^{AB}\,,\\
&x^{AB} = \frac{1}{2}\epsilon^{ABCD}x_{CD}\,,\\
&x^{AB}x_{BE} = \frac{1}{2}\epsilon^{ABCD}x_{CD}x_{BE} = x^{2}\delta^{A}_{E}\,,\\
&x^{2} = x^{\nu}x_{\nu} = -\frac{1}{8}\epsilon_{ABCD}x^{AB}x^{CD}\,.
\end{aligned} \tag{A.3}$$

Some useful formulæ:

$$\begin{aligned} X_{[ab]} &= \epsilon_{ab} X^c{}_c, \; X^{[ab]} = -\epsilon^{ab} X^c{}_c \\ \epsilon^{ABCD}\epsilon_{AEFG} &= \big(\delta^B_E\delta^C_F\delta^D_G + \delta^C_E\delta^D_F\delta^B_G + \delta^D_E\delta^B_F\delta^C_G \\ &\quad -\delta^B_F\delta^C_E\delta^D_G - \delta^C_F\delta^D_E\delta^B_G - \delta^D_F\delta^B_E\delta^C_G\big) \end{aligned} \tag{A.4}$$

APPENDIX B

An Analytic Four-Loop Cut

In this appendix, we present a nontrivial cut of the four-loop four-point amplitude of $\mathcal{N}=4$ sYM. In particular, we analytically evaluate the cut shown in Fig. 2.1, which is a nonplanar permutation of the cut (k) in Fig. 2.4. Since this cut consists of only four- and five-point subamplitudes, the calculation is not significantly more difficult than the two-loop example in section 2.3.3. The cut is evaluated by carrying out the Grassmann integration,

$$\begin{aligned} C^{\text{4-loop}} &= \int \left(\prod_{i=1}^{7} d^2\eta_{l_i} d^2\tilde{\eta}_{l_i}\right) \mathcal{A}_5^{\text{tree}}(p_1,p_2,l_1,l_2,l_3)\, \mathcal{A}_4^{\text{tree}}(-l_1,-l_2,l_4,l_5) \\ &\qquad \times \mathcal{A}_4^{\text{tree}}(-l_4,-l_5,l_6,l_7)\, \mathcal{A}_5^{\text{tree}}(p_3,p_4,-l_3,-l_6,-l_7)\,. \end{aligned} \tag{B.1}$$

Here we have seven on-shell internal momenta labeled l_i, and four component tree amplitudes. In this cut, we can use the supermomentum delta functions to localize six of the seven internal supercoordinates $\eta_{l_i}, \tilde{\eta}_{l_i}$. The remaining supercoordinate integration is handled in the same way as in the example of section 2.3.3.

A solution to the supercoordinate delta-function constraints is

$$\begin{aligned} q_{l_1} &\to -s_{l_1 l_2}^{-1} \not{l}_1 \not{l}_2 q_{l_3}\,, \qquad \tilde{q}_{l_1} \to -s_{l_1 l_1}^{-1} \not{l}_1 \not{l}_2 \tilde{q}_{l_3}\,, \\ q_{l_2} &\to -s_{l_1 l_2}^{-1} \not{l}_2 \not{l}_1 q_{l_3}\,, \qquad \tilde{q}_{l_2} \to -s_{l_1 l_2}^{-1} \not{l}_2 \not{l}_1 \tilde{q}_{l_3}\,, \\ q_{l_4} &\to -s_{l_4 l_5}^{-1} \not{l}_4 \not{l}_5 q_{l_3}\,, \qquad \tilde{q}_{l_4} \to -s_{l_4 l_5}^{-1} \not{l}_4 \not{l}_5 \tilde{q}_{l_3}\,, \\ q_{l_5} &\to -s_{l_4 l_5}^{-1} \not{l}_5 \not{l}_4 q_{l_3}\,, \qquad \tilde{q}_{l_5} \to -s_{l_4 l_5}^{-1} \not{l}_5 \not{l}_4 \tilde{q}_{l_3}\,, \\ q_{l_6} &\to -s_{l_6 l_7}^{-1} \not{l}_6 \not{l}_7 q_{l_3}\,, \qquad \tilde{q}_{l_6} \to -s_{l_6 l_7}^{-1} \not{l}_6 \not{l}_7 \tilde{q}_{l_3}\,, \\ q_{l_7} &\to -s_{l_6 l_7}^{-1} \not{l}_7 \not{l}_6 q_{l_3}\,, \qquad \tilde{q}_{l_7} \to -s_{l_6 l_7}^{-1} \not{l}_7 \not{l}_6 \tilde{q}_{l_3}\,, \end{aligned} \tag{B.2}$$

where we have ignored all dependence on $\{q_1, q_2, q_3, q_4\}$, since these will drop out after the final η_{l_3} integration. As usual, we take the Mandelstam invariants to be $s_{l_i l_j} = (l_i + l_j)^2$. Because of extra factors of these invariants coming from the Grassmann integrations — seen in eq. (2.6) — we must also multiply the final cut by $s^2_{l_1 l_2} s^2_{l_4 l_5} s^2_{l_6 l_7}$. The rest of the calculation is similar to the derivation of eq. (2.8), giving,

$$
\begin{aligned}
C^{\text{4-loop}} \;=\; & \frac{s_{23}(l_4+l_5)^2(l_6+l_7)^2 \mathcal{A}_4^{\text{tree}}(p_1,p_2,p_3,p_4)}{s_{12}(p_1+l_3)^2(p_2+l_1)^2(p_3-l_7)^2(p_4-l_3)^2(l_2+l_3)^2(l_2-l_4)^2(l_5-l_6)^2(l_3+l_6)^2} \\
& \times \langle l_3^a | \Bigg(\not{p}_1 \not{p}_2 \not{l}_1 \not{l}_2 + \frac{\not{l}_2 \not{l}_3 \not{p}_1 \not{p}_2 \not{l}_1 \not{l}_2 + \not{l}_1 \not{l}_2 \not{l}_3 \not{p}_1 \not{p}_2 \not{l}_1}{(l_1+l_2)^2} \\
& \quad - \frac{\not{l}_1 \not{l}_2 (\not{l}_3 \not{p}_1 \not{p}_2 \not{l}_1 - \not{l}_3 \not{l}_1 \not{p}_2 \not{p}_1) - (\not{l}_1 \not{p}_2 \not{p}_1 \not{l}_3 - \not{p}_1 \not{p}_2 \not{l}_1 \not{l}_3) \not{l}_2 \not{l}_1}{2(l_1+l_2)^2} \Bigg) | l_{3\dot{a}}] \\
& \times \langle l_{3a} | \Bigg(\not{l}_6 \not{l}_7 \not{p}_3 \not{p}_4 + \frac{\not{l}_7 \not{p}_3 \not{p}_4 \not{l}_3 \not{l}_6 \not{l}_7 + \not{l}_6 \not{l}_7 \not{p}_3 \not{p}_4 \not{l}_3 \not{l}_6}{(l_6+l_7)^2} \\
& \quad + \frac{(\not{l}_7 \not{p}_3 \not{p}_4 \not{l}_3 - \not{l}_7 \not{l}_3 \not{p}_4 \not{p}_3) \not{l}_7 \not{l}_6 - \not{l}_6 \not{l}_7 (\not{l}_3 \not{p}_4 \not{p}_3 \not{l}_7 - \not{p}_3 \not{p}_4 \not{l}_3 \not{l}_7)}{2(l_6+l_7)^2} \Bigg) | l_3^{\dot{a}}] \,. \qquad \text{(B.3)}
\end{aligned}
$$

This expression is just a gamma trace, and although it appears to be chiral, the γ_7 term in the trace actually drops out. In fact, the five-point tree amplitude itself is non-chiral, although this property is not manifest in the present form.

One can compare this to the cut of the amplitude derived in ref. [67] using (mostly) four-dimensional methods,

$$
\begin{aligned}
C^{\text{4-loop}} \;=\; & \frac{s_{12} s_{23} \mathcal{A}_4^{\text{tree}}(p_1,p_2,p_3,p_4)}{(p_2+l_1)^2(p_3-l_7)^2(l_1-l_5)^2(l_4-l_7)^2} \\
& \times \Bigg(\frac{s_{12}^2 (l_2-l_6)^2}{(l_2+l_3)^2(l_3+l_6)^2} + \frac{s_{23}(l_4+l_5)^4}{(p_1+l_3)^2(p_4-l_3)^2} \\
& \quad + \frac{s_{12}(l_4+l_5)^2(p_1+l_3+l_6)^2}{(p_1+l_3)^2(l_3+l_6)^2} + \frac{s_{12}(l_4+l_5)^2(p_4-l_2-l_3)^2}{(p_4-l_3)^2(l_2+l_3)^2} \Bigg) \,. \qquad \text{(B.4)}
\end{aligned}
$$

We have evaluated these two expressions numerically using six-dimensional momenta to verify their equality.

APPENDIX C

Proof of variable inversion formulæ

In this appendix, we derive the inversion properties in eq. (3.8).

- $I[\lambda^A_{\{ij\}a}] = \frac{x_{iAB}\lambda^{Ba}_{\{ij\}}}{\sqrt{x_i^2 x_j^2}} = \frac{x_{jAB}\lambda^{Ba}_{\{ij\}}}{\sqrt{x_i^2 x_j^2}}$

  Our starting point is the constraint equation $(x_i - x_j)_{AB} = \tilde{\lambda}_{\{ij\}A\dot{a}}\tilde{\lambda}^{\dot{a}}_{\{ij\}B}$. Contracting both sides with $\lambda^{Ba}_{\{ij\}}$ provides an equation linear in λ, but loses normalization information. We then proceed with the inversion

$$\begin{aligned} 0 &= I[(x_i - x_j)_{AB}\lambda^{Ba}_{\{ij\}}] \\ &= (x_j^{-1})^{AC}(x_i - x_j)_{CD}(x_i^{-1})^{DB} I[\lambda^{Ba}_{\{ij\}}]. \end{aligned} \tag{C.1}$$

  This implies that $(x_i^{-1})^{DB} I[\lambda^{Ba}_{\{ij\}}]$ is in the null space of $(x_i - x_j)_{CD}$, so

$$\begin{aligned} (x_i^{-1})^{DB} I[\lambda^{Ba}_{\{ij\}}] &= M_{ab}\lambda^{Db}_{\{ij\}} \\ \Rightarrow \quad I[\lambda^{Aa}_{\{ij\}}] &= x_{iAB}M_{ab}\lambda^{Bb}_{\{ij\}} \\ &= x_{jAB}M_{ab}\lambda^{Bb}_{\{ij\}}\,, \end{aligned} \tag{C.2}$$

  where M_{ab} is a normalization matrix, which we partially fix by inverting the original

constraint equation

$$
\begin{aligned}
& I[(x_i - x_j)^{AB}] = I[\lambda^{Aa}_{\{ij\}}] I[\lambda^{B}_{\{ij\}a}] \\
\Rightarrow \quad & (x_i^{-1})_{AC} (x_i - x_j)^{CD} (x_j^{-1})_{DB} = x_{iAC} M_{ab} \lambda^{Cb}_{\{ij\}}\, x_{jBD} M^{ac} \lambda^{D}_{\{ij\}c} \\
\Rightarrow \quad & (x_i - x_j)^{CD} = -x_i^2 x_j^2 M_{ab} M^{ac} \lambda^{Cb}_{\{ij\}} \lambda^{D}_{\{ij\}c} \\
\Rightarrow \quad & M_{ab} M^{ac} = -\frac{\delta^c_b}{x_i^2 x_j^2} \,. \qquad \text{(C.3)}
\end{aligned}
$$

This is the only constraint on M. Without loss of generality, we choose $M_{ab} = \epsilon_{ab} (x_i^2 x_j^2)^{-1/2}$.

- $I[\eta_{\{ij\}a}] = -\sqrt{\frac{x_i^2}{x_j^2}} \Big(\eta^a_{\{ij\}} + (x_i^{-1})_{AB} \theta_i^A \lambda^{Ba}_{\{ij\}} \Big)$

  To invert η, we begin with the constraint equation $(\theta_i - \theta_j)^A = \lambda^{Aa}_{\{ij\}} \eta_{\{ij\}a}$. Inverting, we have

$$
\begin{aligned}
& I[(\theta_i - \theta_j)^A] = I[\lambda^{Aa}_{\{ij\}}] I[\eta_{\{ij\}a}] \\
\Rightarrow \quad & (x_i^{-1})_{AB}\, \theta_i^B - (x_j^{-1})_{AB}\, \theta_j^B = \frac{x_{iAB}}{\sqrt{x_i^2 x_j^2}} \lambda^B_{\{ij\}a} I[\eta_{\{ij\}a}] \\
& \qquad\qquad = \frac{x_{jAB}}{\sqrt{x_i^2 x_j^2}} \lambda^B_{\{ij\}a} I[\eta_{\{ij\}a}] \,. \qquad \text{(C.4)}
\end{aligned}
$$

Multiplying the above equations by x_i and x_j, respectively, we get

$$
\begin{aligned}
\theta_i^A - (x_i x_j^{-1})^A{}_B\, \theta_j^B &= \sqrt{\frac{x_i^2}{x_j^2}} \lambda^A_{\{ij\}a} I[\eta_{\{ij\}a}] \,, \\
(x_j x_i^{-1})^A{}_B\, \theta_i^B - \theta_j^A &= \sqrt{\frac{x_j^2}{x_i^2}} \lambda^A_{\{ij\}a} I[\eta_{\{ij\}a}] \,. \qquad \text{(C.5)}
\end{aligned}
$$

Adding these two equations gives

$$
(\theta_i - \theta_j)^A - (x_i x_j^{-1})^A{}_B\, \theta_j^B + (x_j x_i^{-1})^A{}_B\, \theta_i^B = \frac{x_i^2 + x_j^2}{\sqrt{x_i^2 x_j^2}} \lambda^A_{\{ij\}a} I[\eta_{\{ij\}a}] \,. \qquad \text{(C.6)}
$$

We rewrite the LHS as

$$\begin{aligned}
&-\lambda^A_{\{ij\}a}\eta^a_{\{ij\}} - \frac{(x_ix_j)^A{}_B\,\theta^B_j}{x_j^2} + \frac{(x_jx_i)^A{}_B\,\theta^B_i}{x_i^2} \\
&\qquad = -\lambda^A_{\{ij\}a}\eta^a_{\{ij\}} - \frac{(x_ix_j)^A{}_B\,\theta^B_i - x_i^2(\theta_i-\theta_j)^A}{x_j^2} + \frac{(x_jx_i)^A{}_B\,\theta^B_i}{x_i^2} \\
&\qquad = -\frac{x_i^2+x_j^2}{x_j^2}\left(\lambda^A_{\{ij\}a}\eta^a_{\{ij\}} + \theta^A_i - (x_jx_i^{-1})^A{}_B\,\theta^B_i\right) \\
&\qquad = -\frac{x_i^2+x_j^2}{x_j^2}\left(\lambda^A_{\{ij\}a}\eta^a_{\{ij\}} + (x_i-x_j)^{AB}(x_i^{-1})_{BC}\,\theta^C_i\right) \\
&\qquad = -\frac{x_i^2+x_j^2}{x_j^2}\lambda^A_{\{ij\}a}\left(\eta^a_{\{ij\}} - \lambda^{Ba}_{\{ij\}}(x_i^{-1})_{BC}\,\theta^C_i\right)\,. \qquad \text{(C.7)}
\end{aligned}$$

where in the second line we used $(x_i - x_j)_{AB}(\theta_i - \theta_j)^B = 0$, and in the third line we used $(x_i - x_j)^{AB}(x_i - x_j)_{BC} = 0$. We can now read off the solution.

- $I[u_{ia}] = \frac{\beta u_i^a}{\sqrt{x_{i+2}^2}}\,, \quad I[\tilde{u}_{i\dot{a}}] = \frac{\tilde{u}_i^{\dot{a}}}{\beta\sqrt{x_{i+2}^2}}$

  Here, we begin with the definition $\langle i_a|i+1_{\dot{b}}] = u_{ia}\tilde{u}_{i+1\dot{b}}$. Contracting both sides with u_i^a and inverting, we have

$$I[u_i^a]I\left[\langle i_a|i+1_{\dot{b}}]\right] = -I[u_i^a]\frac{\langle i^a|i+1^{\dot{b}}]}{\sqrt{x_i^2x_{i+2}^2}} = 0\,. \qquad \text{(C.8)}$$

  Since u_{ia} is the only vector annihilated by the matrix $\langle i|i+1]$, we conclude that

$$I[u_i^a] = \alpha_i u_{ia}\,, \qquad \text{(C.9)}$$

  for some α_i. Returning to the original equation defining u and $\tilde{u}$, we get a set of constraints on α_i,

$$\begin{aligned}
&\alpha_1\tilde{\alpha}_2 = -(x_1^2x_3^2)^{-1/2}\,, && \tilde{\alpha}_1\alpha_2 = -\,(x_1^2x_3^2)^{-1/2}\,, \\
&\alpha_2\tilde{\alpha}_3 = -(x_2^2x_1^2)^{-1/2}\,, && \tilde{\alpha}_2\alpha_3 = -\,(x_2^2x_1^2)^{-1/2}\,, \\
&\alpha_3\tilde{\alpha}_1 = -(x_3^2x_2^2)^{-1/2}\,, && \tilde{\alpha}_3\alpha_1 = -\,(x_3^2x_2^2)^{-1/2}\,. \qquad \text{(C.10)}
\end{aligned}$$

The solution to these equations is

$$\alpha_i = \frac{\beta}{\sqrt{x_{i+2}^2}}\,, \qquad\qquad \tilde{\alpha}_i = \frac{1}{\beta\sqrt{x_{i+2}^2}}\,. \tag{C.11}$$

- $I[w_{ia}] = -\frac{1}{\beta}\sqrt{x_{i+2}^2}w_i^a\,, \quad I[\tilde{w}_{i\dot{a}}] = -\beta\sqrt{x_{i+2}^2}\tilde{w}_i^{\dot{a}}$

  Because w is defined as the pseudoinverse of u via $u_{ia}w_{ib} - u_{ib}w_{ia} = \epsilon_{ab}$, its inversion is straightforward. The definition inverts as

$$\begin{aligned} \epsilon^{ba} &= I[u_{ia}]I[w_{ib}] - I[u_{ib}]I[w_{ia}]\,, \\ &= \frac{\beta}{\sqrt{x_{i+2}^2}}\left(u_i^a I[w_{ib}] - u_i^b I[w_{ia}]\right)\,. \end{aligned} \tag{C.12}$$

  This is again the definition of w as the psuedoinverse of u,

$$\frac{\beta}{\sqrt{x_{i+2}^2}} I[w_{ia}] = -w_i^a\,, \tag{C.13}$$

  whence the result follows.

References

[1] T. Dennen, Y. -t. Huang and W. Siegel, JHEP **1004**, 127 (2010) [arXiv:0910.2688 [hep-th]].

[2] Z. Bern, J. J. Carrasco, T. Dennen, Y. -t. Huang and H. Ita, Phys. Rev. D **83**, 085022 (2011) [arXiv:1010.0494 [hep-th]].

[3] T. Dennen and Y. -t. Huang, JHEP **1101**, 140 (2011) [arXiv:1010.5874 [hep-th]].

[4] Z. Bern, T. Dennen, Y. -t. Huang and M. Kiermaier, Phys. Rev. D **82**, 065003 (2010) [arXiv:1004.0693 [hep-th]].

[5] Z. Bern and T. Dennen, Phys. Rev. Lett. **107**, 081601 (2011) [arXiv:1103.0312 [hep-th]].

[6] Z. Bern, S. Davies, T. Dennen and Y. -t. Huang, arXiv:1202.3423 [hep-th].

[7] Z. Bern, L. J. Dixon and V. A. Smirnov, Phys. Rev. D **72**, 085001 (2005) [hep-th/0505205].

[8] L. F. Alday and J. M. Maldacena, JHEP **0706**, 064 (2007) [arXiv:0705.0303 [hep-th]].

[9] J. M. Drummond, J. Henn, G. P. Korchemsky and E. Sokatchev, Nucl. Phys. B **828**, 317 (2010) [arXiv:0807.1095 [hep-th]].

[10] N. Berkovits and J. Maldacena, JHEP **0809**, 062 (2008) [arXiv:0807.3196 [hep-th]].

[11] E. Witten, Commun. Math. Phys. **252**, 189 (2004) [hep-th/0312171].

[12] F. Cachazo, P. Svrcek and E. Witten, JHEP **0409**, 006 (2004) [hep-th/0403047].

[13] H. Elvang, D. Z. Freedman and M. Kiermaier, JHEP **0904**, 009 (2009) [arXiv:0808.1720 [hep-th]].

[14] R. Britto, F. Cachazo and B. Feng, Nucl. Phys. B **715**, 499 (2005) [hep-th/0412308].

R. Britto, F. Cachazo, B. Feng and E. Witten, Phys. Rev. Lett. **94**, 181602 (2005) [hep-th/0501052].

[15] Z. Bern, J. J. M. Carrasco and H. Johansson, Phys. Rev. D **78**, 085011 (2008) [arXiv:0805.3993 [hep-ph]].

[16] L. J. Mason and D. Skinner, JHEP **1001**, 064 (2010) [arXiv:0903.2083 [hep-th]].

[17] N. Arkani-Hamed, F. Cachazo, C. Cheung and J. Kaplan, JHEP **1003**, 020 (2010) [arXiv:0907.5418 [hep-th]].

[18] Z. Bern, J. J. Carrasco, L. J. Dixon, H. Johansson and R. Roiban, Phys. Rev. Lett. **103**, 081301 (2009) [arXiv:0905.2326 [hep-th]].

[19] Z. Bern, J. J. Carrasco, L. J. Dixon, H. Johansson, D. A. Kosower and R. Roiban, Phys. Rev. Lett. **98**, 161303 (2007) [hep-th/0702112].

[20] Z. Bern, L. J. Dixon and R. Roiban, Phys. Lett. B **644**, 265 (2007) [hep-th/0611086].

[21] N. Berkovits, M. B. Green, J. G. Russo and P. Vanhove, JHEP **0911**, 063 (2009) [arXiv:0908.1923 [hep-th]].

[22] N. Berkovits, Phys. Rev. Lett. **98**, 211601 (2007) [hep-th/0609006].

[23] M. B. Green, J. G. Russo and P. Vanhove, Phys. Rev. Lett. **98**, 131602 (2007) [hep-th/0611273].

[24] P. S. Howe and K. S. Stelle, Phys. Lett. B **554**, 190 (2003) [hep-th/0211279].

[25] G. Bossard, P. S. Howe and K. S. Stelle, Phys. Lett. B **682**, 137 (2009) [arXiv:0908.3883 [hep-th]].

[26] Z. Bern, L. J. Dixon, D. C. Dunbar and D. A. Kosower, Nucl. Phys. B **425**, 217 (1994) [hep-ph/9403226].

[27] Z. Bern, L. J. Dixon, D. C. Dunbar and D. A. Kosower, Nucl. Phys. B **435**, 59 (1995) [hep-ph/9409265].

[28] R. Britto, F. Cachazo and B. Feng, Nucl. Phys. B **725**, 275 (2005) [hep-th/0412103].

[29] Z. Xu, D. -H. Zhang and L. Chang, TUTP-84/3-TSINGHUA;
Z. Xu, D. -H. Zhang and L. Chang, Nucl. Phys. B **291**, 392 (1987);
M. L. Mangano and S. J. Parke, Phys. Rept. **200**, 301 (1991) [hep-th/0509223];
L. J. Dixon, In *Boulder 1995, QCD and beyond* 539-582 [hep-ph/9601359].

[30] A. Ferber, Nucl. Phys. B **132**, 55 (1978);
V. P. Nair, Phys. Lett. B **214**, 215 (1988).

[31] M. T. Grisaru and W. Siegel, Nucl. Phys. B **201**, 292 (1982) [Erratum-ibid. B **206**, 496 (1982)];
Z. Bern, L. J. Dixon, D. C. Dunbar, M. Perelstein and J. S. Rozowsky, Nucl. Phys. B **530**, 401 (1998) [hep-th/9802162].

[32] Z. Bern and A. G. Morgan, Nucl. Phys. B **467**, 479 (1996) [hep-ph/9511336];
Z. Bern, L. J. Dixon, D. C. Dunbar and D. A. Kosower, Phys. Lett. B **394**, 105 (1997) [hep-th/9611127]. C. Anastasiou, R. Britto, B. Feng, Z. Kunszt and P. Mastrolia, Phys. Lett. B **645**, 213 (2007) [hep-ph/0609191];
R. Britto and B. Feng, JHEP **0802**, 095 (2008) [arXiv:0711.4284 [hep-ph]];
W. T. Giele, Z. Kunszt and K. Melnikov, JHEP **0804**, 049 (2008) [arXiv:0801.2237 [hep-ph]];
S. D. Badger, JHEP **0901**, 049 (2009) [arXiv:0806.4600 [hep-ph]].

[33] C. Cheung and D. O'Connell, JHEP **0907**, 075 (2009) [arXiv:0902.0981 [hep-th]].

[34] A. Galperin, E. Ivanov, S. Kalitsyn, V. Ogievetsky and E. Sokatchev, Class. Quant. Grav. **1**, 469 (1984).

[35] A. Karlhede, U. Lindstrom and M. Rocek, Phys. Lett. B **147**, 297 (1984).
U. Lindstrom and M. Rocek, Commun. Math. Phys. **128**, 191 (1990).

[36] R. Boels, JHEP **1001**, 010 (2010) [arXiv:0908.0738 [hep-th]].

[37] R. Britto, F. Cachazo and B. Feng, Nucl. Phys. B **715**, 499 (2005) [arXiv:hep-th/0412308];
R. Britto, F. Cachazo, B. Feng and E. Witten, Phys. Rev. Lett. **94**, 181602 (2005) [arXiv:hep-th/0501052].

[38] N. Arkani-Hamed and J. Kaplan, JHEP **0804**, 076 (2008) [0801.2385 [hep-th]].

[39] Z. Bern, J. J. M. Carrasco, H. Ita, H. Johansson and R. Roiban, Phys. Rev. D **80**, 065029 (2009) [0903.5348 [hep-th]].

[40] Z. Bern, L. J. Dixon and D. A. Kosower, Phys. Rev. D **72**, 125003 (2005) [hep-ph/0505055].

[41] Z. Bern, L. J. Dixon, D. C. Dunbar and D. A. Kosower, Nucl. Phys. B **425**, 217 (1994) [hep-ph/9403226]; Nucl. Phys. B **435**, 59 (1995) [hep-ph/9409265];
Z. Bern, L. J. Dixon and D. A. Kosower, Ann. Rev. Nucl. Part. Sci. **46**, 109 (1996) [hep-ph/9602280]; JHEP **0408**, 012 (2004) [arXiv:hep-ph/0404293].

[42] Z. Bern, L. J. Dixon and D. A. Kosower, Nucl. Phys. B **513**, 3 (1998) [hep-ph/9708239].

[43] Z. Bern and A. G. Morgan, Nucl. Phys. B **467**, 479 (1996) [hep-ph/9511336].

[44] Z. Bern, L. J. Dixon, D. C. Dunbar and D. A. Kosower, Phys. Lett. B **394**, 105 (1997) [hep-th/9611127];
Z. Bern, L. J. Dixon and D. A. Kosower, JHEP **0001**, 027 (2000) [hep-ph/0001001].

[45] R. Britto, F. Cachazo and B. Feng, Nucl. Phys. B **725**, 275 (2005) [hep-th/0412103].

[46] E. I. Buchbinder and F. Cachazo, JHEP **0511**, 036 (2005) [[hep-th/05061xo26].

[47] R. Britto, B. Feng and P. Mastrolia, Phys. Rev. D **73**, 105004 (2006) [hep-ph/0602178];
C. Anastasiou, R. Britto, B. Feng, Z. Kunszt and P. Mastrolia, Phys. Lett. B **645**, 213 (2007) [hep-ph/0609191], JHEP **0703**, 111 (2007) [hep-ph/0612277].
P. Mastrolia, Phys. Lett. B **644**, 272 (2007) [hep-th/0611091];
R. Britto, B. Feng and G. Yang, JHEP **0809**, 089 (2008) [0803.3147 [hep-ph]].

[48] G. Ossola, C. G. Papadopoulos and R. Pittau, Nucl. Phys. B **763**, 147 (2007) [hep-ph/0609007].

[49] D. Forde, Phys. Rev. D **75**, 125019 (2007) [0704.1835 [hep-ph]].

[50] R. Britto and B. Feng, Phys. Rev. D **75**, 105006 (2007) [hep-ph/0612089];
W. B. Kilgore, 0711.5015 [hep-ph];
R. Britto, B. Feng and P. Mastrolia, Phys. Rev. D **78**, 025031 (2008) [0803.1989 [hep-ph]].

[51] Z. Bern, J. J. M. Carrasco, H. Johansson and D. A. Kosower, Phys. Rev. D **76**, 125020 (2007) [0705.1864 [hep-th]].

[52] F. Cachazo and D. Skinner, 0801.4574 [hep-th].

[53] W. T. Giele, Z. Kunszt and K. Melnikov, JHEP **0804**, 049 (2008) [0801.2237 [hep-ph]].

[54] S. D. Badger, JHEP **0901**, 049 (2009) [0806.4600 [hep-ph]].

[55] F. A. Berends, R. Kleiss, P. De Causmaecker, R. Gastmans and T. T. Wu, Phys. Lett. B **103**, 124 (1981);
P. De Causmaecker, R. Gastmans, W. Troost and T. T. Wu, Nucl. Phys. B **206**, 53 (1982);
Z. Xu, D. H. Zhang and L. Chang, TUTP-84/3-TSINGHUA;
R. Kleiss and W. J. Stirling, Nucl. Phys. B **262**, 235 (1985);
J. F. Gunion and Z. Kunszt, Phys. Lett. B **161**, 333 (1985);
Z. Xu, D. H. Zhang and L. Chang, Nucl. Phys. B **291**, 392 (1987).

[56] M. L. Mangano and S. J. Parke, Phys. Rept. **200**, 301 (1991);
L. J. Dixon, in *QCD & Beyond: Proceedings of TASI '95*, ed. D. E. Soper (World Scientific, 1996) [hep-ph/9601359].

[57] V. P. Nair, Phys. Lett. B **214**, 215 (1988);
A. Brandhuber, P. Heslop and G. Travaglini, Phys. Rev. D **78**, 125005 (2008) [0807.4097 [hep-th]].

[58] M. Bianchi, H. Elvang and D. Z. Freedman, JHEP **0809**, 063 (2008) [0805.0757 [hep-th]];
J. M. Drummond, J. Henn, G. P. Korchemsky and E. Sokatchev, 0808.0491 [hep-th];
N. Arkani-Hamed, F. Cachazo and J. Kaplan, JHEP **1009**, 016 (2010) [0808.1446 [hep-th]];
H. Elvang, D. Z. Freedman and M. Kiermaier, JHEP **0904**, 009 (2009) [0808.1720 [hep-th]].

[59] Z. Bern *et al.*, 0803.0494 [hep-ph].

[60] C. F. Berger *et al.*, Phys. Rev. D **78**, 036003 (2008) [0803.4180 [hep-ph]].

[61] Z. Bern, L. J. Dixon and D. A. Kosower, Phys. Rev. D **73**, 065013 (2006) [hep-ph/0507005];
D. Forde and D. A. Kosower, Phys. Rev. D **73**, 061701 (2006) [hep-ph/0509358];
C. F. Berger, Z. Bern, L. J. Dixon, D. Forde and D. A. Kosower, Phys. Rev. D **74**, 036009 (2006) [hep-ph/0604195].

[62] Z. Bern, L. J. Dixon and D. A. Kosower, JHEP **0408**, 012 (2004) [hep-ph/0404293].

[63] N. Arkani-Hamed, J. L. Bourjaily, F. Cachazo, S. Caron-Huot and J. Trnka, 1008.2958 [hep-th].

[64] R. H. Boels, 1008.3101 [hep-th].

[65] Z. Bern, L. J. Dixon, D. A. Kosower, R. Roiban, M. Spradlin, C. Vergu and A. Volovich, Phys. Rev. D **78**, 045007 (2008) [0803.1465 [hep-th]];
C. Vergu, 0908.2394 [hep-th];
D. A. Kosower, R. Roiban and C. Vergu, 1009.1376 [hep-th].

[66] Z. Bern, J. S. Rozowsky and B. Yan, Phys. Lett. B **401**, 273 (1997) [arXiv:hep-ph/9702424].

[67] Z. Bern, J. J. M. Carrasco, L. J. Dixon, H. Johansson and R. Roiban, 1008.3327 [hep-th].

[68] Z. Bern, M. Czakon, L. J. Dixon, D. A. Kosower and V. A. Smirnov, Phys. Rev. D **75**, 085010 (2007) [hep-th/0610248].

[69] Z. Bern, L. J. Dixon, D. C. Dunbar, M. Perelstein and J. S. Rozowsky, Nucl. Phys. B **530**, 401 (1998) [arXiv:hep-th/9802162].

[70] Z. Bern, J. J. Carrasco, L. J. Dixon, H. Johansson, D. A. Kosower and R. Roiban, Phys. Rev. Lett. **98**, 161303 (2007) [arXiv:hep-th/0702112]; Z. Bern, J. J. M. Carrasco, L. J. Dixon, H. Johansson and R. Roiban, Phys. Rev. D **78**, 105019 (2008) [arXiv:0808.4112 [hep-th]].

[71] Z. Bern, J. J. Carrasco, L. J. Dixon, H. Johansson and R. Roiban, Phys. Rev. Lett. **103**, 081301 (2009) [arXiv:0905.2326 [hep-th]].

[72] L. F. Alday, J. M. Henn, J. Plefka and T. Schuster, JHEP **1001**, 077 (2010) [0908.0684 [hep-th]];
J. M. Henn, S. G. Naculich, H. J. Schnitzer and M. Spradlin, JHEP **1004**, 038 (2010) [1001.1358 [hep-th]]; JHEP **1008**, 002 (2010) [1004.5381 [hep-th]].

[73] Z. Bern, J. S. Rozowsky and B. Yan, Phys. Lett. B **401**, 273 (1997) [arXiv:hep-ph/9702424].

[74] H. Kawai, D. C. Lewellen and S. H. H. Tye, Nucl. Phys. B **269**, 1 (1986);
Z. Bern, A. De Freitas and H. L. Wong, Phys. Rev. Lett. **84**, 3531 (2000) [hep-th/9912033];
Z. Bern, Living Rev. Rel. **5**, 5 (2002) [gr-qc/0206071];
N. E. J. Bjerrum-Bohr, P. H. Damgaard, B. Feng and T. Sondergaard, 1005.4367 [hep-th].

[75] J. M. Drummond, J. Henn, V. A. Smirnov and E. Sokatchev, JHEP **0701**, 064 (2007) [hep-th/0607160];
A. Brandhuber, P. Heslop and G. Travaglini, Nucl. Phys. B **794**, 231 (2008) [0707.1153 [hep-th]].

[76] J. M. Drummond, J. Henn, G. P. Korchemsky and E. Sokatchev, Nucl. Phys. B **795**, 52 (2008) [0709.2368 [hep-th]];
J. M. Drummond, J. Henn, G. P. Korchemsky and E. Sokatchev, Nucl. Phys. B **826**, 337 (2010) [0712.1223 [hep-th]].

[77] R. Ricci, A. A. Tseytlin and M. Wolf, JHEP **0712**, 082 (2007) [arXiv:0711.0707 [hep-th]].

[78] N. Beisert, R. Ricci, A. A. Tseytlin and M. Wolf, Phys. Rev. D **78**, 126004 (2008) [arXiv:0807.3228 [hep-th]].

[79] G. P. Korchemsky, J. M. Drummond and E. Sokatchev, Nucl. Phys. B **795**, 385 (2008) [arXiv:0707.0243 [hep-th]];
A. Brandhuber, P. Heslop and G. Travaglini, Nucl. Phys. B **794**, 231 (2008) [arXiv:0707.1153 [hep-th]].

[80] J. M. Drummond, J. Henn, G. P. Korchemsky and E. Sokatchev, Nucl. Phys. B **795**, 52 (2008) [0709.2368 [hep-th]];
J. M. Drummond, J. Henn, G. P. Korchemsky and E. Sokatchev, Nucl. Phys. B **826**, 337 (2010) [0712.1223 [hep-th]].

[81] J. M. Drummond, J. M. Henn and J. Plefka, JHEP **0905**, 046 (2009) [arXiv:0902.2987 [hep-th]].

[82] J. M. Drummond and J. M. Henn, JHEP **0904**, 018 (2009) [arXiv:0808.2475 [hep-th]];

[83] Z. Bern, M. Czakon, L. J. Dixon, D. A. Kosower and V. A. Smirnov, Phys. Rev. D **75**, 085010 (2007) [arXiv:hep-th/0610248];
Z. Bern, J. J. M. Carrasco, H. Johansson and D. A. Kosower, Phys. Rev. D **76**, 125020 (2007) [arXiv:0705.1864 [hep-th]];
Z. Bern, L. J. Dixon, D. A. Kosower, R. Roiban, M. Spradlin, C. Vergu and A. Volovich, Phys. Rev. D **78**, 045007 (2008) [arXiv:0803.1465 [hep-th]];

[84] G. P. Korchemsky and E. Sokatchev, Nucl. Phys. B **839**, 377 (2010) [arXiv:1002.4625 [hep-th]].

[85] N. Arkani-Hamed, J. L. Bourjaily, F. Cachazo, S. Caron-Huot and J. Trnka, arXiv:1008.2958 [hep-th];
J. M. Drummond and J. M. Henn, arXiv:1008.2965 [hep-th].

[86] A. Hodges, arXiv:0905.1473 [hep-th].

[87] N. Arkani-Hamed, F. Cachazo and C. Cheung, JHEP **1003**, 036 (2010) [arXiv:0909.0483 [hep-th]].

[88] L. Mason and D. Skinner, JHEP **0911**, 045 (2009) [arXiv:0909.0250 [hep-th]].

[89] A. Brandhuber, P. Heslop and G. Travaglini, JHEP **0908**, 095 (2009) [arXiv:0905.4377 [hep-th]];JHEP **0910**, 063 (2009) [arXiv:0906.3552 [hep-th]];
N. Beisert, J. Henn, T. McLoughlin and J. Plefka, JHEP **1004**, 085 (2010) [arXiv:1002.1733 [hep-th]].

[90] L. F. Alday, J. M. Henn, J. Plefka and T. Schuster, JHEP **1001**, 077 (2010) [arXiv:0908.0684 [hep-th]];
J. M. Henn, S. G. Naculich, H. J. Schnitzer and M. Spradlin, JHEP **1004**, 038 (2010) [arXiv:1001.1358 [hep-th]];
J. M. Henn, Nucl. Phys. Proc. Suppl. **205-206**, 193 (2010) [arXiv:1005.2902 [hep-ph]].

[91] A. Brandhuber, P. Heslop and G. Travaglini, Phys. Rev. D **78**, 125005 (2008) [arXiv:0807.4097 [hep-th]].

[92] Z. Bern, J. J. M. Carrasco, L. J. Dixon, H. Johansson and R. Roiban, arXiv:1008.3327 [hep-th].

[93] T. Bargheer, F. Loebbert and C. Meneghelli, Phys. Rev. D **82**, 045016 (2010) [arXiv:1003.6120 [hep-th]]. S. Lee, Phys. Rev. Lett. **105**, 151603 (2010) [arXiv:1007.4772 [hep-th]];
Y. t. Huang and A. E. Lipstein, JHEP **1011**, 076 (2010) [arXiv:1008.0041 [hep-th]].

[94] S. Caron-Huot and D. O'Connell, arXiv:1010.5487 [hep-th].

[95] R. Roiban, M. Spradlin and A. Volovich, JHEP **0404**, 012 (2004) [hep-th/0402016].

[96] R. Roiban, M. Spradlin and A. Volovich, Phys. Rev. D **70**, 026009 (2004) [hep-th/0403190].

[97] Z. Bern, Living Rev. Rel. **5**, 5 (2002) [gr-qc/0206071].

[98] Z. Bern, A. De Freitas and H. L. Wong, Phys. Rev. Lett. **84**, 3531 (2000) [arXiv:hep-th/9912033].

[99] N. E. J. Bjerrum-Bohr, P. H. Damgaard and P. Vanhove, Phys. Rev. Lett. **103**, 161602 (2009) [arXiv:0907.1425 [hep-th]];
S. Stieberger, arXiv:0907.2211 [hep-th].

[100] C. R. Mafra, JHEP **1001**, 007 (2010) [arXiv:0909.5206 [hep-th]].

[101] H. Tye and Y. Zhang, arXiv:1003.1732 [hep-th].

[102] N. E. J. Bjerrum-Bohr, P. H. Damgaard, T. Sondergaard and P. Vanhove, arXiv:1003.2403 [hep-th].

[103] Z. Bern, J. J. M. Carrasco and H. Johansson, Phys. Rev. Lett. **105**, 061602 (2010) [arXiv:1004.0476 [hep-th]].

[104] Z. Bern and A. K. Grant, Phys. Lett. B **457**, 23 (1999) [arXiv:hep-th/9904026];

[105] W. Siegel, Phys. Rev. D **48**, 2826 (1993) [arXiv:hep-th/9305073].

[106] V. Del Duca, L. J. Dixon and F. Maltoni, Nucl. Phys. B **571**, 51 (2000) [arXiv:hep-ph/9910563].

[107] R. Kleiss and H. Kuijf, Nucl. Phys. B **312**, 616 (1989).

[108] A. Gorsky and A. Rosly, JHEP **0601**, 101 (2006) [arXiv:hep-th/0510111];
P. Mansfield, JHEP **0603**, 037 (2006) [arXiv:hep-th/0511264];
J. H. Ettle and T. R. Morris, JHEP **0608**, 003 (2006) [arXiv:hep-th/0605121];
H. Feng and Y. t. Huang, JHEP **0904**, 047 (2009) [arXiv:hep-th/0611164].

[109] R. Kleiss and H. Kuijf, Nucl. Phys. B **312**, 616 (1989).

[110] V. Del Duca, L. J. Dixon and F. Maltoni, Nucl. Phys. **B571**, 51-70 (2000) [hep-ph/9910563].

[111] M. B. Green, J. H. Schwarz and L. Brink, Nucl. Phys. B **198**, 474 (1982).

[112] F. Cachazo, arXiv:0803.1988 [hep-th].

[113] P. S. Howe and K. S. Stelle, Int. J. Mod. Phys. A **4**, 1871 (1989); N. Marcus and A. Sagnotti, Nucl. Phys. B **256**, 77 (1985).

[114] M. T. Grisaru and W. Siegel, Nucl. Phys. B **201**, 292 (1982) [Erratum-ibid. B **206**, 496 (1982)].

[115] Z. Bern, J. J. M. Carrasco, L. J. Dixon, H. Johansson and R. Roiban, arXiv:1201.5366 [hep-th].

[116] E. Cremmer and B. Julia, Nucl. Phys. B **159**, 141 (1979).

[117] M. B. Green, J. G. Russo and P. Vanhove, JHEP **1006**, 075 (2010) [arXiv:1002.3805 [hep-th]]; H. Elvang and M. Kiermaier, JHEP **1010**, 108 (2010) [arXiv:1007.4813 [hep-th]]; G. Bossard, P. S. Howe and K. S. Stelle, JHEP **1101**, 020 (2011) [arXiv:1009.0743 [hep-th]]; N. Beisert, H. Elvang, D. Z. Freedman, M. Kiermaier, A. Morales and S. Stieberger, Phys. Lett. B **694**, 265 (2010) [arXiv:1009.1643 [hep-th]].

[118] M. B. Green, J. G. Russo and P. Vanhove, JHEP **1006**, 075 (2010) [arXiv:1002.3805 [hep-th]]; J. Bjornsson and M. B. Green, JHEP **1008**, 132 (2010) [arXiv:1004.2692 [hep-th]].

[119] P. S. Howe and U. Lindström, Nucl. Phys. B **181**, 487 (1981).

[120] G. Bossard, P. S. Howe, K. S. Stelle and P. Vanhove, Class. Quant. Grav. **28**, 215005 (2011) [arXiv:1105.6087 [hep-th]].

[121] R. Kallosh, arXiv:1103.4115 [hep-th].

[122] A. K. Das, Phys. Rev. D **15**, 2805 (1977); E. Cremmer, J. Scherk and S. Ferrara, Phys. Lett. B **74**, 61 (1978).

[123] Z. Bern, J. J. Carrasco, D. Forde, H. Ita and H. Johansson, Phys. Rev. D **77**, 025010 (2008) [arXiv:0707.1035 [hep-th]].

[124] Z. Bern, L. J. Dixon and R. Roiban, Phys. Lett. B **644**, 265 (2007) [arXiv:hep-th/0611086].

[125] D. C. Dunbar, J. H. Ettle and W. B. Perkins, Phys. Rev. D **83**, 065015 (2011) [arXiv:1011.5378 [hep-th]].

[126] M. T. Grisaru, Phys. Lett. B **66**, 75 (1977); E. T. Tomboulis, Phys. Lett. B **67**, 417 (1977); S. Deser, J. H. Kay and K. S. Stelle, Phys. Rev. Lett. **38**, 527 (1977); S. Ferrara and B. Zumino, Nucl. Phys. B **134**, 301 (1978).

[127] Z. Bern, C. Boucher-Veronneau and H. Johansson, Phys. Rev. D **84**, 105035 (2011) [arXiv:1107.1935 [hep-th]]; C. Boucher-Veronneau and L. J. Dixon, JHEP **1112**, 046 (2011) [arXiv:1110.1132 [hep-th]].

[128] Z. Bern and D. A. Kosower, Nucl. Phys. B **379**, 451 (1992); Z. Bern, A. De Freitas, L. J. Dixon and H. L. Wong, Phys. Rev. D **66**, 085002 (2002) [arXiv:hep-ph/0202271].

[129] N. Marcus and A. Sagnotti, Nuovo Cim. A **87**, 1 (1985).

[130] Z. Bern, J. J. M. Carrasco, L. J. Dixon, H. Johansson and R. Roiban, Phys. Rev. D **82**, 125040 (2010) [arXiv:1008.3327 [hep-th]].

[131] A. V. Smirnov, JHEP **0810**, 107 (2008) [arXiv:0807.3243 [hep-ph]].

[132] M. Czakon, Comput. Phys. Commun. **175**, 559 (2006) [arXiv:hep-ph/0511200].

[133] A. V. Smirnov and M. N. Tentyukov, Comput. Phys. Commun. **180**, 735 (2009) [arXiv:0807.4129 [hep-ph]].

[134] A. I. Davydychev and M. Y. Kalmykov, Nucl. Phys. B **699**, 3 (2004) [hep-th/0303162].

[135] A. G. Grozin, Int. J. Mod. Phys. A **19**, 473 (2004) [hep-ph/0307297].